

THE REGULATION OF TCF POP-1 ASYMMETRY AND ITS FUNCTION IN
EARLY CELL FATE SPECIFICATION IN *CAENORHABDITIS ELEGANS*

APPROVED BY SUPERVISORY COMMITTEE

Mentor: Rueyling Lin, Ph.D.

Committee Chairman: Leon Avery, Ph.D., M.B.A.

Committee Member: Zhijiang James Chen, Ph.D.

Committee Member: Keith A. Wharton, Jr., M.D., Ph.D.

DEDICATION

I would like to dedicate this work to my parents.

THE REGULATION OF TCF POP-1 ASYMMETRY AND ITS FUNCTION IN
EARLY CELL FATE SPECIFICATION IN *CAENORHABDITIS ELEGANS*

by

SHU-YI HUANG

DISSERTATION

Presented to the Faculty of the Graduate School of Biomedical Sciences

The University of Texas Southwestern Medical Center at Dallas

In Partial Fulfillment of the Requirements

For the Degree of

DOCTOR OF PHILOSOPHY

The University of Texas Southwestern Medical Center at Dallas

Dallas, Texas

September, 2009

Copyright

by

SHU-YI HUANG, 2009

All Rights Reserved

fr

ACKNOWLEDGEMENTS

I would like to thank my mentor, Dr. Rueyling Lin, for her guidance and advice both in science and in life.

I thank my dissertation committee, Drs. Leon Avery, James Chen, and Keith Wharton for their time and suggestions.

I thank Dr. Scott Robertson for great discussions and advice. I appreciate especially his patience in helping me trouble-shoot on a daily basis.

For Lin lab members, I am particularly grateful to Dr. Miao-chia Lo, who started the work on analyzing the C-terminus of POP-1 and helped me starting my project in the Lin lab. I am thankful for Dr. Premnath Shetty, who contributed primary data for the work of Chapter Two. I thank Manisha Patel and Jessica Medina for everyday help in the lab. I also thank Drs. Eric Rogers, Yuichi Nishi, and Tugba Guven-Ozcan for discussion, emotional support, and a great lab environment.

I thank the Genetics and Development Program of the Division of Basic Science at the University of Texas Southwestern Medical Center. I especially thank Amy Haughey and Margaret Allen for all their administrative expertise.

THE REGULATION OF TCF POP-1 ASYMMETRY AND ITS FUNCTION IN
EARLY CELL FATE SPECIFICATION IN *CAENORHABDITIS ELEGANS*

SHU-YI HUANG, Ph.D.

The University of Texas Southwestern Medical Center at Dallas, 2009

RUEYLING LIN, Ph.D.

Cell-cell signaling pervades all aspects of development. Signaling pathways need to be highly robust to ensure reproducible outcomes. In the cases of several major pathways, including the Wnt signaling pathway, default repression and signal-dependent activation are both mediated by the same response elements and transcription factors. My work focuses on how the *C. elegans* TCF protein POP-1 is converted from a repressor into an activator upon Wnt and MAPK signaling.

C. elegans embryos exhibit a nearly invariant cell lineage composed primarily of a stepwise binary diversification of anteroposterior blastomere identities. The nuclear level of TCF/POP-1 is lowered in all posterior cells in the A-P cell divisions. I showed that the β -catenin homolog, SYS-1, exhibits reiterated asymmetry which is reciprocal to that of POP-1. SYS-1 functions as a limiting coactivator for POP-1. The SYS-1-to-POP-1 ratio is critical for both anterior and posterior cell fates. A high ratio drives the posterior cell fate whereas a low ratio drives the anterior cell fate in multiple A-P divisions throughout development. I showed genetically that while POP-1 nuclear asymmetry is mainly regulated by the MAPK pathway, SYS-1 asymmetry is regulated solely by the Wnt pathway.

Besides the quantitative differences between A-P nuclei, the Wnt and MAPK pathways also modify POP-1 qualitatively, affecting the transcriptional activity of POP-1. I showed that LIT-1/WRM-1-dependent phosphorylation of POP-1 reduces its binding to the coactivator SYS-1. Deleting the PCA domain also weakens the interaction between POP-1 and SYS-1 independent of LIT-1/WRM-1 phosphorylation. The PCA domain is required for POP-1 nuclear asymmetry and all LIT-1/WRM-1-dependent phosphorylation of POP-1. Within the PCA domain, mutating POP-1 threonine 426 to aspartic acid, but not alanine, shows similar effects to deleting the PCA domain.

This study shows that Wnt and MAPK signaling pathways regulate the TCF protein POP-1 both quantitatively for its nuclear asymmetry, and qualitatively for its transcriptional activity. The two pathways not only change the levels of POP-1 and SYS-

1 but also modify the strength of binding, strongly favoring the formation of POP-1/SYS-1 activation complex in the posterior cell, thereby driving A-P differential cell fates.

TABLE OF CONTENTS

TITLE FLY	i
DEDICATION	ii
TITLE PAGE	iii
ACKNOWLEDGEMENT	v
ABSTRACT	vi
TABLE OF CONTENTS	ix
PRIOR PUBLICATIONS	xii
LIST OF FIGURES	xiii
LIST OF TABLES	xv
LIST OF ABBREVIATIONS.....	xvi
CHAPTER ONE: Introduction	1
A common theme in development: activation and repression of signaling pathways. 1	
Endoderm specification in <i>C. elegans</i>	2
Inputs from Wnt and MAPK pathways specify E fate.....	5
The SKN-1/MED-1 pathway for EMS fate specification.....	6
Other contributions	8
Wnt signaling pathways	9
Canonical Wnt signaling pathway	11
Noncanonical Wnt signaling pathway	12
Wnt signaling in <i>Caenorhabditis elegans</i>	13
Cross-regulation of the Wnt signaling pathway by the MAPK pathway	14
POP-1 Asymmetry in MS and E	17

POP-1 nuclear level is lowered by nuclear export in posterior nuclei	17
TCF family of transcription factors: homology and diversity	19
POP-1 acts both as a repressor and an activator for endoderm genes	24
POP-1 functions as a repressor	24
POP-1 functions as an activator	25
Global POP-1 asymmetry beyond MS and E	26
Aims of the study	27
Identification of SYS-1 as the limiting coactivator for POP-1	27
Characterization of the C-terminal domain of POP-1	28
The domains and residues of POP-1 important for the POP-1/SYS-1 interaction	29
CHAPTER TWO: Binary cell fate specification during C. elegans embryogenesis driven	
by reiterated reciprocal asymmetry of TCF POP-1 and its coactivator β-catenin SYS-1	30
Introduction	30
Results	33
Discussion	55
Materials and methods	63
CHAPTER THREE: Deletion analysis of POP-1 C-terminus	66
Introduction	66
Results	71
Discussion	77
Materials and methods	82
CHAPTER FOUR: Mutational analysis within the PCA domain of POP-1	86
Introduction	86

Results	88
Discussion	102
Materials and methods.....	106
CHAPTER FIVE: Differential presentation of mabRL2 epitope <i>in vivo</i>	110
Introduction	110
Results	112
Discussion	126
Materials and methods.....	131
CHAPTER SIX: Regulation of the interaction between POP-1 and its coactivator SYS-1	136
Introduction	136
Results	139
Discussion	144
Materials and methods.....	146
CHAPTER Seven: Conclusions	149
BIBLIOGRAPHY	154

PRIOR PUBLICATIONS

Shuyi Huang, Premnath Shetty, Scott M. Robertson and Rueyling Lin. “Binary cell fate specification during *C. elegans* embryogenesis driven by reiterated reciprocal asymmetry of TCF POP-1 and its coactivator β -catenin SYS-1.” *Development* 134, 2685-2695. (2007)

Shuyi Huang, Premnath Shetty, Scott Robertson, and Rueyling Lin. Meeting abstract. “Binary cell fate specification during *C. elegans* embryogenesis driven by reiterated reciprocal asymmetry of TCF/POP-1 and its coactivator β -catenin/SYS-1.” International Worm Meeting, 2007. Oral presentation.

Shuyi Huang, Premnath Shetty, and Rueyling Lin. Meeting abstract. “Wnt signaling regulates reciprocal asymmetric nuclear levels of TCF/POP-1 and its coactivator β -catenin/SYS-1 between A-P sister cells in early *C. elegans* embryos.” *C. elegans* Development and Evolution Meeting, 2006. Oral presentation.

LIST OF FIGURES

Figure 1.1. Simplified illustrations of four major developmental signaling pathways: the Notch, Wnt, Hedgehog, and nuclear receptor pathways	2
Figure 1.2. Early lineage of the <i>C. elegans</i> embryo.....	4
Figure 1.3. POP-1 asymmetry and endoderm induction in <i>C. elegans</i> embryos	6
Figure 1.4. The intracellular branches of the Wnt signaling pathway	11
Figure 1.5. Model for POP-1 nuclear asymmetry in MS and E.....	19
Figure 1.6. The isoforms of vertebrate TCF family proteins	21
Figure 1.7. Sequence alignment of the C-clamp of TCF E-tails.....	24
Figure 2.1. SYS-1 is required for the activation of Wnt target genes in E and gut formation	35
Figure 2.2. GFP::SYS-1 expression during the cell cycle.....	41
Figure 2.3. Reciprocal nuclear asymmetry of GFP::SYS-1 and POP-1 between A-P sisters.....	43
Figure 2.4. GFP::SYS-1 nuclear asymmetry between A-P sisters is Wnt signal- and proteasome-dependent.....	45
Figure 2.5. Increased level of SYS-1 causes extra gut at the expense of pharynx.....	50
Figure 2.6. Altering the SYS-1/POP-1 ratio also affects cell fate decisions at other A-P divisions	51
Figure 2.7. Pathways regulating the reciprocal asymmetry of POP-1 and SYS-1	56
Figure 3.1. Architecture of GFP::POP-1 transgene and its expression pattern.....	69
Figure 3.2. Deletion analysis of POP-1 on the domain C-terminal to the HMG box	72
Figure 3.3. Amino acid sequence of the PCA domain of POP-1	74

Figure 3.4. Phosphorylation of POP-1 variants in HeLa cells	77
Figure 4.1. The effects of T426 mutations on GFP::POP-1 nuclear asymmetry	90
Figure 4.2. The epistasis of Exp sites and T426 on GFP::POP-1 nuclear asymmetry	93
Figure 4.3. The effects of mutations within the PCA domain on GFP::POP-1 nuclear asymmetry	96
Figure 4.4. The effects of C436S mutation on GFP::POP-1 nuclear asymmetry compared to endogenous POP-1 asymmetry in <i>mom-2(or42)</i>	99
Figure 4.5. Phosphorylation of POP-1 variants in HeLa cells	101
Figure 5.1. Mapping the mabRL2 epitope	113
Figure 5.2. Hyperphosphorylated POP-1 in wildtype embryos is not detected by mabRL2 and is sensitive to the methods of embryo extract preparation.....	115
Figure 5.3. Western blot analysis of dounced wildtype embryo extracts as detected by 94I and mabRL2	116
Figure 5.4. Comparison between N-terminal and C-terminal GFP fusion transgenes of POP-1	118
Figure 5.5. Western blot analysis of GFP::POP-1 variants as detected by 94I and mabRL2	120
Figure 5.6. Time course analysis of wildtype and <i>lit-1(t1512ts)</i> embryo extracts treated with phosphatase	122
Figure 5.8. Western blot analysis of POP-1 treated with various reducing agents	125
Figure 5.9. Flow chart of the fractionation of embryo extract after douncing.....	133
Figure 6.1. Coimmunoprecipitation of POP-1 _{WT} and POP-1 _{D9E} with SYS-1.....	140
Figure 6.1. Coimmunoprecipitation of POP-1 variants with SYS-1.....	142

LIST OF TABLES

Table 2.1. Penetrance of gutless phenotype in various mutants with altered SYS-1 or POP-1 levels.....	36
Table 2.2. Defects for POP-1 and GFP::SYS-1 asymmetry in various genetic backgrounds	47
Table 2.3. Predicted changes of cell fates resulting from an A-P cell fate change for MSa and MSp	52
Table3.1. Deletion analysis of POP-1 on the domain C-terminal to the HMG box.....	75
Table 4.1. Epistasis analysis of POP-1 T426 and the Exp sites.....	92
Table 4.2. Mutational analysis of the PCA domain of POP-1	97

LIST OF ABBREVIATIONS

2-ME – 2-mercaptoethanol
3-AT – 3-amino-1,2,4-triazole
Act sites – LIT-1/WRM-1-dependent phosphorylation sites that favor activation when phosphorylated
A-P – Anteroposterior
APC – Adenomatous polyposis coli
bZIP – The Basic Leucine Zipper DNA binding Domain
CamKII – Calcium-calmodulin dependent kinase II
C-clamp – Cysteine-clamp, previously known as CR domains, which recognizes an additional GC element downstream of the WRE
CKII – Casein Kinase II
CMV – Cytomegalovirus
COS-7 – African Green Monkey SV40-transformed kidney fibroblast cell line
CRM1 – An export receptor for leucine-rich nuclear export signal (NES)-dependent protein transport
CtBP – C-terminal Binding Protein
DIC – Differential interference contrast
DMEM – Dulbecco's Modified Eagle Medium
Dsh – Dishevelled
DTT – Dithiothreitol
E. coli – *Escherichia coli*
EST – Expressed sequence tag
Exp sites – Export sites, amino acids that are phosphorylated by LIT-1/WRM-1 and are important for POP-1 nuclear export
FBS – Fetal bovine serum
Flag – A polypeptide protein tag with the sequence N – DYKDDDDK – C and of 1012 Da in size
Fz – Frizzled
GAL4 – Gal4 is a modular protein consisting broadly of a DNA-binding domain and an activation domain
GFP – Green Fluorescent Protein
GSK-3 – Glycogen Synthase Kinase-3
HeLa – An immortal cell line derived from cervical cancer cells taken from a patient named Henrietta Lacks
HMG domain – High Mobility Group DNA-binding domain
HRP – Horseradish Peroxidase
ICAT – Inhibitor of β -catenin and TCF-4
IP – Immunoprecipitation
LRP – Low density lipoprotein receptor-Related Protein
MAPK – Mitogen-Activated Protein Kinase
Mom – More mesoderm
Myc – A polypeptide protein tag derived from c-myc with the sequence N – EQKLISEEDL – C and of 1202 Da in size

PAGE – Polyacrylamide gel electrophoresis
 PCA – POP-1 C-terminal Acidic domain, corresponding to ~amino acids 400-438 of POP-1
 PCR – Polymerase Chain Reaction
 PKC – Protein Kinase C
 Pop – POsterior Pharynx defect
 PPase – Phosphatase
 RNAi – RNA interference
 SDS – Sodium Dodecyl Sulfate
 TOPFLASH – A luciferase reporter of β -catenin-mediated transcriptional activation by multimerization of the optimal WREs
 UTR – Untranslated region
 VENUS – A yellow fluorescent protein with improved maturation and brightness
 VP16 – A virial phosphoprotein of herpes simplex virus and a potent transcriptional activator.
 VPC – Vulva Precursor Cells
 Wnt – A gene family named after *Wg* (*Wingless*) and *Int*; a major class of secreted morphogenic ligands
 WRE – Wnt-response element, C/T-C-T-T-T-G-A/T-A/T
 WT – Wildtype

CHAPTER ONE

Introduction

COMMON THEME IN DEVELOPMENT:

ACTIVATION AND REPRESSION OF SIGNALING PATHWAYS

Cell-cell signaling pervades all aspects of development in all animals. It is rather surprising that the variety of signaling pathways and basic cell responses to signals appears to be quite limited (Gerhart, 1999). Among the signal transduction pathways identified to date, seven major pathways (Wnt, TGF- β , Hedgehog, receptor tyrosine kinase (RTK), nuclear receptor, Jak/STAT, and Notch) are used repeatedly to control the vast majority of cell fate decisions during early development of complex metazoan such as vertebrates, arthropods, and nematodes (Barolo and Posakony, 2002; Pires-daSilva and Sommer, 2003). Mutations in these pathways often result in cancer or other diseases. The primary consequence of signaling is the activation of specific target genes by signal-regulated transcription factors. Signaling pathways need to be highly robust to ensure reproducible outcomes of developmental processes, but at the same time, they need to be flexible enough to allow changes during development and evolution (Pires-daSilva and Sommer, 2003). In the case of Wnt, Hedgehog, nuclear receptor, and Notch pathways, the default repression and signal-dependent activation are both mediated by the same response elements and the same transcription factor (Barolo and Posakony, 2002). A signaling event elevates the level of coactivator(s), reduces the level of corepressor(s), and/or increase the affinity of transcription factor for coactivator(s) over corepressors(s),

promoting the formation of transcription factor/coactivator complex, and activating downstream genes (Figure 1.1).

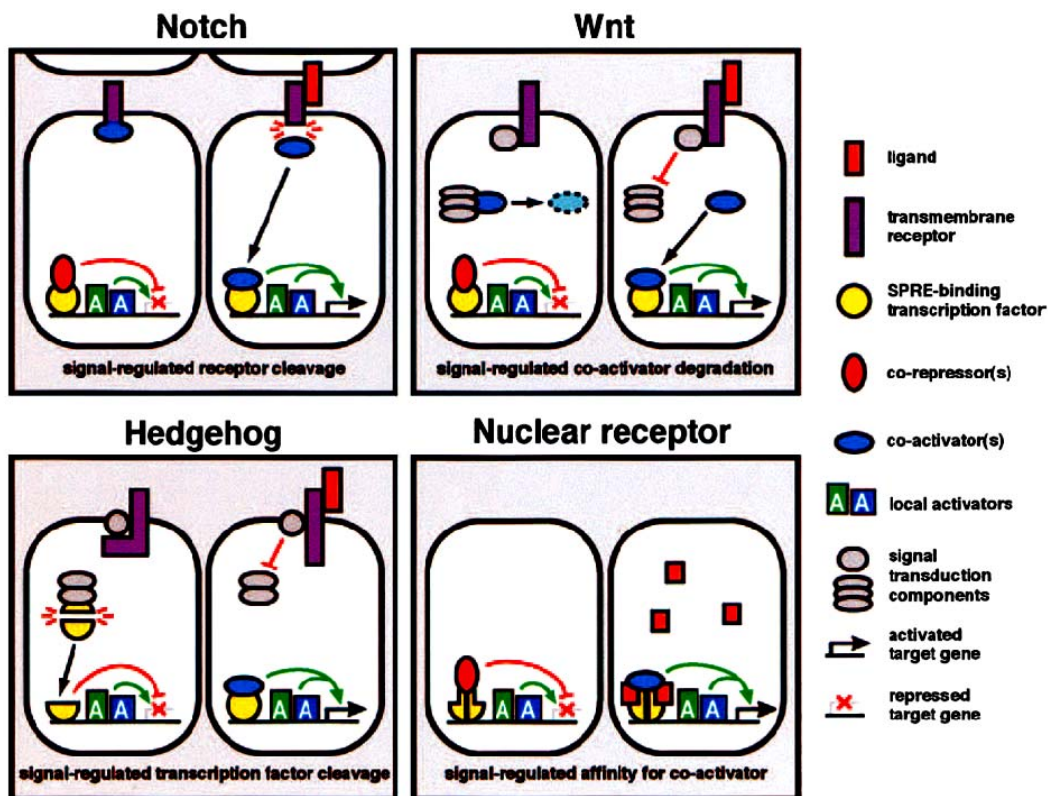


Figure 1.1. Simplified illustrations of four major developmental signaling pathways: the Notch, Wnt, Hedgehog, and nuclear receptor pathways. In each case, the downstream transcription factor binds to signaling pathway response elements (SPREs) and functions both in the default repression state and the signal-dependent activation of target gene by different mechanisms. (Adapted from Barolo and Posakony, 2002)

ENDODERM SPECIFICATION IN *C. ELEGANS*

The nematode *C. elegans* has a nearly invariant cell lineage (Sulston et al., 1983). The point of sperm entry defines the posterior of the one cell embryo. Fertilization causes segregation of many maternal factors along the antero-posterior (A-P) axis, resulting in the one cell embryo dividing into a larger somatic cell, AB, and a smaller germ cell, P1. AB goes on to divide along the A-P axis (ABa/p), then divide once along the left-right axis (ABal/ABar and ABpl/ABpr). The following five rounds of division in the AB lineage are all oriented along the A-P axis. Eventually AB gives rise to hypodermis, neurons, anterior pharynx, and other tissues. The germ cell P1 continues to divide in a stem cell-like fashion, producing a germ cell and a sister somatic cell in the following three cell cycles. The somatic cell produced by P1 is EMS, which divides along the A-P axis and produces two daughter cells with different cell fates. The posterior daughter, E, clonally generates the entire intestine (endoderm) of the worm. The anterior sister of E, MS, produces mesodermal cells, including the posterior pharynx (Gonczy and Rose, 2005). The germ cell produced by P1 is P2, which gives rise to the somatic cell C and the germ cell P3. P3 divides one more time to give the somatic cell D and the germ cell P4 before P4 becomes restricted to produce only the germline lineage. AB, E, MS, C, D, and P4 are referred to as the six founder cells in *C. elegans* embryogenesis because they produce descendants that have mostly synchronous cell divisions (Figure 1.2). The early cell fate specifications provide a good system for understanding the mechanisms underlying how one precursor cell becomes specified and results in two daughter cells acquiring different cell fates. This study focuses on how multiple signaling pathways input into the specification of MS vs. E fate.

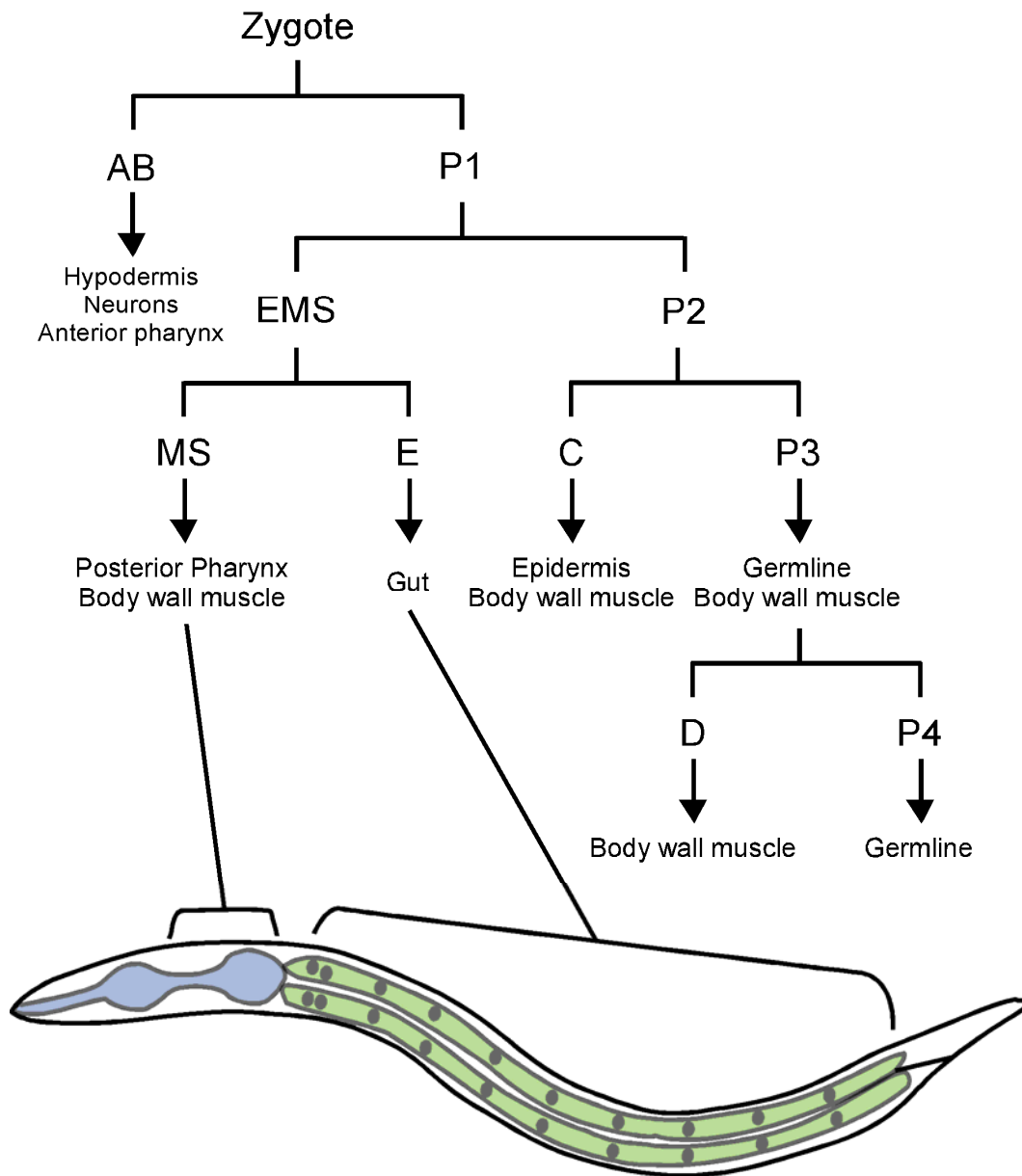


Figure 1.2. Early lineage of the *C. elegans* embryo. The founder cells (AB, MS, E, C, D and P4), as well as cells that give rise to founder cells (P1, P2, P3 and EMS), are shown. The designation of founder cell was based on the observation that these cells produce descendants that have mostly synchronous cell divisions. Tissues derived from the founder cells are noted. An adult hermaphrodite is used to illustrate the MS- and E-derived tissues relevant to this study.

Inputs from the Wnt and MAPK pathways specify E fate

Blastomere recombination experiments demonstrated that at the four cell stage, a signaling event from P2 to EMS is required for the induction of endoderm (E) fate (Goldstein, 1992). Maternal-effect lethal screens have identified two classes of mutants that are important for the specification of E fate. One class, the Mom mutants, shows various degrees of a gutless phenotype and extra mesodermal cells resulting from E adopting an MS-like fate (Figure 1.3). Cloning of these genes revealed that they are genes in the Wnt and MAPK pathways. The Wnt pathway components *mom-1*/porcupine, *mom-2*/Wnt, and *mom-3*/Wntless are all required in the signaling cell, P2, while *mom-5*/Frizzled, *mom-4*/TAK1, *lit-1*/Nlk, and *wrm-1*/β-catenin function in the signal-receiving cell EMS for endoderm fate specification. Mutation(s) affecting either pathway cause an incompletely penetrant gutless phenotype, while mutation(s) knocking down both pathways result in 100% gutless phenotype.

The other class, the Pop mutant, has only one gene, which is the TCF homolog, *pop-1* (for posterior pharynx defective). The phenotype of *pop-1*(-) is the lack of MS-derived posterior pharynx and extra gut cells, resulting from MS taking an E-like fate (Lin et al., 1995 (Figure 1.2)). This suggests that the primary function of POP-1 is to repress E fate in MS. POP-1 protein is primarily localized to the nucleus, and the levels of POP-1 protein are higher in the anterior MS nucleus than it is in the nucleus of its posterior sister, E. This phenomenon is termed “POP-1 nuclear asymmetry” and is regulated by the *mom* genes. Genetic analysis shows that *pop-1* is epistatic to all *mom* mutants, supporting that *pop-1* functions downstream of the Wnt and MAPK pathways.

The effect of POP-1 on the induction of endoderm fate regulated by the Wnt and MAPK pathways is the focus of this study.

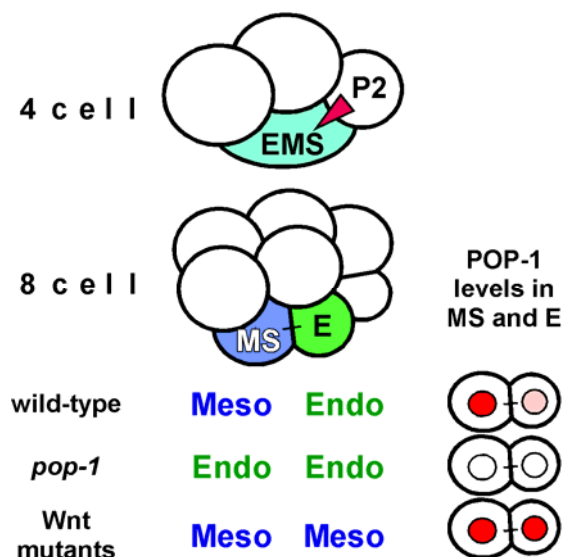


Figure 1.3. POP-1 asymmetry and endoderm induction in *C. elegans* embryos.

Upper: Schematic views of wildtype *C. elegans* embryo at 4- and 8-cell stages. Lower: Fates of MS and E and their POP-1 nuclear levels in wildtype, *pop-1*, or Wnt mutants. Meso = mesoderm. Endo = endoderm.

The SKN-1/MED-1 pathway for EMS fate specification

The bZIP/homeodomain transcription factor SKN-1 (Bowerman et al., 1993) plays an important role in the specification of EMS fate (Bowerman et al., 1992). All embryos from *skn-1* mutant mothers lack pharynx. The pharynx is formed by the ABa and MS descendants, while an MS to ABa signal is required for the specification of ABa-derived anterior pharynx. Therefore, the complete lack of pharyngeal tissue in *skn-1* mutant suggesting the loss of MS fate. While maternally supplied *skn-1* mRNA is evenly distributed in early embryos, the level of SKN-1 protein is higher in P1 than AB at the 2-

cell stage (Bowerman et al., 1993). Mutations in which SKN-1 protein is distributed evenly, both AB and P1 produce cell types similar to the wildtype MS blastomere. At the 4-cell stage, the level of SKN-1 protein is equal between EMS and P2. The germline protein PIE-1 inhibits *skn-1(+)* function in P2, distinguishing the germline cell fate from EMS (Mello et al., 1992). In a *pie-1* mutant, both P2 and EMS take on MS-like fates. As for the two daughter cells of EMS, MS and E both have equal levels of SKN-1 protein but they take on different cell fates, indicating that SKN-1 is not sufficient for the specification of MS vs. E fate.

In EMS, SKN-1 directly activates the expression of two nearly identical GATA factors, *med-1* and *med-2*, that are important for the EMS fate. All *med-1(-); med-2(-)* embryos lack pharynx, and some (15-50%) also lack gut. Expressing SKN-1 leads to the ectopic expression of *med-1* and *med-2*, which in turn are able to convert non-EMS blastomeres into mesoendodermal progenitors. Moreover, forced expression of *med-1* and *med-2* can also force non-EMS cells to adapt the EMS fate independent of SKN-1 activity (Maduro et al., 2001). These observations suggest that a primary function of the maternal SKN-1 protein is to activate the zygotic expression of *med-1* and *med-2*, which is sufficient to promote the EMS fate.

DNase footprinting and gel shift assays revealed that rather than the canonical GATA binding site (HGATAR), MED-1 appears to recognize a related DNA sequence (RAGATATAC) (Broitman-Maduro et al., 2005). Multiple MED-1 binding sites have been identified in the promoter regions of two other GATA factor genes, *end-1* and *end-*

3, that are key regulators of the endoderm fate. Overexpression of either *end-1* or *end-3* can reprogram non-endodermal cells to become intestinal cells (Zhu et al., 1998). The function of *end-1* and *end-3* may be partially redundant: mutations of either *end-1* or *end-3* alone result in no or mild phenotypes in terms of gut formation (Maduro et al., 2007), while *end-1(-); end-3(-)* embryos are 100% gutless (Maduro, 2008). Although MED-1 can bind to the regulatory regions of *end-1* and *end-3* promoters, the weak gutless phenotype of *med-1(-); med-2(-)* suggests input from parallel pathways into the specification of endoderm.

Other contributions

It has been shown that two tyrosine kinase-related genes, *src-1* and *mes-1*, regulate not only the division orientation of EMS blastomere but also contribute to the specification of endoderm fate parallel to the Wnt pathway (Bei et al., 2002). Depleting *mes-1* or *src-1* strongly enhances the gutless and spindle orientation defects of the MOM-2/MOM-5 pathway, suggesting MES-1/SRC-1 function in a parallel pathway. The gutless phenotype in these double mutants is *pop-1*-dependent, suggesting the pathways converge upstream of or on *pop-1*. Interestingly, while *src-1(RNAi)* enhances the gutless phenotype of *mom-4(ne19)*, *mes-1(bn74)* has little effect on *mom-4(ne19)*. Chimera studies showed that *mes-1* is required in both P2 and EMS to control the EMS division axis, while *src-1* is only required in EMS. At the four cell stage, phosphotyrosine (pTyr) signal is enriched at the P2/EMS junction. This enrichment is dependent on *mes-1(+)* activity, and *src-1* is required for most of the visible pTyr signal throughout the whole embryo. MES-1 is predicted to be a single-pass transmembrane protein similar to

receptor-type tyrosine kinases (Berkowitz and Strome, 2000) and it is also enriched at the P2/EMS boarder. It is likely that MES-1 functions in bidirectional signaling at the cell contact upstream of SRC-1 in the regulation of the division axis and cell fate of EMS.

The caudal-like homeodomain protein PAL-1 has also been implicated in the specification of endoderm fate. PAL-1 is required in the C blastomere for its mesoectoderm fate (Hunter and Kenyon, 1996). PAL-1 is present at high levels with SKN-1 in both C MS, and E. The GSK-3 β homolog GSK-3 is required in C to repress SKN-1 function and allow the PAL-1-dependent C fate. In most *skn-1(-)* embryos, E and MS take on C-like fates, suggesting C fate is the default state and PAL-1 is active in E and MS. The role of PAL-1 in endoderm fate is revealed when the SKN-1/MED-1,2 pathway is inactivated. For the embryos that do make gut in the absence of SKN-1 or MED-1,2, PAL-1 functions parallel to POP-1 and activates endoderm development (Maduro et al., 2005b).

WNT SIGNALING PATHWAYS

Wnt signaling controls diverse developmental processes such as proliferation, differentiation, polarity, and cell migration (Kestler and Kuhl, 2008). Overactivation of the Wnt pathway caused by mutations of pathway components accounts for over 90% of colon cancers and a substantial percentage of many other cancers (Giles et al., 2003; Polakis, 2000). In addition, mutations of the Wnt pathway components are the cause of

many other diseases that affect the cardiovascular, nervous, bone, kidney and other systems (Klaus and Birchmeier, 2008). The Wnt signaling pathway also plays an important role in stem cell maintenance (Nusse, 2008).

Since the discovery of the first gene in Wnt signaling pathway, *Int1* (Integration 1) in mice (Nusse and Varmus, 1982), many components and target genes of the pathway have been identified from research covering a wide spectrum of model organisms, including worms, flies, frogs, mice and humans (Klaus and Birchmeier, 2008). Wnt signaling is evolutionarily conserved and is employed throughout all phyla of the animal kingdom. The simplest free-living animals, placozoans, which represent a primitive metazoan form, have a complete Wnt pathway (Srivastava et al., 2008). Work in the Cnidaria has shown the diversity of Wnt genes, and regulatory components of Wnt signaling, evolved early in metazoan evolution, prior to the divergence of cnidarians and bilaterians. Evidence from Hydra and the sea anemone, *Nematostella*, demonstrates a role for Wnt signaling in axis formation and patterning, as well as in gastrulation and germ-layer specification (Lee et al., 2006).

Based on the intracellular mediators involved in the signal-receiving cells, Wnt signaling pathways can be divided into two classes: the canonical Wnt/ β -catenin pathway, and the β -catenin-independent, noncanonical Wnt pathway (Figure 1.4).

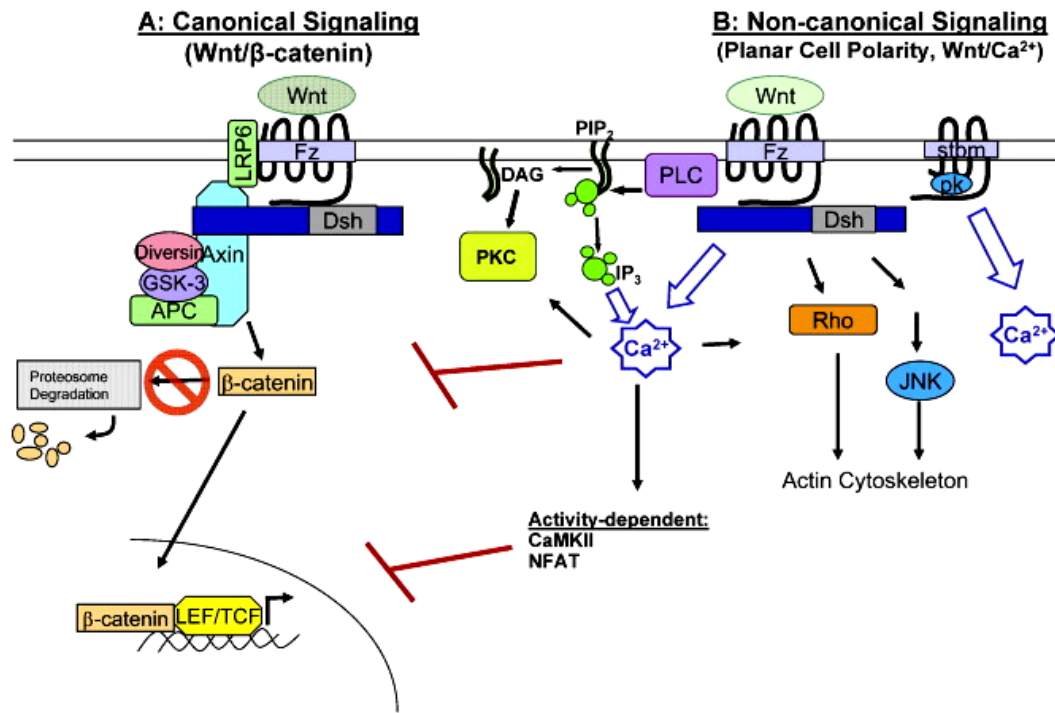


Figure 1.4. The intracellular branches of the Wnt signaling pathway. Schematic view of the Wnt signaling pathway including: (A) the canonical Wnt/β-catenin, and (B) the non-canonical PCP and Wnt/Ca²⁺ signaling pathways. (A) When the canonical pathway is inactive, a destruction complex, including Axin, Dsh, GSK-3 and APC, targets β-catenin for proteasomal degradation. Upon Wnt binding, Fz interacts with Dsh and leads to β-catenin stabilization. Nuclear β-catenin interacts with LEF/TCF to promote the transcription of Wnt target genes. (B) The non-canonical Wnt pathways are independent of β-catenin. Wnt binding to Fz leads to the release of intracellular Ca²⁺ and the activation of PKC, CaMKII, and NFAT. Increased intracellular Ca²⁺ and activated calcium sensors have been shown to antagonize β-catenin. The PCP pathway signals through GTPases (Rho) and C-Jun N-terminal kinase (JNK) to polarize the cytoskeleton. Fz, Frizzled; LRP, low density lipoprotein receptor; APC, adenomatous polyposis coli; GSK-3, glycogen synthase kinase 3; Dsh, Dishevelled; TCF, T cell factor; LEF, lymphoid enhancer factor; PKC, protein kinase C; PLC, phospholipase C; JNK, c-jun NH2-terminal kinase; stbm, Strabismus; pk, Prickle. (Adapted from (Slusarski and Pelegri, 2007))

Canonical Wnt signaling pathway

The hallmark of the activation of the canonical Wnt signaling pathway is the accumulation of cytoplasmic β-catenin and its nuclear translocation (Cadigan and Nusse,

1997; Gordon and Nusse, 2006; Polakis, 2000). In the absence of Wnt, β -catenin is targeted for proteasomal degradation by a destruction complex which includes Dishevelled (Dsh), Axin, adenomatous polyposis coli (APC), and glycogen synthase kinase 3 β (GSK-3). Without β -catenin, the T cell-specific transcription factor/lymphoid enhancer-binding factor 1 (TCF/LEF) family of transcription factors are associated with corepressors such as CtBP and groucho, resulting in the repression of Wnt target genes. Upon Wnt binding to a receptor complex composed of Frizzled (Fz) and LRP, the destruction complex is inhibited, and β -catenin is stabilized. Accumulation of cytoplasmic β -catenin is followed by its translocation to the nucleus where it interacts with TCF transcription factors and activates the expression of target genes. Therefore, in the canonical Wnt signaling pathway, the Wnt signal dictates whether TCFs function in β -catenin-free repressor complexes or in β -catenin-containing activator complexes in the canonical Wnt signaling pathway.

Noncanonical Wnt signaling pathway

Noncanonical Wnt signaling pathways (Figure 1.4.B) do not involve β -catenin/TCF-mediated transcription, although they do share some upstream components with the canonical pathway, such as Frizzled and Dishevelled. The Noncanonical Wnt pathways have been further categorized as the Wnt/JNK pathway and Wnt/Calcium pathway. The Wnt/JNK pathway is also called planar cell polarity (PCP) pathway in *Drosophila*, and it regulates the polarization and migration of cells. While some Wnts have been shown to activate this pathway in vertebrates, the involvement of a distinct Wnt ligand is still not

clear in *Drosophila*. Activation of the Wnt/JNK pathway leads to the activation of Rho GTPases and in turn the activation of downstream mediators such as JNK or rho kinase (ROK). For the Wnt/Calcium pathway, the cellular response upon Wnt binding is intracellular calcium release and activation of calcium sensitive enzymes, such as calcium-calmodulin dependent kinase II (CamKII) and protein kinase C (PKC). This pathway is important in modulating cell adhesion and cytoskeletal dynamics.

Wnt signaling in *Caenorhabditis elegans*

C. elegans shares many conserved Wnt pathway components with flies and vertebrates, but with some notable differences. Similar to other organisms, *C. elegans* has multiple genes encoding Wnt ligands (*lin-44*, *egl-20*, *mom-2*, *cwn-1* and *cwn-2*), Frizzled receptors (*lin-17*, *mom-5*, *mig-1* and *cfz-2*), and Disheveled (*mig-5*, *dsh-1*, *dsh-2*). There are also homologs of Porcupine (*mom-1*), Casein Kinase Ia (*kin-19*), GSK3 β (*gsk-3*), and Axin (*pry-1* and *axl-1*).

On the other hand, worms appear to encode only a single TCF gene, *pop-1*, and a single APC gene, *apr-1*. There is no clear LRP homolog identified to date. However, since worm Wnt pathway genes are sometimes quite diverged, it is possible that functional homologs exist but are not identified due to low similarities to known genes at the level of primary sequence. Indeed, the axin-related gene *axl-1* was initially overlooked (Oosterveen et al., 2007). Lastly, the *C. elegans* genome has three β -catenin genes (*bar-1*, *wrm-1* and *hmp-2*) with highly divergent primary sequences, with the functions of vertebrate β -catenin dispersed among the three. HMP-2 localizes to

epithelial cell junctions with HMP-1/ α -catenin and HMR-1/cadherin, and it seems to be exclusively involved in cell adhesion (Korswagen et al., 2000). BAR-1 only functions in processes involving the canonical Wnt pathways, such as the migration of Q neuroblasts and the cell fate specification of vulva precursor cells (VPCs) (Eisenmann et al., 1998; Maloof et al., 1999). WRM-1 functions in many asymmetric divisions throughout development, including EMS, T cells, and Z1/Z4 (somatic gonad precursors, SGPs) divisions (Herman, 2001; Rocheleau et al., 1997; Siegfried and Kimble, 2002). However, it only interacts with POP-1/TCF weakly and the interaction does not require the β -catenin binding domain of POP-1 (Natarajan et al., 2001).

There is evidence for other non-canonical Wnt pathways. Phospholipase C (*plc-1*) and inositol triphosphate receptor (*itr-1*) have been shown to be required for the intercalation of the embryonic epidermis (Thomas-Virnig et al., 2004; Vazquez-Manrique et al., 2008). A PCP-like pathway has been suggested to be required for B cell asymmetry (Wu and Herman, 2006) and the PHA neuronal lineage (Hawkins et al., 2005). However, detailed mechanisms are not clear.

Crosstalk between the Wnt signaling pathway and the MAPK pathway

The mitogen-activated protein kinase (MAPK) pathway is a kinase cascade involved in the transduction of extracellular stimulation that lead to intracellular responses (Zarubin and Han, 2005). Various extracellular signals activate the MAPK pathway, which consist of a core of three protein kinases: the MAP kinase kinase kinase (MAPKKK), the MAP kinase kinase (MAPKK), and the MAP kinase (MAPK). Activated MAPKKK

phosphorylates and activates MAPKK, which in turn phosphorylates and activates MAPK. The active MAPK then acts on the downstream targets and regulates gene expression. Activation of the MAPK pathway leads to cellular responses such as cell proliferation, differentiation, motility, and apoptosis based on cues derived from the cell surface, the metabolic state of the cell, and the intracellular environment. Defects in the MAPK pathway have been linked to cancer, immune disorders and neurodegenerative diseases.

A conserved MAPK pathway has been shown to interact with the Wnt pathway. The pathway is composed of TAK1 (for TGF- β -activated kinase 1), TAB1 (for TAK1 binding protein), and NLK (for NEMO-like kinase). TAK1 is related to mitogen-activated protein-kinase-kinase kinase (MAPKKK) (Yamaguchi et al., 1995). TAB1 was identified as a TAK1 interacting protein, and it activates TAK1 by binding to the catalytic domain of TAK1 (Shibuya et al., 1996). TAK1 functions upstream of NLK, a MAP kinase-related kinase, and enhances the kinase activity of NLK (Ishitani et al., 1999). There is no known MAP-kinase kinase (MAPKK) in this pathway. The influence of the TAK1-NLK pathway on the Wnt pathway was first discovered by genetic studies in *C. elegans*. The *C. elegans* genome encodes TAK1 (*mom-4*), NLK (*lit-1*), and TAB1 (*tap-1*) (Ishitani et al., 1999; Meneghini et al., 1999). The β -catenin WRM-1 is required for the activation of LIT-1 kinase activity. Active LIT-1 phosphorylates POP-1 and promotes the nuclear export of POP-1 (Meneghini et al., 1999; Rocheleau et al., 1999; Shin et al., 1999).

Activation of the TAK1-NLK pathway negatively regulates the Wnt signaling pathway as shown by TOPFLASH assays and by Wnt-dependent processes in *Xenopus*, *Drosophila*, and zebrafish (Ishitani et al., 1999; Thorpe and Moon, 2004; Zeng and Verheyen, 2004). In mammalian cells, phosphorylation of TCF-4 by NLK inhibits the DNA binding of TCF/ β -catenin complex but not that of TCF alone (Ishitani et al., 1999). Moreover, NLK does not interact directly with TCF proteins. Rather, it can interact with TCF when β -catenin is present. Thus, β -catenin may be required for a stable interaction between NLK and TCF. Another proposed mechanism of NLK-dependent downregulation of TCF is by promoting degradation of TCF (Yamada et al., 2006). The NLK-associated RING finger protein (NARF) induces the ubiquitylation of TCF and the ubiquitylated TCF is subsequently degraded by the proteasome. The ubiquitylation of TCF by NARF is enhanced by NLK kinase activity, suggesting that NARF functions as a ubiquitin-ligase (E3) for TCF degradation and suppresses the Wnt signaling pathway.

The signal activating the TAK1-NLK pathway is not known in *C. elegans*. In other systems, TAK1 can be activated by TGF- β , BMP, or IL1 (Ninomiya-Tsuji et al., 1999; Shibuya et al., 1998; Yamaguchi et al., 1995). Also, the TAK1-NLK pathway has been shown to be activated upon Wnt1 or Wnt5a signaling (Ishitani et al., 2003; Smit et al., 2004). However, Wnt1 stimulation activates the canonical, β -catenin-dependent pathway (Klaus and Birchmeier, 2008), while Wnt5a is known to activate the noncanonical, Wnt/Calcium pathway (Kohn and Moon, 2005). Therefore, how different Wnt signals affect the TAK1-NLK pathway is not well understood.

POP-1 ASYMMETRY IN MS AND E

Immunocytochemistry reveals that the nuclear protein levels of POP-1 are different between nuclei of sister blastomeres born along the anteroposterior axis, a phenomenon termed “POP-1 asymmetry” (Lin et al., 1998). For the MS and E sister blastomeres, POP-1 protein is present at higher levels in the anterior MS nucleus than it is in the posterior E nucleus, and the asymmetric levels of POP-1 in MS and E requires P2 to EMS signaling and is important for the specification of E fate (Lin et al., 1998).

POP-1 asymmetry in MS and E is regulated by the Wnt and MAPK pathways, while the MOM-4/LIT-1/WRM-1 pathway plays a more important role (Lin et al., 1998; Lo et al., 2004; Maduro et al., 2002; Meneghini et al., 1999; Park and Priess, 2003; Rocheleau et al., 1999; Shin et al., 1999; Thorpe et al., 1997). Wnt pathway components, *mom-2*/Wnt, *mom-5*/Frizzles, *apc-1*/APC, all have incompletely penetrant effects on endoderm formation and POP-1 asymmetry, although they are fully penetrant for the spindle orientation defect, which is independent of POP-1 function. On the other hand, *mom-4*/TAK1, *lit-1*/Nlk, and *wrm-1*/β-catenin all have 100% POP-1 asymmetry defects (Meneghini et al., 1999).

POP-1 nuclear level is lowered by nuclear export in posterior nuclei

Quantification of GFP::POP-1 showed that the total cellular levels of POP-1 in A-P sister blastomeres are equal, and that POP-1 nuclear asymmetry is the result of

nucleocytoplasmic redistribution of POP-1 (Maduro et al., 2002). Also, cotransfecting LIT-1, WRM-1, and POP-1 results in nuclear-to-cytoplasmic redistribution of POP-1 in a mammalian tissue culture system (Rocheleau et al., 1999). Indeed, POP-1 nuclear asymmetry requires the 14-3-3 protein, PAR-5, and the exportin CRM1 homolog, XPO-1 (previously known as *crm-1* or *imb-4*) (Lo et al., 2004). Phosphorylation of POP-1 by LIT-1/WRM-1 complex promotes the interaction between POP-1 and PAR-5. Mutating LIT-1 phosphorylation sites or depleting XPO-1 by RNAi both result in the loss of nuclear POP-1 asymmetry, and these embryos often fail to produce endoderm. Although the β -catenin WRM-1 is required for POP-1 asymmetry, it only interacts with POP-1 weakly (Natarajan et al., 2001). It is likely that its only requirement is to activate the kinase activity of LIT-1 (Rocheleau et al., 1999). Moreover, nuclear levels of LIT-1 and WRM-1 are asymmetric, with higher levels in the posterior E as compared to its anterior sister MS. This pattern is reciprocal to that of nuclear POP-1 asymmetry. The asymmetric distribution of WRM-1 and LIT-1 is also under the control of the Wnt and MAPK pathways. Therefore, the Wnt and MAPK pathways increase the nuclear levels of LIT-1/WRM-1 complex, which phosphorylates POP-1 and promotes the interaction between POP-1 and PAR-5 and leads to the nuclear export of POP-1 in E (Figure 1.5).

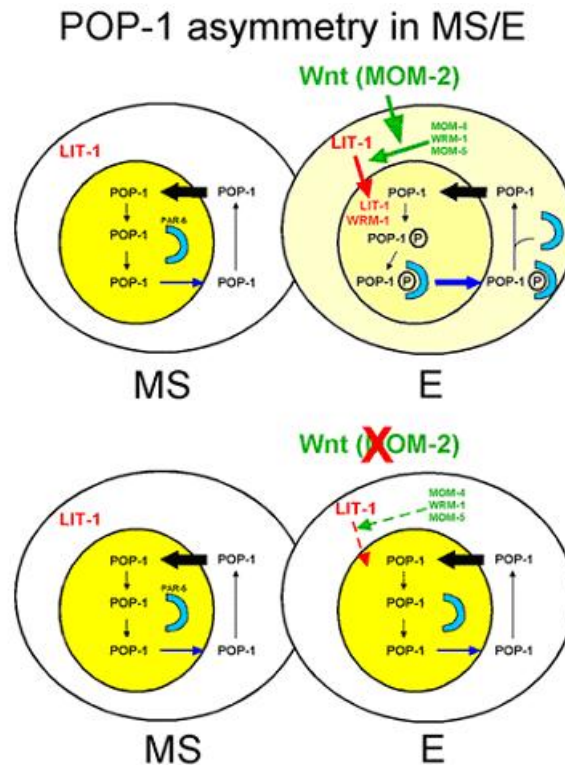


Figure 1.5. Model for POP-1 nuclear asymmetry in MS and E. Lo et al. (2004) proposed that POP-1 nuclear asymmetry throughout the early *C. elegans* embryo is a result of a PAR-5-mediated nuclear export that occurs in the posterior cells. (Upper panel) the upstream Wnt/MAP kinase components result in a high nuclear LIT-1 and WRM-1 in posterior cells. The higher levels of nuclear LIT-1 and WRM-1 result in hyperphosphorylation of POP-1 in the posterior nuclei. Phosphorylation of POP-1 by LIT-1 creates a binding site(s) for PAR-5 (blue crescent). Binding to PAR-5 facilitates the nuclear export of POP-1, resulting in the lowering of nuclear POP-1 in posterior cells. (Lower panel) In the absence of Wnt signaling (MOM-2), LIT-1 and WRM-1 are not enriched in the nucleus, and the nuclear level of POP-1 remains high in E. The levels of POP-1 are indicated by different shades of yellow, with the brightest yellow representing the highest level.

TCF FAMILY OF TRANSCRIPTION FACTORS:

HOMOLOGY AND DIVERSITY

TCF proteins are a family of evolutionarily conserved sequence-specific DNA-binding transcription factors that function downstream of the canonical Wnt signaling pathway. TCF proteins share four conserved functional domains (Figure 1.6): (1) an N-terminal β -catenin binding domain; (2) a context-dependent repression domain; (3) an HMG-type DNA binding domain with nuclear localization signal (NLS); and (4) a C-terminal tail (Hoppler and Kavanagh, 2007). While invertebrates tend to have only one *Tcf* gene and rarely display alternative transcripts, most vertebrates encode four family members, *Tcf-1*, *Lef-1*, *Tcf-3*, and *Tcf-4* (or in HUGO nomenclature, *TCF7*, *LEF1*, *TCF7L1*, and *TCF7L2*, respectively) with diverse isoforms produced from each gene by extensive alternative splicing and promoter usage (Waterman, 2004). Each of these isoforms contains certain domains and lacks others. Since the different domains mediate different protein-DNA or protein-protein interactions, the isoforms produced from the same gene may have very different activity. The selective expression of these isoforms could perform tissue- or stage-specific functions, further increasing the diversity of outcomes of Wnt signals.

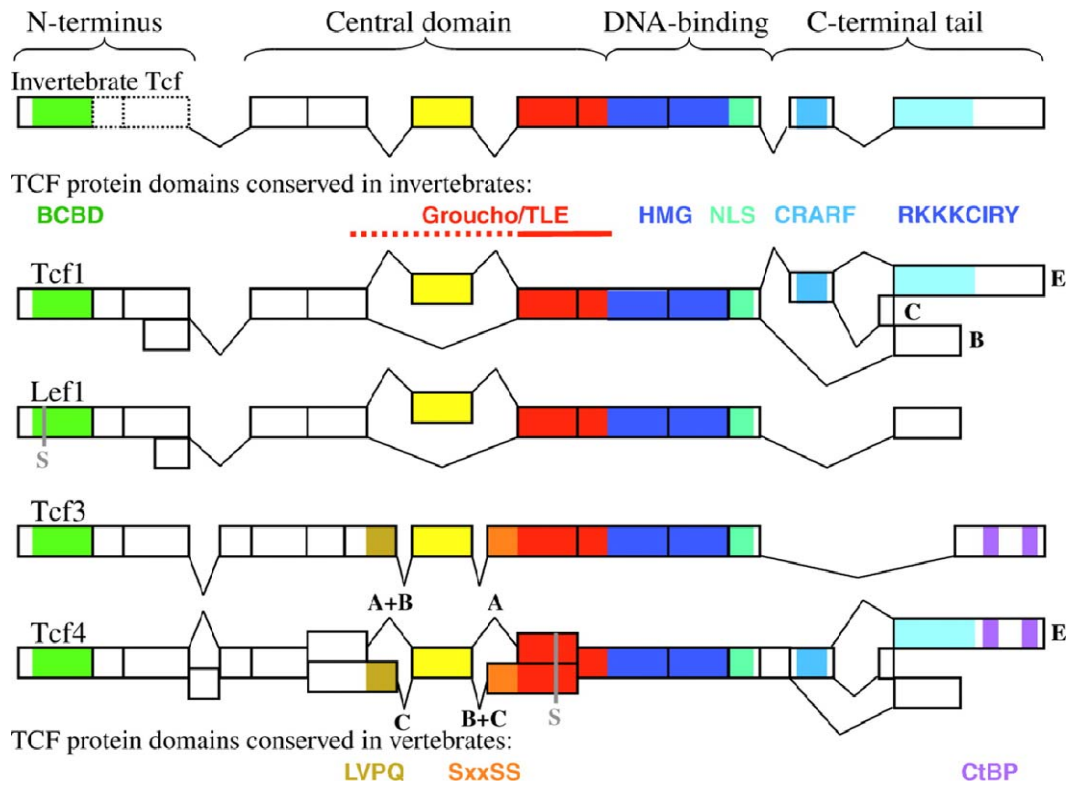


Figure 1.6. The isoforms of vertebrate TCF family proteins. The exon structure is shown for a generic invertebrate *Tcf* gene and generic vertebrate *Tcf-1*, *Lef-1*, *Tcf-3* and *Tcf-4* genes. There are four major domains of TCF proteins: N-terminal β -catenin binding domain (BCBD in green), central repression domain, DNA-binding HMG domain (dark blue) and C-terminal tail. Other conserved motifs include the LVPQ and SxxSS motives in the central domain (olive and orange), the groucho/TLE transcriptional co-repressors (red), the nuclear localization signal (NLS in turquoise), the C-clamp (blue and cyan), and the CtBP-binding domain (purple). The identified SUMOylation sites in LEF1 (K25) and in TCF4 (K297) are marked in grey. Alternative translation initiation sites for TCF-1 and LEF-1 are indicated, which produce N-TCF isoforms lacking the β -catenin-binding domain.

The N-terminal β -catenin binding domain of TCF proteins is about 50 amino acids long and is highly conserved, with >60% sequence identity among orthologs (Arce et al., 2006). Binding to β -catenin induces conformational changes in this domain including the formation of an alpha helix which lies along a positively charged groove of

the middle armadillo repeats of β -catenin and salt bridges forming the lysine-aspartic “charged button,” both of which are conserved in all TCF/ β -catenin interactions (Liu et al., 2008). Alternative promoter usage in mammalian *Tcf-1* and *Lef-1* genes results in certain isoforms that lack the β -catenin binding domain. These isoforms are therefore non-responsive to Wnt/ β -catenin signaling and act as constitutive repressors (Hoppler and Kavanagh, 2007).

The central context-dependent repression domain is located between the β -catenin binding domain and the HMG domain. The sequence identity level among vertebrate TCF proteins in this domain is as low as 15% (Arce et al., 2006). Although the primary sequences are not conserved, the overall function of this domain appears to be conserved. The context-dependent repression domain participates in repression by recruiting the corepressors of the Groucho family. Groucho co-repressors function with a multitude of transcription factors of distinct families. TCF acts as a repressor upon binding to Groucho-family proteins. The mechanism of transcription repression by Groucho is believed to be through the recruitment of histone deacetylases (HDACs).

The high mobility group (HMG) DNA binding domain is the best conserved domain in the TCF/LEF family of proteins, with >90% sequence identity among vertebrates and ~50% between *C. elegans* and mammalian TCF-1 and LEF-1. The HMG box of TCF proteins recognizes the core consensus sequence C/T-C-T-T-T-G-A/T-A/T (also termed the Wnt-response element or WRE), in the minor groove of the double helix.

Upon binding, TCF is known to bend DNA 90° -130°, and is believed to facilitate interactions between proteins bound at nonadjacent sites (Giese et al., 1992). The nuclear localization signal adjacent to the HMG domain in TCF proteins participates in DNA binding directly. It is able to form non-specific contacts between its positively charged side chains with the phosphate backbone of DNA. These additional contacts increase the affinity of TCF-DNA binding by 100-fold into the nanomolar range.

Alternative splicing at the C-terminus of TCF family proteins gives rise to isoforms with a variety of C-terminal “tails” with or without two conserved domains: the Cysteine-clamp (C-clamp, previously also called CR domains; Figure 1.7), and corepressor CtBP binding motifs. The C-clamp contains conserved cysteines with aromatic and basic amino acids and binds to double-strand DNA but not single-strand DNA or RNA. The C-clamp recognizes an additional GC element downstream of the WRE; therefore, it may allow regulation of different sets of target genes. Among the alternatively spliced tails, the “E-tail” is produced from *Tcf-1* and *Tcf-4*, but not *Tcf-3* or *Lef-1*. All the invertebrate TCF proteins examined to date have C-termini most similar to the E-tail; therefore, it is likely to be the ancestral form. The invertebrate and mammalian TCF-1 E-tails contain the C-clamp but not the CtBP binding motifs. TCF-4 E-tail has both the C-clamp and the CtBP binding motifs, while the C-terminal domain of TCF-3 only contains the CtBP binding motifs but not the C-clamp.

	<u>CR 1</u>		<u>CR 2</u>
Consensus	KKCRARFGQ+	----	WC--CRRKKKC-RQQ
hTCF1E...	SP KKCRARFGLN QQTD	WC	GP CRRKKKCIRYL PG
hTCF4E...	AP KKCRARFGLD QQNN	WC	GP CRRKKKCVRYI QG
hTCF3E...	QLSQTSQQQVQEAEG-	ALAS	KS KKPCVQYL PP
dTCF	...NM KKCRARFGLD QQSQ	WC	KP CRRKKKCIRY MEA
pop-1	...DQ KKCRARF GVNTEM	WC	KF CKRKKKCEYAT DR
PBF	...EA KKCRKVYGI EHRDQ	WC	TACR WKKACQ RFLD*
G4EF	...DA KKCRKVYGM ERRDL	WC	TACR WKKACQ RFLD*

Figure 1.7. Sequence alignment of the C-clamp of TCF E-tails. Sequences from the human LEF/TCF family are aligned with the TCF orthologs. (Amino acid sequences for TCF orthologs were derived from the following GenBank™ entries: *Drosophila melanogaster* (dTCF, [AMINO ACIDSC47464](#)); *C. elegans* (POP-1, [AMINO ACIDSC05308](#)); Prf-1/PBF ([AMINO ACIDSF73463](#)); and G4EF ([AMINO ACIDSF97516](#))). Two cysteine-rich (CR) regions of consensus CR1 and CR2 in the C-clamp are indicated above the alignment. The asterisk after the PBF and G4EF proteins indicates the end of the protein.

The tails are the least understood features of TCF proteins. Many studies on TCF function have been done with reporters carrying multimerized optimal WREs (i.e., TOPFLASH). The activation of these reporters are β -catenin-dependent but tail-independent. Therefore, in many studies the effects of the C-terminal tails are ignored. It is thus crucial to study the regulation of endogenous genes by the TCF/LEF proteins to reveal the function of the C-terminal domain.

POP-1 ACTS BOTH AS A REPRESSOR AND AN ACTIVATOR

POP-1 functions as a repressor

POP-1 is required to repress endoderm fate in MS. *pop-1(-)* embryos have extra gut due to an MS to E fate transformation, and endoderm genes, such as *end-1* and *end-3*, are derepressed in the MS lineage. POP-1 can interact with the histone deacetylase, HDA-1, and the Groucho family co-repressor, UNC-37 (Calvo et al., 2001). Both Groucho/UNC-37 and HDAC/HDA-1 show ubiquitous localization without A-P asymmetry (Pflugrad et al., 1997). Inhibition of *unc-37* and *hda-1* by RNAi result in derepression of an *end-1* reporter in MS. POP-1 co-repressor complex represses the transcription of *end-1* in MS. These data suggests that POP-1 represses transcription of endoderm genes by recruiting HDA-1 and UNC-37.

POP-1 functions as an activator

Because *pop-1(-)* embryos still make gut, it was believed that POP-1 is only required for repressing endoderm genes in MS while a low nuclear level of POP-1 in E results in the alleviation of its repression, allowing the induction of endoderm fate. However, work from our lab shows that POP-1 is required for the full activation of endoderm genes (Shetty et al., 2005). E-specific reporters are repressed in MS and activated in E in a POP-1-dependent manner *in vivo*. POP-1 directly interacts with at least one E-specific gene, *end-1*. The activation of E-specific reporters requires the β -catenin binding domain of POP-1. Also, the lowering of the nuclear level of POP-1 is required for the activation of E-specific reporters. When nuclear export of POP-1 is blocked, resulting in a high nuclear level of POP-1 in E, POP-1 represses E fate and the embryos are gutless. These results support the presence of a limiting coactivator β -catenin. In the MS nucleus, if the

level of coactivator is limiting, the high level of nuclear POP-1 acts as a repressor and repress endoderm fate. In E, a low level of nuclear POP-1 can bind to coactivator and activate endoderm genes. While canonical Wnt signaling in other systems increases the level of β -catenin in response to Wnt signaling, Wnt signaling lowers the nuclear level of TCF protein in worms. Both effects result in the increase of TCF/ β -catenin activation complex, and the activation of Wnt target genes.

GLOBAL POP-1 ASYMMETRY BEYOND MS AND E

POP-1 asymmetry reiterates throughout embryogenesis in all sister blastomeres resulting from divisions along the anterior-posterior axis, but not from those dividing along the left-right or dorsal-ventral axes. Lineage analysis compared wildtype and *pop-1(-)* embryos shows that POP-1 asymmetry affects multiple A-P cell fate decisions. POP-1 asymmetry is also observed in certain larval lineages (such as seam cells, Q neuroblasts, T cells, and somatic gonad precursors, etc.).

By the 24-cell stage, both AB and EMS descendants have the ability to generate POP-1 asymmetry cell-autonomously (Park and Priess, 2003). At the 24-cell stage, when a single AB descendent is isolated and allowed to divide, it can give rise to two daughter cells with asymmetric levels of POP-1. When two isolated AB descendants are placed next to each other and allowed to divide, they are able to signal to each other so that their spindles align, and they show reciprocal POP-1 asymmetry. These results show that

starting at around the 24-cell stage and beyond, the blastomeres not only can generate POP-1 asymmetry cell autonomously, but they can also mutually induce POP-1 asymmetry. This process is MOM-2/Wnt-independent, but MOM-5/Frizzled and MOM-4/MAPK are required for the establishment of POP-1 asymmetry in the recombined blastomeres. Interestingly, in the context of intact embryos, POP-1 asymmetry is present in some *mom-5* mutant embryos but not in *mom-2; mom-5* double mutant embryos. This result suggests that in intact embryos, MOM-2/Wnt can induce POP-1 asymmetry independent of MOM-5/Frizzled. However, in both isolated blastomeres and intact embryos, MOM-4/MAPK, LIT-1/Nlk, and WRM-1/ β -catenin are essential for the global POP-1 asymmetry throughout embryogenesis.

AIMS OF THE STUDY

The major aim of this study was to investigate the quantitative and qualitative regulation of POP-1 in relation to its subcellular localization (nuclear asymmetry) and transcriptional activity. The goal of this study is to understand how POP-1 is converted from a repressor to an activator by the Wnt and MAPK signaling.

Identification of SYS-1 as the limiting coactivator for POP-1

Since POP-1 is converted from a repressor to an activator in response to Wnt/MAPK signaling in a β -catenin-dependent manner, Chapter Two focuses on the identification of the β -catenin coactivator for POP-1 in E fate specification. I showed that SYS-1 is the

limiting coactivator for POP-1 in E, and it showed reciprocal asymmetry to that of POP-1. The Wnt and MAPK pathway components regulated SYS-1 and POP-1 asymmetries, respectively, to effectively increase the SYS-1-to-POP-1 ratio. Contrary to the canonical Wnt pathway which is activated by increasing the level of β -catenin, it is the SYS-1-to-POP-1 ratio that is important for the decision between anterior vs. posterior cell fates in multiple divisions during embryogenesis.

Characterization of the C-terminal domain of POP-1

Prior to this study, there was very little understanding of the role of the POP-1 C-terminal region beyond the HMG domain. I tested *cis*- elements for their contributions in the regulation of POP-1 nuclear asymmetry and transcriptional repression activities. The results showed that the C-terminal most 39 amino acid (PCA domain, see Chapter Three) and POP-1_{T426} are crucial for POP-1 asymmetry and LIT-1/WRM-1-dependent phosphorylation of POP-1. I have also identified a second repression domain located between the HMG domain and the PCA domain, and the PCA domain itself may function as an activation domain. Therefore, there are two distinct domains of POP-1 required for proper nuclear asymmetry, and two domains for the repression activity of POP-1. Chapters Two and Three describe the deletion and mutational analyses, respectively.

Chapter Five includes an analysis of the epitope of the monoclonal antibody against POP-1, mabRL2. Hyperphosphorylated POP-1 in wildtype embryo extracts is not recognized by mabRL2, suggesting the epitope for mabRL2 is not accessible to mabRL2 in hyperphosphorylated POP-1. The epitope of mabRL2 represents a qualitative

difference in POP-1 which is missing or blocked in the hyperphosphorylated POP-1. Our working model is that an unknown posttranslational modification at or near the mabRL2 epitope makes the epitope inaccessible in hyperphosphorylated POP-1. My attempts to identify the molecular nature of this posttranslational modification are described in Chapter Five.

The domains and residues of POP-1 important for the POP-1/SYS-1 interaction

I tested the relative binding affinity between POP-1 variants and SYS-1 in a mammalian tissue culture system. It was previously believed that the interaction between TCF proteins and their coactivator β -catenin is strictly through the N-terminal β -catenin interaction domain of TCF, and that POP-1 was no exception (Liu et al., 2008). My results suggest that additional domains of POP-1 may also contribute to POP-1/SYS-1 binding. In addition, LIT-1/WRM-1-dependent phosphorylation weakened the interaction between POP-1 and SYS-1. The results are presented in detail in Chapter Six.

All experiments presented here were conducted in the Lin laboratory at the University of Texas Southwestern Medical Center from March, 2004 to August, 2009.

CHAPTER TWO

BINARY CELL FATE SPECIFICATION DURING *C. ELEGANS* EMBRYOGENESIS DRIVEN BY REITERATED RECIPROCAL ASYMMETRY OF TCF POP-1 AND ITS COACTIVATOR β -CATENIN SYS-1

INTRODUCTION

Cell fates of *C. elegans* embryos are determined early in the embryo, through a combination of spatiotemporally controlled expression of maternally-supplied transcription factors and highly specific cell-cell interactions (Kemphues and Strome, 1997; Schnabel and Priess, 1997). After initial fate specification, each blastomere generates specific terminally differentiated cell types following a series of primarily antero-posterior (A-P) cell divisions.

Lineage analyses using genetic mutants suggest that most of the invariant lineage during *C. elegans* embryogenesis is built by a stepwise binary diversification of blastomere identities (Kaletta et al., 1997). Mutations in the gene *lit-1*, which encodes a Nemo-like MAP kinase (Ishitani et al., 1999; Rocheleau et al., 1999), suggest that the LIT-1 protein is involved in at least six consecutive binary switches that cause the posterior cell of two equivalent cells at each A-P cleavage to assume the posterior fate. The nuclear level of LIT-1 is higher in posterior cells where its activity is required, compared to their anterior sisters (Lo et al., 2004; Takeshita and Sawa, 2005).

The A-P asymmetry of LIT-1 levels is reciprocal to that of the *C. elegans* TCF protein, POP-1, which is detected at a higher level in the nuclei of anterior cells of all A-P divisions examined (Lin et al., 1998; Lin et al., 1995). In the absence of POP-1, anterior cells adopt the fate of posterior sisters. Both LIT-1 and POP-1 A-P asymmetry require the MAP kinase kinase kinase MOM-4, a *C. elegans* β -catenin WRM-1, and a lesser contribution from other components of the Wnt pathway (Lin et al., 1998; Lo et al., 2004; Maduro et al., 2002; Meneghini et al., 1999; Park and Priess, 2003; Rocheleau et al., 1999; Shin et al., 1999; Thorpe et al., 1997). WRM-1 has been shown to bind directly to LIT-1 and activate its kinase activity in vitro (Rocheleau et al., 1999). We have shown previously that LIT-1/WRM-1 phosphorylates POP-1 at specific sites, thereby promoting its interaction with a 14-3-3 protein, leading to nuclear export (Lo et al., 2004). Therefore, in the posterior cells, as compared to their anterior sisters, nuclear levels of LIT-1 are high and nuclear POP-1 levels are lowered.

The source of signal(s) for A-P asymmetric cell fate specification are known in very few cases (Lin et al., 1998; Park and Priess, 2003; Thorpe et al., 1997). At the 4-cell stage, a Wnt/MAPK signal from P2 to EMS specifies the posterior daughter of EMS, E, to become an endoderm precursor (Goldstein, 1992). The anterior daughter of EMS, MS, generates mesoderm. Most mutations in either the Wnt or MAP kinase signaling pathways result in a non-fully penetrant transformation of E to MS (the Mom phenotype) (Kaletta et al., 1997; Rocheleau et al., 1997; Thorpe et al., 1997). Mutation in *pop-1* results in MS adopting the fate of E (Lin et al., 1995). We and others have shown that POP-1 both represses E fate in the MS blastomere (Calvo et al., 2001; Lin et al., 1995; Rocheleau et al., 1997; Thorpe et al.,

1997), as well as promoting endoderm formation from E (Broitman-Maduro et al., 2005; Shetty et al., 2005). We showed that Wnt/MAPK signaling converts POP-1 from a repressor to an activator of target genes (Shetty et al., 2005). Activation of these target genes in E by POP-1 specifically required that the POP-1 nuclear level in E be lowered. In addition, a requirement for the N-terminal domain of POP-1, similar in sequence to the N-terminal domains of other TCF proteins involved in binding β -catenin (van de Wetering et al., 1997), suggested a β -catenin co-activator.

The *C. elegans* genome encodes four β -catenin-related proteins, HMP-2, BAR-1, WRM-1, and SYS-1 (Costa et al., 1998; Eisenmann et al., 1998; Kidd et al., 2005; Rocheleau et al., 1997). WRM-1 is required for asymmetric cell fates in *C. elegans* embryogenesis (Rocheleau et al., 1997). However, WRM-1 has never been shown to physically interact with POP-1, nor has it been shown to function as a TCF/POP-1 co-activator (Kidd et al., 2005; Korswagen et al., 2000; Natarajan et al., 2001; Rocheleau et al., 1999). SYS-1 is required for asymmetric divisions of the somatic gonad precursors (Kidd et al., 2005; Miskowski et al., 2001), and has recently been implicated in the specification of endoderm precursor (Phillips et al., 2007). While animals homozygous for a reduction of function mutation are sterile, *sys-1(RNAi)* resulted in a very low penetrance gutless phenotype.

We show here that SYS-1 is a limiting coactivator for POP-1 in the activation of Wnt/MAPK-responsive genes in the E blastomere. SYS-1 exhibits a reiterated asymmetry that is reciprocal to the reiterated asymmetry of nuclear POP-1 through all A-

P divisions examined. We show that the SYS-1-to-POP-1 ratio appears critical for both the anterior and posterior cell fates in multiple divisions: a high ratio drives the posterior cell fate whereas a low ratio drives the anterior cell fate. In addition, SYS-1 and POP-1 levels are regulated in opposite directions by two pathways known to regulate endoderm specification. We propose that SYS-1 levels are increased primarily by the MOM-2/MOM-5 pathway whereas nuclear POP-1 levels are decreased primarily by the MOM-4/WRM-1/LIT-1 pathway. Together, these two pathways efficiently increase the SYS-1-to-POP-1 ratio in the posterior cell, promoting asymmetric cell fates.

RESULTS

***sys-1* activity is required for the activation of Wnt-responsive genes in the E blastomere**

To investigate the potential role of the β -catenin SYS-1 as a co-activator for POP-1 in the E blastomere, we examined the effect of *sys-1* depletion on the expression of the Wnt-responsive, E-specific genes, *sdz-23* and *end-1* (Robertson et al., 2004; Shetty et al., 2005; Zhu et al., 1997). Depletion of *sys-1* by RNAi resulted in a reduction in the expression levels of both *sdz-23* and *end-1* reporter genes in all embryos examined ($n > 200$) (Figure 2.1 A, C, E, F; data not shown). Although the extent of reduction is similar to that observed when *pop-1* is removed, *sys-1*-depletion does not result in derepression of either E-specific reporter in the MS lineage (Figure 2.1 A-D) or defects in GFP::POP-1 asymmetry (data not shown). These results suggest that the requirement for

sys-1 in activation of Wnt target gene expression in E is downstream or independent of the regulation of nuclear POP-1 levels.

sys-1(RNAi) produces nearly 100% dead embryos (Figure 2.1 H). These RNAi embryos are arrested without proper morphogenesis but nonetheless with differentiated tissue types, such as epidermal, pharyngeal, and muscle cells. Despite pleiotropic terminal phenotypes, 3-4% of *sys-1(RNAi)* embryos were consistently observed to lack intestine (n=497, Figure 2.1 I), a percentage gutless similar to *pop-1(RNAi)* embryos (Broitman-Maduro et al., 2005). It has been shown that the transcription factor SKN-1 functions in parallel with the POP-1 pathway to specify endoderm (Broitman-Maduro et al., 2005). Depletion of *pop-1* in the *skn-1(zu67)* mutant background enhances the *skn-1(zu67)* gutless phenotype from 64% to almost 100%. We observed that *sys-1(RNAi)* also enhances the *skn-1(zu67)* gutless phenotype to 100% (n=68), consistent with SYS-1 functioning in the same pathway as POP-1 in endoderm specification.

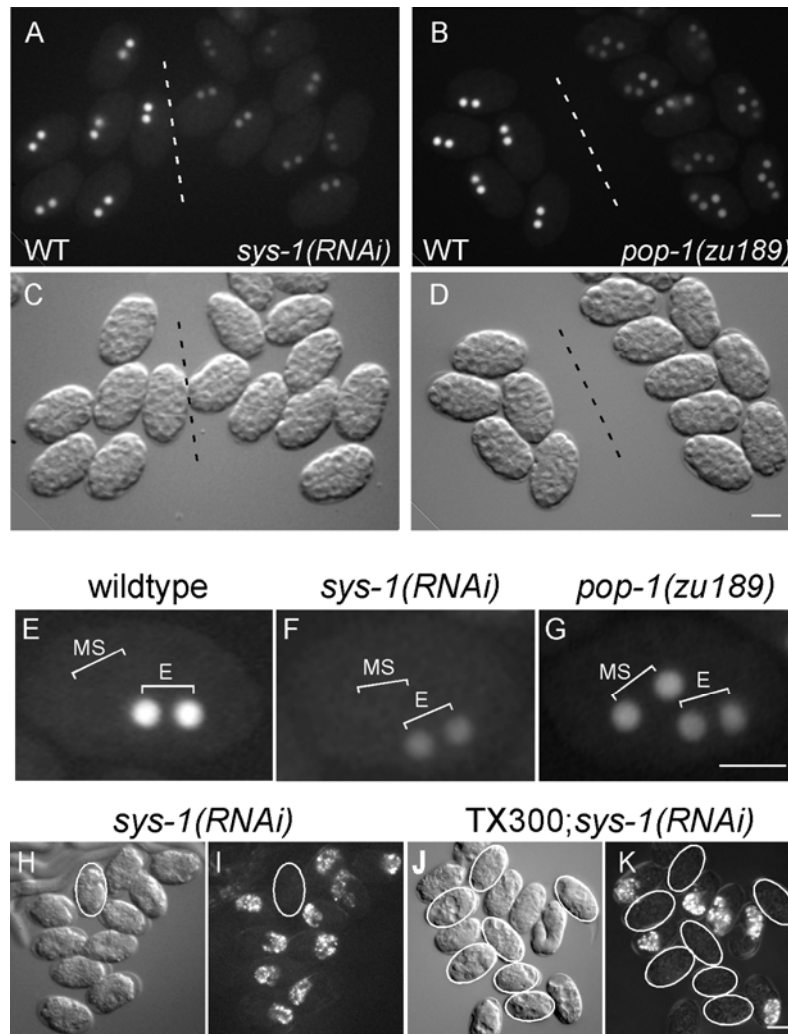


Figure 2.1. SYS-1 is required for the activation of Wnt target genes in E and gut formation. (A-D) Micrographs of embryos carrying the *Psdz-23::gfp::H2B* transgene, in wildtype, *sys-1(RNAi)*, or *pop-1(zu189)* backgrounds. All embryos are shown at the stage when two MS and two E daughters are present, with DIC (bottom) and the corresponding nuclear GFP::H2B fluorescence image (top). In each panel, wildtype (left of the dashed line) and RNAi/mutant embryos (right of dashed line) were imaged together. Note the reduced GFP fluorescence in *sys-1(RNAi)* and *pop-1(zu189)* embryos compared to that in wildtype embryos. Four GFP-positive cells were observed in *pop-1(RNAi)* embryos due to derepression in the MS lineage. (E-G) Representative wildtype, *sys-1(RNAi)* and *pop-1(RNAi)* embryos from the above panels showing reporter GFP expression. (H-K) Terminally differentiated *sys-1(RNAi)* (H, I) or *telIs3;sys-1(RNAi)* (J, K) embryos shown under DIC (H, J) or birefringence optics revealing intestinal specific gut granules (white speckles in I and K). Embryos lacking gut granules are outlined in white. Bar: 20 μ m.

Elevated POP-1 or reduced SYS-1 levels enhance the Mom phenotype whereas elevated SYS-1 levels suppress it

We observed a strong enhancement of the gutless phenotype upon *sys-1(RNAi)* in all *mom* mutants examined (Table 2.1). A striking example is the enhancement of *lit-1(tl534)* from 0% (n=116) to 100% (n=126) gutless. Conversely, we observed a strong suppression of the gutless phenotype in most *mom* mutants or RNAi embryos carrying a transgene expressing GFP::SYS-1 either in all (*teIs98(P_{pie-1}gfp::sys-1)*) or the EMS (*teEx321(P_{med-1}gfp::sys-1)*) lineages. For example, the penetrance of the Mom phenotype in *apr-1(RNAi)* and *mom-4(ne19)* embryos dropped from 29% (n=70) and 40% (n=65) to 0% (n=20) and 1% (n=67), respectively, in the *teEx321* background. Both the SYS-1 reduction-of-function and overexpression results above suggest that the level of SYS-1 is important for endoderm specification.

Table 2.1. Penetrance of gutless phenotype in various mutants with altered SYS-1 or POP-1 levels

	reported	this study
<i>skn-1(zu67)</i>	67 ^a	63 (46) ^b
<i>sys-1 (RNAi)</i>		4 (429)
<i>skn-1(zu67);sys-1 (RNAi)</i>		100 (68)
<i>skn-1(RNAi)(inj)</i> ^c		74(46)
<i>skn-1(RNAi)</i>		72(163)
<i>skn-1(RNAi)(inj);mom-2 (or42)</i>	100 ^d	100 (71)
<i>skn-1(RNAi)(inj);mom-4 (ne19)</i>		100 (79)
<i>skn-1(RNAi); mom-5(or57)</i>		96%(179)
<i>teEx321(P_{med-1}gfp::sys-1)</i> ^e		0 (134)
<i>teIs3(P_{med-1}gfp::pop-1)</i> ^f		0 (150)
<i>teIs98(P_{pie-1}gfp::sys-1)</i> ^f		0 (392)
<i>skn-1(RNAi); teIs98</i>		16 (215)

	reported	this study
<i>mom-1(or10)</i>	85 ^d	83 (55)
<i>mom-1(or10);sys-1(RNAi)</i>		93 (41)
<i>mom-1(or10);tels3</i>		93 (41)
<i>mom-2(or42)</i>	73 ^d	72 (105)
<i>mom-2(RNAi)</i>	14 ^h	28 (49)
<i>mom-2(or42);sys-1(RNAi)</i>		100 (229)
<i>mom-2(or42);teEx321</i>		10 (39)
<i>mom-2(RNAi)^g;tels3</i>		60 (67)
<i>mom-2(or42);tels98</i>		28(145)
<i>mom-2(or42);tels98;skn-1(RNAi)</i>		94 (467)
<i>mom-3(or78)</i>	65 ^d	70 (60)
<i>mom-3(or78);sys-1(RNAi)</i>		81 (80)
<i>mom-3(or78);teEx321</i>		13 (15)
<i>mom-3(or78);tels3</i>		84 (50)
<i>mom-4(ne19)</i>	43 ^h	40 (65)
<i>mom-4(ne19);sys-1(RNAi)</i>		100 (246)
<i>mom-4(ne19);teEx321</i>		1 (67)
<i>mom-4(ne19);tels3</i>		75 (56)
<i>mom-5(or57)</i>	5 ^d	14 (113)
<i>mom-5(or57);sys-1(RNAi)</i>		60 (134)
<i>mom-5(or57);teEx321</i>		0 (62)
<i>mom-5(or57);tels3</i>		65 (93)
<i>mom-5(or57);tels98</i>		4(131)
<i>mom-5(or57);tels98;skn-1(RNAi)</i>		52(188)
<i>apr-1(RNAi)</i>	26 ^h	29 (70)
<i>apr-1(RNAi);teEx321</i>		0 (20)
<i>apr-1(RNAi);tels3</i>		71 (62)
<i>lit-1(t1534)</i>	0 ⁱ	0 (116)
<i>lit-1(t1534);sys-1(RNAi)</i>		100 (126)
<i>lit-1(t1534);tels3</i>		94 (56)
<i>lit-1(I512)</i>	100 ⁱ	99 (224)
<i>lit-1(t1512);teEx321</i>		65 (31)

	reported	this study
<i>wrm-1(RNAi)</i>	100 ^h	100 (122)
<i>wrm-1(RNAi);sys-1(RNAi)</i>		100 (87)
<i>wrm-1(RNAi);teEx321</i>		100 (143)
<i>wrm-1(RNAi);teIs3</i>		100 (170)
<i>med-1/2(RNAi)</i> ^j	7-52%	16(61)
<i>med-1/2(RNAi);mom-2(or42)</i>		85(66)
<i>med-1/2(RNAi);mom-4(ne19)</i>		46(57)
<i>med-1/2(RNAi);mom-2(or42);teEx321</i>		23(31)
<i>med-1/2(RNAi);mom-4(ne19);teEx321</i>		19(27)

^a Bowerman et al, 1992.

^b Numbers indicate percentage gutless. Numbers in parentheses indicate total number of embryos scored.

^c All *skn-1(RNAi)* was performed by feeding except the ones indicated as injection (inj)

^d Thorp et al, 1997.

^e *teEx321* was crossed into adult mutant hermaphrodites and GFP positive embryos were scored.

^f Balanced *mom* mutant strains carrying *teIs3* and *teIs98* were generated. Embryos were collected from mutant hermaphrodites and scored for gut formation.

^g *teIs3* is on V, the same linkage group as *mom-2*, therefore *mom-2(RNAi)* was performed.

^h Rocheleau et al, 1997.

ⁱ Kaletta, et al, 1997.

^j 7% gutless (Goszczynski, et al, 2005). 52% gutless (Maduro et al, 2001). 6 mg/ml ds *med-1/2* RNA was injected and embryos laid 24 hours post injection were assayed for gut formation.

We then asked whether an increase in the level of POP-1 would also affect the penetrance of the gutless phenotype in *mom* mutants. Worms carrying extra copies of *pop-1* transgenes (*teIs3* [*P_{med-1gfp}::pop-1*]) expressing GFP::POP-1 in the EMS lineage display normal POP-1 nuclear asymmetry and no developmental defect (Lo et al., 2004). We observed a strong enhancement of the Mom phenotype with *teIs3* (Table 2.1), which increases the percentage of gutless embryos from 29% (n=70) and 43% (n=65) to 71% (n=62) and 75% (n=56), respectively, for *apr-1(RNAi)* and *mom-4(ne19)*. This effect is similar to that observed for depletion of *sys-1* and opposite to that observed following an increase in SYS-1 levels. These results demonstrate that both POP-1 and SYS-1 levels

are important for the specification of endoderm. A high level of SYS-1 promotes, whereas a low level of SYS-1 or a high level of POP-1 antagonizes the endoderm fate.

We believe that the observed effect on the gutless phenotype upon altering the levels of SYS-1 or POP-1 results from an altered POP-1 activity and not an altered SKN-1-dependent pathway. We found, for example, that *teIs98(P_{pie-1gfp::sys-1})* suppresses the gutless phenotype in *skn-1(RNAi)* embryos (Table 2.1). The penetrance of the gutless phenotype dropped from 76% (n=163) in *skn-1(RNAi)* embryos to 16% (n=215) following *skn-1(RNAi)* in *teIs98*. This SKN-1-independent suppression was also observed in *mom-2(or42)* and *mom-5(or57)* mutant backgrounds (Table 2.1). Because expression of GFP::SYS-1 in *teEx321(P_{med-1gfp::sys-1})* depends on the SKN-1 activity, we inactivated the SKN-1 pathway by *med-1/2* RNAi. *med-1* and *med-2* are transcription factors downstream of *skn-1*. It has been shown that depletion of both *med-1* and *med-2* by RNAi results in gutless embryos (Calvo et al., 2001). We performed *med-1/2(RNAi)* in *mom-2(or42)*, *mom-4(ne19)*, *mom-2(or42);teEx321*, and *mom-4(ne19);teEx321* embryos. In every case we examined, *teEx321* suppressed the gutless phenotype when *med-1* and *med-2* were depleted by RNAi (Table 2.1).

Genetic interaction between POP-1 and SYS-1

We also observed a genetic interaction between POP-1 and SYS-1 in the formation of endoderm. First, the low penetrance gutless phenotype observed following *sys-1(RNAi)* was enhanced by over 10-fold (59%, n=205) in the *teIs3(P_{med-1gfp::pop-1})* background (Figure 2.1 J, K). Second, whereas *sys-1(q544)/+* animals produce no dead embryos, *sys-*

l(q544)/+; teIs3 produce 42% dead embryos and larvae (n=105), and 4% of these embryos are gutless. The increased severity of *sys-1* depletion in a genetic background in which the POP-1 level is elevated demonstrates that, while both POP-1 and SYS-1 absolute levels are important, their abundance relative to each other is more important for the specification of endoderm. A high SYS-1-to-POP-1 ratio promotes the endoderm fate.

Nuclear SYS-1 levels are higher in E than MS, reciprocal to nuclear POP-1

We determined the localization of GFP::SYS-1 in the MS and E blastomeres and their descendants in *teEx321(P_{med-1}gfp::sys-1)* embryos by immunofluorescence using an anti-GFP antibody. GFP::SYS-1 has a dynamic subcellular localization throughout the cell cycle (Figure 2.2). At telophase, it was observed in the nucleus, the cytoplasm, and on centrosomes. The overall level of nuclear and cytoplasmic GFP becomes different between MS and E, with a higher level in E compared to MS, during early interphase (Figure 2.3 A). The centrosomal GFP signal disappears during interphase, reappears at prometaphase, and is very intense and equal between sisters during metaphase. Using VENUS-tagged full-length SYS-1 (VNS::SYS-1), Phillips et al (2007) have recently also reported that VNS::SYS-1 associates with centrosome and is at a higher level in E than in MS.

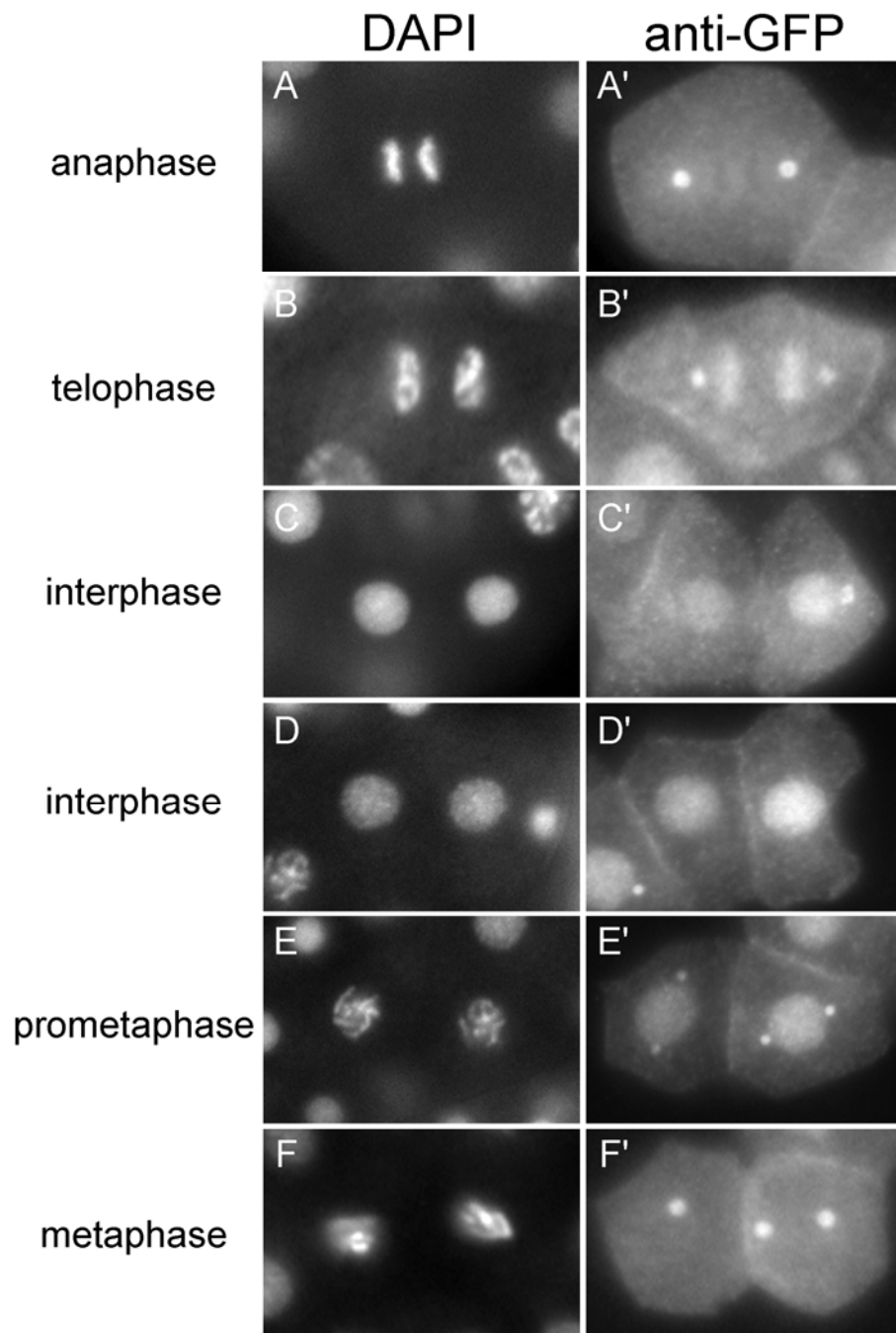


Figure 2.2. GFP::SYS-1 expression during the cell cycle. Anti-GFP staining (right panels) along with corresponding DAPI staining (left panels) at the indicated stages during the cell cycle. Note the dynamic centrosomal staining pattern. GFP::SYS-1 asymmetry was first detected at early interphase.

The asymmetric GFP::SYS-1 levels observed between MS and E (MS<E) is reciprocal to the POP-1 nuclear asymmetry (Lin et al., 1995) (Figure 2.3 A-D). Strikingly, just as POP-1 asymmetry is reiterated following all A-P divisions observed, the reciprocal GFP::SYS-1 asymmetry is also reiterated in subsequent A-P divisions in the EMS lineage (Figure 2.3 E-L). MS and its descendants divide along the A-P axis five times during embryogenesis. We followed the first three rounds of A-P divisions in the MS lineage in fixed embryos and observed a higher level of cytoplasmic and nuclear GFP in all posterior cells compared to their anterior sisters (Figure 2.3 E-H; data not shown). E divides A-P, giving rise to Ea and Ep, both of which then divide left-right, after which the four E descendants undergo several more rounds of A-P divisions to generate the entire intestine. We observed asymmetric GFP::SYS-1 in all A-P divisions of the E lineage (Figure 2.3 E-H, K-L). The only time that the GFP::SYS-1 levels were observed to be equal was in the two pairs of sisters derived from the left-right divisions of Ea and Ep (Figure 2.3 I, J). We also observed cortical GFP staining in cells with low GFP::SYS-1 (Figure 2.3 E, G). However, this asymmetric cortical staining is not consistently detected with our fixation protocol and therefore was not analyzed further in this study.

GFP::SYS-1 is expressed in all lineages in early *telIs98(P_{pie-1}gfp::sys-1)* embryos. The anterior blastomere, AB, of a 2-cell embryo undergoes first a dorsal-ventral then left-right divisions before dividing anteroposteriorly five times. We observed GFP::SYS-1 asymmetry in all AB descendants that derived from A-P divisions that we could identify, including those generating 8, 16, and 32 AB cells (will be referred to as AB8, AB16, and AB32 cells). This reiterated reciprocal asymmetry of nuclear POP-1 and GFP::SYS-1

levels suggests that SYS-1 functions as a coactivator for POP-1 in the posterior cell following multiple A-P divisions in multiple lineages.

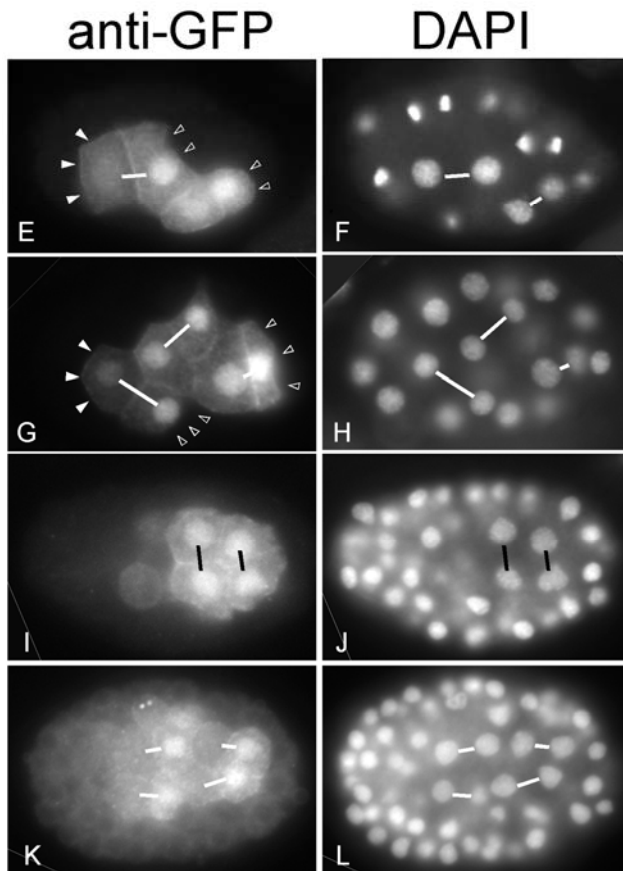
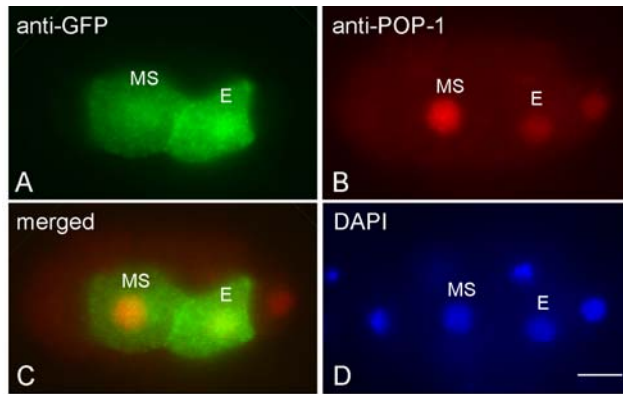


Figure 2.3. Reciprocal nuclear asymmetry of GFP::SYS-1 and POP-1 between A-P sisters.

Immunofluorescence micrographs of *teEx321* embryos at 1MS/1E stage stained with anti-GFP antibody (a), anti-POP-1 mABRL2 (b), and DAPI (c) to visualize nuclei. (d) Merged image. Anti-GFP (left) and corresponding DAPI (right) stainings at 2E stage (e-h), 4E stage (i,j) and 8E stage (k,l) of embryogenesis. White lines connect nuclei of sister cells born from A-P divisions whereas black lines connect nuclei born from left-right divisions. The cortical GFP signal appeared asymmetric, which was observed at the anterior cortex of anterior cells (Solid arrowheads) but not at the posterior cortex of the posterior sisters (open arrowheads). Bar: 10 μ m.

Differential regulation of SYS-1 and POP-1 A-P asymmetry by the Wnt and MAPK pathways

We asked whether GFP::SYS-1 asymmetry is regulated by the Wnt and/or MAPK pathways by depleting a component in either pathway via genetic mutation or RNAi. We first assayed the effect in the EMS lineage by scoring in MSa/MSp and Ea/Ep pairs of sisters as stronger GFP::SYS-1 staining at this stage permitted easier scoring (Figure 2.3 E, F; Figure 2.4B, a-c). GFP::SYS-1 asymmetry between MSa/MSp and Ea/Ep pairs of sisters was abolished or defective in most *mom-2(or42)*, *mom-5(RNAi)*, *mom-5(or57)*, or *apr-1(RNAi)* embryos (Figure 2.4A, a-d; 2.4B, d-f; Table 2.2). Double staining with anti-POP-1 antibody also showed defects in nuclear POP-1 asymmetry, although the POP-1 asymmetry defect tended to be less penetrant with subtle asymmetry still often observed between sister blastomeres in these mutant embryos (Table 2.2). Both GFP::SYS-1 and nuclear POP-1 asymmetries were restored in these mutants following the 2E/4MS stage. Conversely, in *mom-4(ne19)*, *lit-1(RNAi)*, *lit-1(t1512)*, or *wrm-1(RNAi)* embryos, we observed no or very little defect in GFP::SYS-1 asymmetry, despite a complete abolishment of POP-1 asymmetry (Figure 2.4A, e-h; 2.4B, g-i; Table 2.2).

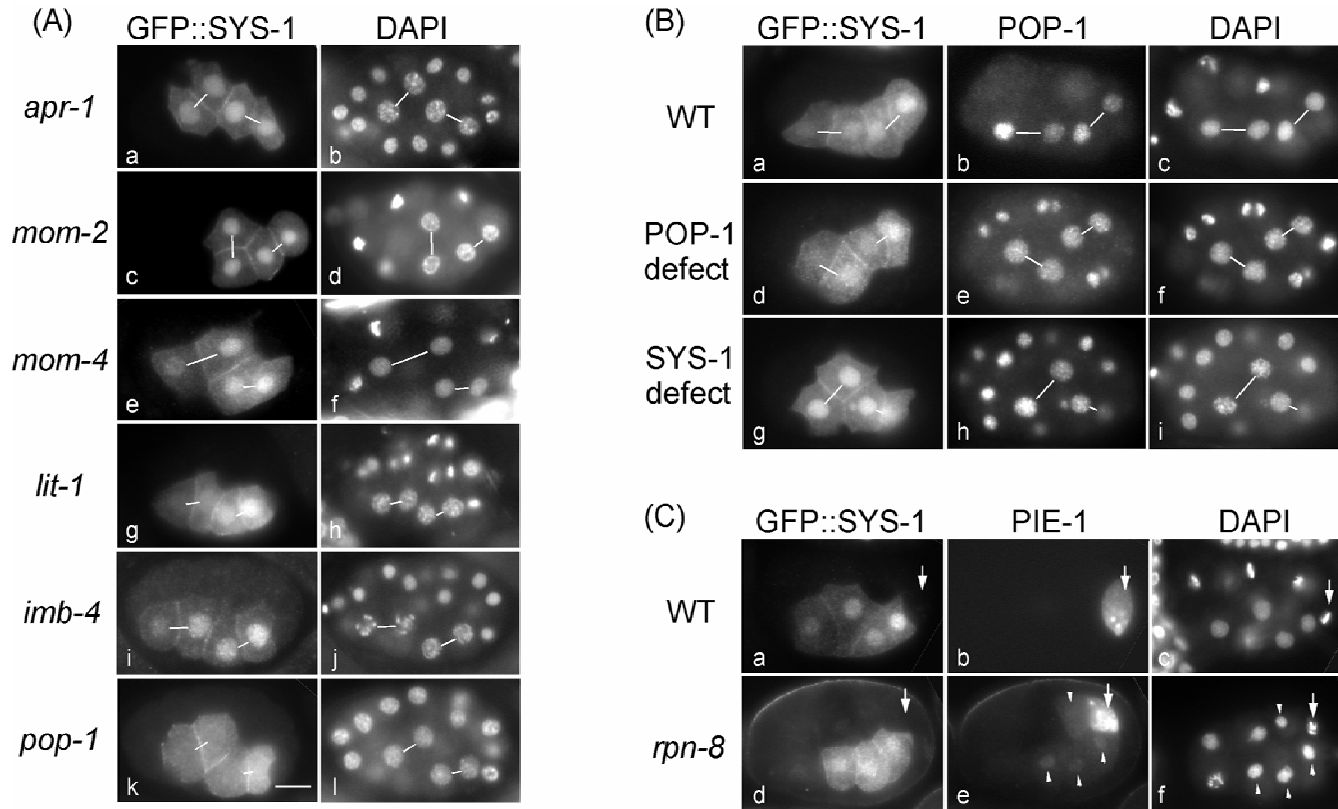


Figure 2.4. GFP::SYS-1 nuclear asymmetry between A-P sisters is Wnt signal- and proteasome-dependent. All embryos shown are at the 2E/2MS stage, with lines connecting the MSa/MSp and Ea/Ep A-P sisters. (A) Immunofluorescence micrographs of GFP::SYS-1 in various mutant backgrounds (indicated to the left). Left column: anti-GFP. Right column: DAPI. (B) Independent regulation of GFP::SYS-1 (a, d, g) and POP-1 (b, e, h) asymmetry. (a-c) wildtype (d-f) *mom-5(or57)*; GFP::SYS-1 symmetric, POP-1 asymmetric. (g-i) *wrm-1(RNAi)*: GFP::SYS-1 asymmetric, POP-1 symmetric. (C) wildtype (a-c) and *rpn-8(RNAi)* embryo (d-f) double stained with antibodies to GFP and PIE-1. Arrow: germline precursor. Arrowheads: somatic nuclei that stain weakly with the PIE-1 antibody. Bar: 10 μ m.

We also scored the effect of *wrm-1*, *mom-2*, and *mom-5* depletion on GFP::SYS-1 in AB8 and AB16 cells (Table 2.2). In both *mom-2(or42)* and *mom-5(or57)* mutants (n=5 and 6 respectively), we observed a 100% loss of GFP::SYS-1 asymmetry in AB8 cells. This asymmetry defect decreased by the AB16 and AB32 stages to 17% and 0% (n=12) for *mom-2(or42)*, and 65% and 11% (n=17) for *mom-5(or57)* embryos, respectively. The defect for nuclear POP-1 asymmetry is less penetrant at the same stages (Table 2.2). In *wrm-1(RNAi)* embryos, despite a fully penetrant defect for nuclear POP-1 asymmetry, we detected no loss of GFP::SYS-1 asymmetry in AB8, AB16, or AB32 cells (n=6, 10 and 3 respectively). Taken together, our results demonstrate that genes regulating endoderm specification contribute differentially to SYS-1 and POP-1 asymmetry. GFP::SYS-1 asymmetry is regulated by *mom-2*, *mom-5*, and *apr-1*, but not *mom-4*, *wrm-1*, or *lit-1*. On the contrary, *mom-4*, *wrm-1*, and *lit-1* influence nuclear POP-1 asymmetry much more than *mom-2*, *mom-5*, and *apr-1*.

Depletion of *pop-1* (*zu189* or *RNAi*) resulted in a decrease in GFP::SYS-1 nuclear staining and a concomitant increase in cytoplasmic signal in all expressing cells, without abolishing the differential GFP levels between A-P sisters (Figure 2.4A k, l; data not shown), suggesting that POP-1 regulates nuclear localization or nuclear retention of SYS-1.

Table 2.2. Defects for POP-1 and GFP::SYS-1 asymmetry in various genetic backgrounds

	MSa/MSp		Ea/Ep		AB8		AB16		AB32	
	SYS-1 ^a	POP-1	SYS-1	POP-1	SYS-1	POP-1	SYS-1	POP-1	SYS-1	POP-1
Wildtype N2	1 (132) ^b	5 (131)	1 (79)	9 (75)	0 (7)	0 (7)	0 (18)	0 (18)	0 (6)	0 (6)
<i>mom-2(or42)</i>	100 (26)	100 ^c (26)	79 (33)	76 (33)	100 (5)	40 (5)	17 (12)	0 (12)	0 (2)	0 (2)
<i>mom-5(or57)</i>	100 (6)	86 (7)	100 (8)	87 (8)	100 (6)	88 (6)	65 (17)	59 (17)	11 (9)	11 (9)
<i>apr-1(RNAi)</i>	100 (15)	100 (14)	93 (14)	87 (15)						
<i>lit-1(t1512)</i>	0 (19)	100 (19)	22 (9)	100 (9)						
<i>mom-4(ne19)</i>	0 (16)	100 (16)	0 (19)	100 (19)						
<i>wrm-1(RNAi)</i>	0 (37)	100 (37)	0 (20)	100 (20)	0 (6)	100 (6)	0 (10)	100 (10)	0 (3)	100 (3)
<i>wrm-1(ne1982)</i>	11 (19) ^d	53 (19)	0 (22)	32 (22)						

^a. SYS-1 was scored by immunofluorescence using the anti-GFP antibody in *teEx321* embryos.

^b. Numbers indicate percentage of sister pairs scored with abnormal asymmetry. Numbers in parenthesis are total number of pairs scored. Abnormal asymmetry is defined as a pattern different from wildtype. Sister pairs with only subtle difference are scored as abnormal. For AB8, AB16, and AB32, abnormality was scored if some or all pairs of AB cells at that particular stage were scored as abnormal.

^c. Most pairs of sister cells scored as having abnormal POP-1 asymmetry in *mom-2*, *mom-5*, and *apr-1* embryos still have subtle POP-1 asymmetry.

^d. We observed abnormal SYS-1 asymmetry between the MSa/MSp pair in two *ne1982* embryos. One embryo has only a subtle difference between MSa and MSp whereas the other has a reversed asymmetry.

SYS-1 asymmetry is dependent on the proteasome but not on nuclear export

We have shown previously that POP-1 A-P asymmetry is dependent on nuclear export. To analyze whether nuclear export plays a similar role in regulating GFP::SYS-1 asymmetry, we individually depleted by RNAi in *teEx321(P_{med-1}gfp::sys-1)* embryos three genes including *xpo-1* (previously known as *imb-4* or *crm-1*), *ran-3*, and *ran-4*, that have been shown to function in nuclear export. All (n=8) *xpo-1(RNAi)* and 50% of *ran-3(RNAi)* and *ran-4(RNAi)* embryos (n=7 and 3 respectively) exhibit exclusively nuclear GFP::SYS-1, suggesting that these three genes regulate GFP::SYS-1 nuclear export. However, GFP::SYS-1 levels were still observed to be different between A-P sisters in embryos depleted of any of these three genes (Figure 2.4A, i, j; data not shown). This result and the cytoplasmic GFP::SYS-1 observed in *pop-1* mutant embryos suggest that neither nuclear export nor differential subcellular distribution accounts for the GFP::SYS-1 asymmetry between sisters.

GFP::SYS-1 asymmetry is affected, however, by depletion of components of the proteasome. We have depleted individually three components of the proteasome: *rpn-8*, *pas-4*, and *pbs-2* and obtained similar results in each case, namely a similar level of GFP::SYS-1 in almost all GFP-expressing blastomeres (Figure 2.4C, d; data not shown). We showed that this loss of GFP::SYS-1 asymmetry is not due to a loss of embryonic polarity in RNAi embryos. PIE-1 in wildtype embryos is localized to germ cell precursors (Figure 2.4C, a-c) (Mello et al., 1996). This germline precursor-specific localization of PIE-1 requires proper establishment of embryonic polarity and proteasome-mediated degradation of PIE-1 segregated to somatic cells (DeRenzo et al., 2003). Under the

conditions RNAi was performed, in all cases (n=6) we detected GFP::SYS-1 equal between sister blastomeres and PIE-1 primarily in the germline precursor (Figure 2.4C d-f). We also detected a small amount of PIE-1 in somatic cells, consistent with a defect in proteasome-mediated degradation in our RNAi embryos. All together, our result demonstrates that proteasome components regulate GFP::SYS-1 asymmetry.

Elevated SYS-1 expression results in an MS to E fate transformation

Approximately 50% (n=71) of GFP-positive *teEx321(P_{med-1gfp}::sys-1)* embryos either fail to hatch or die as L1 larvae. Immunofluorescence analyses detected no embryos lacking gut (n>1,000). Instead, we observed a small number of embryos (3%, n>500) with approximately twice the number of intestinal cells and missing the posterior portion of pharynx (Figure 2.5), a phenocopy of *pop-1(zul89)* mutant embryos (Lin et al., 1995) and consistent with an MS to E fate transformation. The actual penetrance of this phenocopy would be higher because only approximately 50% of the embryos scored would be transgenic embryos.

This *pop-1* phenocopy was greatly enhanced with a mild reduction of *pop-1* by RNAi. Under mild *pop-1* RNAi conditions in which two control strains, N2 and *telIs18(P_{sdz-23gfp}::H2B)* (Shetty et al., 2005), produced only 13% (n=82) and 29% (n=104) *pop-1*-like embryos, respectively, *teEx321(P_{med-1gfp}::sys-1)* GFP-positive embryos produced 75% (n=49). As elevated SYS-1 levels result in an MS to E fate transformation, this result strongly suggests that the SYS-1 level is limiting with respect to that of POP-1 in MS, precluding MS from making endoderm.

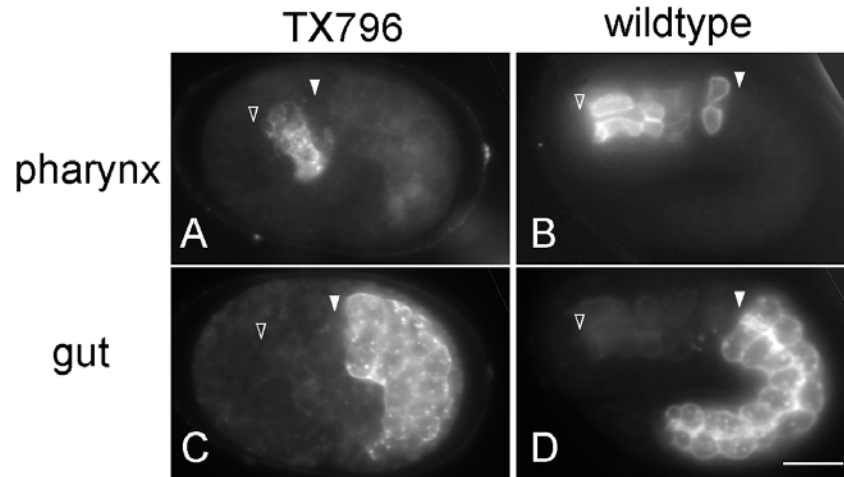


Figure 2.5. Increased level of SYS-1 causes extra gut at the expense of pharynx.

Immunofluorescence of *teEx321* (A, C) or wildtype (B, D) embryos stained with 3NB12 for pharynx (A, B), and ICB4 for gut (C, D). The anterior and posterior tips of the pharynx are indicated by an open and closed arrowhead, respectively. While only a small percentage of *teEx321* embryos exhibit this phenotype, the penetrance increases with mild *pop-1(RNAi)*. Bar: 10 μ m.

The SYS-1-to-POP-1 ratio is also critical for other A-P divisions

To ask whether the SYS-1-to-POP-1 ratio also regulates multiple, reiterating, asymmetric A-P divisions, we examined cell fate changes at other A-P divisions within the MS and E lineages.

The MS lineage

The *C. elegans* pharynx consists of eight muscle types (pm1 through pm8) arranged as eight consecutive rings with three cells in each ring (Figure 2.6 A) (Albertson and Thomson, 1976). An antibody, 3NB12, recognizes pm3, pm4, pm5 and pm7 cells, generating a characteristic staining pattern in wildtype pharynx with a gap in signal

between pm5 and pm7 due to the absence of pm6 cell staining (Figure 2.6 B) (Priess and Thomson, 1987).

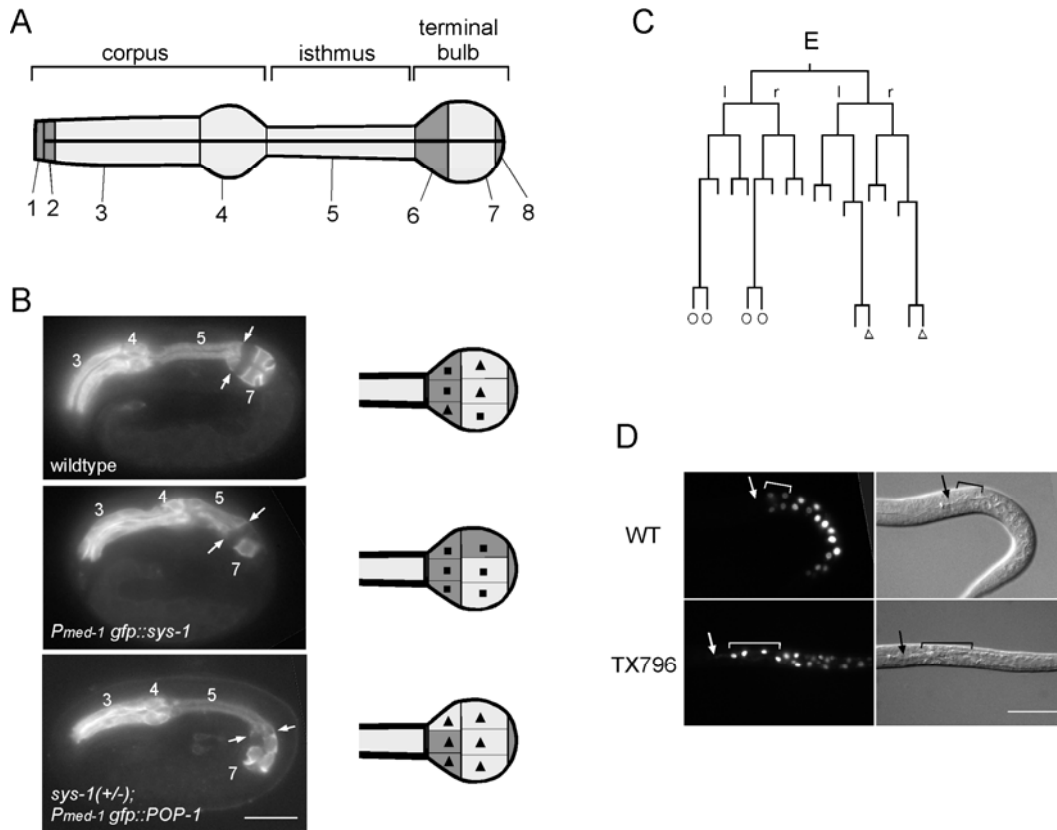


Figure 2.6. Altering the SYS-1/POP-1 ratio also affects cell fate decisions at other A-P divisions. (A) Schematic of the *C. elegans* pharynx showing corpus, isthmus, and terminal bulb, including the location of the eight pharyngeal muscle types (labeled 1 through 8). Gray indicates cells that are not stained by 3NB12. (B) Embryos derived from wildtype, *teEx321*, and *sys-1(q544/+);tel3* stained with 3NB12. Schematics to the right indicate the three pm6 and three pm7 muscle cells in wildtype and predicted cell fate changes following an A-to-P (middle) or a P-to-A (bottom) fate transformation at the division giving rise to MSa and MSp. Triangles and squares denote cells derived from the MSa and MSp lineages, respectively. Bar: 10 μm. (C) The E lineage. Horizontal lines indicate divisions whereas vertical lines are developmental time. All divisions are anterior (left)-posterior (right) except those labeled l/r. The four cells that comprise intestinal ring 1 and the two comprising ring 9 are indicated by open circles and triangles, respectively. (D) PHO-1::GFP expression in wildtype and *teEx321* larvae. Arrow: posterior end of the pharynx; Brackets: cells in the first two intestinal rings in wildtype and the corresponding region in *teEx321*. Bar: 30 μm.

All pm6 and pm7 cells, which form the anterior and posterior portions of the terminal bulb, respectively, are derived from the MS lineage and their complete lineage histories are known (Sulston et al., 1983). One of the three pm6 and two of the three pm7 pharyngeal muscle cells are derived from MSa, whereas the other two pm6 and single pm7 muscle cells are derived from MSp (Sulston et al., 1983). An MSa to MSp fate change would be predicted to result in the MSa-derived pm6 cell (**MSaapappa**) and the MSa-derived pm7 cells (**MSaaaappp** and **MSaapaapp**) adopting the fate of **MSpapappa**, **MSpaaappp** and **MSpapaapp**, respectively (Table 2.3). The net result would be a decrease in one 3NB12-positive pm7 and an increase in one 3NB12-negative pm6 cell at the terminal bulb. The same lineage calculations for an MSp to MSa fate change predicts a net gain of one 3NB12-positive pm7 muscle cell at the expense of one 3NB12-negative pm6 muscle cell (Figure 2.6 B and Table 2.3).

Table 2.3. Predicted changes of cell fates if an A-P cell fate change for MSa and MSp.

	wildtype	MSa → MSp ^a	MSp → MSa ^b
pm6	MSpaaappp	-- ^c	MSaaaappp (pm7) ***
	MSaapappa	MSpapappa (pm6)	--
	MSpapappa	--	MSaapappa (pm6)
pm7	MSaaaappp	MSpaaappp (pm6) ***	--
	MSaapaapp	MSpapaapp (pm7)	--
	MSpapaapp	--	MSaapaapp (pm7)

^a. predicted change in cell fate if an A to P cell fate change occurs at the division giving rise to MSa and MSp.

^b. predicted change in cell fate if a P to A cell fate change occurs at the division giving rise to MSa and MSp.

^c. --: not affected by cell fate change

***: pharyngeal muscle type change

Although presenting a recognizable corpus, isthmus, and terminal bulb, approximately 10% (n=1000) of the *teEx321(P_{med-igfp}::sys-1)* embryos exhibited a decrease in the number of pm7 muscle cells upon 3NB12 staining (Figure 2.6 B). Instead of the three pm7 cells always observed in wildtype embryos, we often observed only two pm7 cells in *teEx321* embryos. On the contrary, ~10% of embryos and larvae derived from *sys-1(q544/+);teIs3(P_{med-igfp}::pop-1)* had four 3NB12-positive cells and a smaller than wildtype 3NB12-negative zone in the terminal bulb (Figure 2.6 B). We did not observe any *teEx321* embryos with extra pm7 muscle cells or progeny of *sys-1(q544/+);teIs3* with missing pm7 muscle cells (n>1,000). Because we are unable to definitively identify pm6 cells in these transgenic animals, we cannot be certain that an observed extra pm7 cell is at the expense of a pm6 cell or that a missing pm7 cell has become a pm6 cell. However, the phenotype observed for *teEx321* is consistent with the lineage prediction for an MSa-to-MSp fate change whereas the *sys-1(q544/+);teIs3* phenotype is consistent with the predicted MSp-to-MSa fate change.

The E lineage

In the E lineage, we also observed *teEx321(P_{med-igfp}::sys-1)* embryos exhibiting defects in cells born as anterior daughters from successive A-P divisions and embryos derived from *sys-1(q544/+);teIs3(P_{med-igfp}::pop-1)* exhibiting defects in cells born as posterior daughters from successive divisions. The entire intestine is clonally-derived from the E blastomere and is composed of 20 cells in 9 sequential rings, 4 cells in the first ring and 2 cells in each of the following 8 rings (Figure 2.6 C) (Sulston et al., 1983). The four cells that comprise ring 1 are two pairs of sister cells (Ealaaa Ealaap, Earaaa,

and Earap), each of which derives from the most anterior lineage of Eal and Ear, respectively (Figure 2.6 C). These four cells would be the most sensitive to any A to P fate transformation within the E lineage. Because the E lineage is clonally restricted to the intestinal fate, all A to P or P to A fate transformations within the E lineage should still give rise to intestinal cells, making the tracking of cell fate changes complicated. Fortunately, intestinal cells derived from different branches of the E lineage exhibit different properties (Fukushige et al., 2005; Schroeder and McGhee, 1998). For example, the gut phosphoesterase PHO-1, which is expressed strongly in all other gut cells, is expressed weakly in the six cells that make up the first two intestinal rings (Figure 2.6 D) (Fukushige et al., 2005). We observed that 100% (n=22) of *teEx321*(*P_{med-igfp}::sys-1*) GFP-positive progeny exhibited bright PHO-1 reporter GFP fluorescence in at least some of the four anterior-most intestinal cells, compared to 0% (n=10) of wildtype embryos (Figure 2.6 D). The first gut ring is also responsible for attaching intestine to the pharyngeal/intestinal valve cells. We observed approximately 13% (n=71) of *teEx321* GFP-positive progeny with intestine unattached to the pharynx (not shown). These results are consistent with lineage defects among the cells comprising ring 1. In addition, the pm8 muscle cell, which attaches the pharynx to the pharyngeal/intestinal valve cells, is derived from MSa (Sulston et al., 1983). pm8 lineage defects, due to an A to P transformation resulting from elevated SYS-1 levels, could also contribute to the unattached anterior intestine phenotype observed in *teEx321* progeny.

The most posterior gut ring, which attaches intestine to the intestinal/rectal valve cells, consists of two cells, Eplppp and Eprppp, each of which is born as the most

posterior lineage of Epl and Epr, respectively (Figure 2.6 C) (Sulston et al., 1983), and would be the most sensitive to any P to A fate transformation within the E lineage. In 23% (n=105) of larvae derived from *sys-1(q544/+);teIs3(P_{med-1gfp}::pop-1)*, the posterior of the intestine is not attached to the rectum (not shown). No defect in intestinal attachment to pharynx was observed (n>1,000). Similarly, no defect in intestinal attachment to rectum was observed in *teEx321(P_{med-1gfp}::sys-1)* embryos (n>1,000). Using the intestinal antibody ICB4 (Kemphues et al., 1988), we observed that although the majority of embryos derived from *teEx321* and *sys-1(q544/+);teIs3* had a disorganized intestine, they had twenty or close to twenty intestinal cells (n=50).

Together, our results show that a high SYS-1-to-POP-1 ratio inhibits the anterior cell fate whereas a low ratio inhibits the posterior fate in multiple A-P divisions during *C. elegans* embryogenesis.

DISCUSSION

We show in this study that the β -catenin SYS-1 functions as a coactivator for TCF/POP-1 in activating Wnt/MAPK-responsive genes in the endoderm precursor. More importantly, we show that the SYS-1-to-POP-1 ratio appears critical for both the anterior and posterior cell fates in multiple asymmetric divisions regulated by Wnt/MAPK signaling: a high ratio drives the posterior cell fate whereas a low ratio drives the anterior cell fate. In posterior cells, GFP::SYS-1 levels are elevated while nuclear POP-1 levels are lowered.

Our results demonstrate that the MOM-2/MOM-5 and MOM-4/WRM-1/LIT-1 pathways, by virtue of their differential effects on SYS-1 and POP-1 nuclear levels, mutually reinforce an increase in the SYS-1-to-POP-1 ratio in posterior cells, thereby robustly promoting A-P cell fate asymmetries (Figure 2.7). As *C. elegans* embryogenesis consists primarily of a series of binary cell fate specifications at A-P divisions, the reiteration of this mechanism may drive much of the invariant lineage.

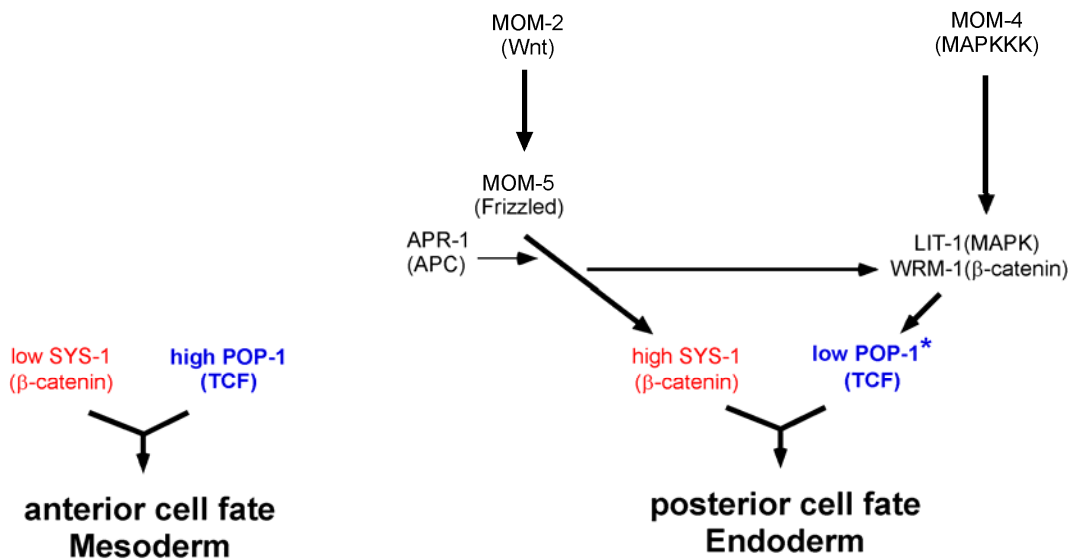


Figure 2.7. Pathways regulating the reciprocal asymmetry of POP-1 and SYS-1.

Schematic of the two pathways regulating nuclear SYS-1 and POP-1 levels: SYS-1 levels are elevated by the MOM-2/MOM-5 pathway and nuclear POP-1 levels are decreased by the MOM-4/WRM-1/LIT-1 pathway with input from the MOM-2/MOM-5 pathway. Each pathway contributes to an increase of the SYS-1-to-POP-1 ratio which drives the posterior cell fate. Asterisk: denotes that POP-1 activity could be regulated via post-translational modification.

SYS-1 functions as a limiting coactivator for POP-1 in the E blastomere

Nuclear POP-1 asymmetry has been observed in several asymmetric A-P sisters whose differential cell fates require MAPK and/or Wnt signaling (Herman, 2001; Lin et al., 1998;

Lin et al., 1995; Siegfried et al., 2004). Signaling and POP-1 activation are required for the posterior cell fate and in all cases these cells have a lower level of nuclear POP-1 (Herman, 2001; Maduro et al., 2005a; Shetty et al., 2005; Siegfried and Kimble, 2002). This requirement for a lowered level of nuclear POP-1 in cells in which POP-1 functions as an activator seems counter-intuitive. One plausible model invoked a co-activator for POP-1 whose amount is limiting with respect to POP-1 (Herman, 2001; Kidd et al., 2005; Shetty et al., 2005; Siegfried et al., 2004). In cells with high nuclear POP-1 levels, only a small portion of POP-1 would be bound to the limiting co-activator, with the majority free to bind to co-repressor(s) resulting in transcriptional repression of target genes. In addition, POP-1 could be qualitatively different between asymmetric sisters, also promoting preferential interaction of POP-1 with co-activator in Wnt/MAPK responsive cells.

We show here that β -catenin/SYS-1, like TCF/POP-1, is important for endoderm fate. Our data argue that the SYS-1-to-POP-1 ratio, more so than absolute SYS-1 and POP-1 levels, is critical in E blastomere fate specification. A high SYS-1-to-POP-1 ratio promotes, whereas a low SYS-1-to-POP-1 ratio antagonizes, E fate. Most convincingly demonstrated, simply increasing SYS-1 levels by introducing extra copies of *gfp::sys-1* was sufficient to transform MS blastomere fate to endoderm, or E fate. These results strongly support the model that SYS-1 levels are limiting with respect to POP-1 levels in the specification of endoderm fate.

Activation of Wnt target genes by coordinate regulation of β -catenin/SYS-1 and TCF/POP-1

A high SYS-1-to-POP-1 ratio can be achieved by decreasing the level of POP-1, increasing the level of SYS-1, or both. Our results demonstrate that GFP::SYS-1 and POP-1 levels are simultaneously regulated in opposite directions. While the MOM-4/WRM-1/LIT-1 pathway plays the major role in lowering nuclear POP-1 levels, GFP::SYS-1 asymmetry is regulated primarily by the MOM-2/MOM-5 pathway, with very little or no input from *wrm-1*, *lit-1*, or *mom-4*. These observations offer an explanation for the synergy observed by us and others between mutations from these two groups of genes: while *mom-2*, *mom-5*, and *mom-4* mutations alone have an incompletely penetrant gutless phenotype, *mom-2;mom-4* and *mom-5;mom-4* embryos have a 100% gutless phenotype (Rocheleau et al., 1997; Rocheleau et al., 1999; Thorpe et al., 1997). Defects in altering the level of either SYS-1 or POP-1 alone would not result in as dramatic a change of the SYS-1-to-POP-1 ratio as defects in altering both. Consistent with our results, Phillips et al have recently shown that SYS-1 asymmetry in somatic gonad precursors is MOM-5-dependent, but LIT-1- and WRM-1-independent (Phillips et al., 2007). *lit-1* or *wrm-1* mutants, unlike *mom-4* mutants, produce 100% gutless embryos. It is possible that the LIT-1/WRM-1 kinase regulates POP-1 transcriptional activity, in addition to its role in regulating POP-1 nuclear levels. Supporting this possibility, phosphorylation of TCF proteins by NLK has been reported to inhibit DNA binding activity of TCFs (Ishitani et al., 2003) or enhance transcription of Wnt targets (Thorpe and Moon, 2004). We propose that these two pathways specify endoderm fate by collaborating to very efficiently elevate the SYS-1-to-POP-1 ratio in the E blastomere, and furthermore that this redundancy helps to insulate a genetic system used in multiple A-P divisions during *C. elegans* embryogenesis from deleterious mutations.

Studies in *Drosophila* also suggest that the β -catenin/TCF ratio plays an important role in Wnt signaling. *wingless* and *armadillo* mutant phenotypes can be partially suppressed by a reduction in dTCF activity, whereas the phenotype of a weak *wingless* allele is enhanced by overexpression of wildtype dTCF (Cavallo et al., 1998). It appears therefore that lower levels of dTCF, or higher levels of ARM, analogous to what we show here, contribute to Wnt signal strength. However, while regulation of β -catenin levels by Wnt is well documented in vertebrates and *Drosophila*, possible regulation of TCF levels by the MAPK pathway is less well documented. A recent report that the NLK kinase promotes TCF degradation by facilitating its interaction with an E3 ligase (Yamada et al., 2006), suggests that simultaneous regulation of β -catenin and TCF levels in opposite directions may not be unique to the *C. elegans* embryo.

The two β -catenins, WRM-1 and SYS-1

It has been suggested that the cellular functions carried out by a single β -catenin in vertebrates and flies are separated to multiple β -catenins in worms (Korswagen et al., 2000). β -catenin has been shown to undergo importin-independent nuclear import, perhaps by directly binding to the nuclear pore complex through its armadillo repeats, which resemble the heat repeats of importin (Fagotto et al., 1998). β -catenin nuclear localization has been shown to then facilitate nuclear import of LEF1 and TCF4 by direct binding (Asally and Yoneda, 2005; Hsu et al., 2006). It is possible that WRM-1 is a

specialized β -catenin that functions as a nuclear import receptor for LIT-1 or additional factors in response to Wnt/MAPK signaling during *C. elegans* embryogenesis.

It is interesting that two β -catenins in *C. elegans*, SYS-1 and WRM-1, both function in endoderm precursor specification, exhibit an elevated level in the posterior cell of all A-P divisions, function in elevating the SYS-1-to-POP-1 ratio, have seemingly very different biological activities and are regulated through different mechanisms. Our current data is consistent with SYS-1 A-P asymmetry being regulated by differential degradation between sister cells. This resembles the down-regulation of vertebrate β -catenins in the absence of Wnt signaling (Krieghoff et al., 2006), but different from WRM-1, whose asymmetric levels are dependent on IMB-4-mediated nuclear export (Nakamura et al., 2005). Recent work has shown that cortically localized WRM-1 represses its nuclear accumulation (Mizumoto and Sawa, 2007). It is interesting to note that GFP::SYS-1 also localized to centrosomes and differentially localized to cortex. However, the functional significance, if any, of centrosomal and cortical SYS-1 requires further investigation.

Pathways regulating endoderm

Analyses of the expression of endoderm specifying genes, *end-1* and *end-3*, demonstrated that both the SKN-1/MED-1 and the POP-1 (and now SYS-1) pathways contribute to the high level expression of these endoderm genes (Maduro et al., 2005a; Shetty et al., 2005). We propose that transcriptional activation of *end-1* and *end-3* by either the SKN-1/MED-1 or POP-1/SYS-1 pathway alone is sufficient to specify endoderm. In MS, where the

SYS-1-to-POP-1 ratio is low, POP-1, in conjunction with co-repressor(s), overrides transcriptional activation by SKN-1/MED-1, resulting in no *end-1* or *end-3* expression and a lack of endoderm fate. In E, a high SYS-1-to-POP-1 ratio allows POP-1 to function as an activator, further elevating *end-1* and *end-3* transcription. Embryos with reduced expression of *end-1* and *end-3* as a result of *skn-1* depletion would be expected to be sensitive to alterations in the SYS-1-to-POP-1 ratio, consistent with the observed synergy between *skn-1* and *mom-2*, *mom-4*, or *mom-5* mutations (Thorpe et al., 1997), and the suppression of *skn-1(zu67)* by *teIs98(P_{pie-1gfp::sys-1})* (this study).

SYS-1 and POP-1 function in MS

In addition to specification of the endoderm precursor, POP-1 is also required for MS fate specification. The role of POP-1 in MS specification is not, however, simply repression of endoderm fate. In embryos in which the endoderm-specifying genes *end-1* and *end-3*, as well as *pop-1*, are deleted, the MS blastomere generates neither pharynx nor intestine (Maduro et al., 2005a; Zhu et al., 1997). This indicates that POP-1 plays an important and direct role in specifying MS fate, independent of its function in endoderm gene repression. We reported previously that in a large percentage of embryos with artificially elevated nuclear POP-1 levels in E, E also generates neither pharynx nor intestine (Lo et al., 2004). Therefore, a high level of nuclear POP-1 in E, while sufficient to repress endoderm, is not sufficient to promote mesoderm. A low level (but not complete absence) of SYS-1 and a high level of nuclear POP-1 would appear to be important for the activation of genes specifying the MS blastomere.

SYS-1 and POP-1 function in reiterated A-P cell fate decisions

We show that in multiple A-P divisions, a low SYS-1-to-POP-1 ratio promotes the anterior cell fate whereas a high SYS-1-to-POP-1 ratio promotes the posterior fate. This suggests that the SYS-1-to-POP-1 ratio may have a broad role in controlling stepwise A-P binary decisions throughout *C. elegans* embryogenesis. One argument against this possibility is that we did not observe the collapse of the affected lineage to either the anterior-most or posterior-most cell fate by overexpressing or removing SYS-1 or POP-1. We anticipated that all transgenic strains isolated expressing altered levels of SYS-1 and/or POP-1 would have a non-fully penetrant defect in all divisions in which these proteins might function. Full collapse of affected lineages would be expected to be 100% lethal and therefore not able to be isolated as a strain. In addition, for transgenes utilizing the *med-1* promoter to drive expression in the E and MS lineages, transcription only occurs early in the lineage (Maduro et al., 2001; Robertson et al., 2004). Therefore there is expected to be a progressive decrease in GFP::SYS-1 levels and a less severely altered SYS-1/POP-1 ratio as the embryo develops. It is also possible that the SYS-1/POP-1 ratio might regulate only a subset of cell divisions, despite exhibiting asymmetric levels in all A-P divisions.

Although asymmetric nuclear POP-1 levels have been observed in all A-P sisters examined, it has been shown that the asymmetry in later embryos (after the AB8 stage) is independent of Wnt/MOM-2 or prior contact with signaling cells (Park and Priess, 2003). POP-1 nuclear asymmetry in later embryos does require LIT-1, WRM-1, and MOM-4 and, in isolated blastomeres that have no prior contact with signaling cells, also requires

Frizzled/MOM-5 (Meneghini et al., 1999; Park and Priess, 2003; Rocheleau et al., 1997; Rocheleau et al., 1999). However, it remains unclear what initiates the later POP-1 asymmetry and the mechanism by which it is maintained through successive A-P divisions. What regulates SYS-1 asymmetry in later embryos is even more unclear as we did not observe a defect in later asymmetry in any mutant examined. Future studies involving isolated blastomeres should help resolve the regulation of SYS-1 asymmetry in later embryos.

MATERIALS AND METHODS

Strains

N2 was used as the wildtype strain. Genetic markers: LGI, *pop-1(zu189)*, *dpy-5(e61)*, *mom-5(or57)*, *mom-4(ne19)*, *sys-1(q544)*, *fog-3(q520)*, *teIs3(P_{med-1}gfp::pop-1)*, *hT1(I;V)*, *szT1(I;X)*; LGII, *rol-1(e91)*, *mom-3(or78)*, *mnC1*; LGIII, *unc-119(ed3)*, *lit-1(t1512)*, *lit-1(t1534)*, *unc32(e189)*; LGIV, *teIs46(P_{end-1}gfp::H2B)*; LGV, *mom-2(or42)*, *DnT1(IV;V)*, *teIs18(P_{sdz-23}gfp::H2B)*; LGX, *mom-1(or10)*, *unc-6(n102)*. Strains: TX796 *teEx321[P_{med-1}gfp::sys-1]*. TX585 *teIs18[P_{sdz-23}gfp::H2B]* *V*. TX691 *teIs46[P_{end-1}gfp::H2B]* *IV* (Shetty et al., 2005). TX932 *sys-1(q544)/fog-3(q520)* *I*; *teIs3[P_{med-1}gfp::pop-1]* *V* (Miskowski et al., 2001). TX964 *teIs98[P_{pie-1}gfp::sys-1]*. JM139 [*P_{pho-1} NLS::gfp::H2B*] (a gift from J. McGhee and J. Yan). *teIs98* was generated by microparticle bombardment (Praitis et al., 2001). All other strains were obtained from the Caenorhabditis Genetics Center (CGC).

RNA interference

sys-1 RNAi was performed by feeding L3 larvae with RNAi bacteria followed by injection. We obtained 3-4% gutless embryos upon *sys-1(RNAi)* into JK2761 but not wildtype N2. RNAi were performed by injection for *xpo-1*, *skn-1*, *med-1/med-2*, *apr-1*, *lit-1*, and *mom-5* (Rogers et al., 2002) and by feeding for *wrm-1*, *pop-1*, *skn-1*, *rpn-8*, *pas-4*, *pbs-2*, *ran-3*, and *ran-4* (Timmons and Fire, 1998). RNAi by feeding for each of the genes listed here resulted in near 100% dead embryos. For experiments in which *pop-1* was mildly depleted, *pop-1* feeding RNAi bacteria were diluted with HT115 bacteria. Embryos laid from 16 to 30 hours after injection or 48-60 hours after feeding were collected and either allowed to differentiate for 12 more hours, a period long enough for wildtype control embryos to hatch, or processed for imaging.

Analysis of embryos and imaging

Expression of Wnt target genes upon *sys-1* depletion was analyzed as described previously (Shetty et al., 2005). Embryos were collected from *mom* mutant or RNAi hermaphrodites, and either assayed for GFP and scored later for gut formation, or fixed for immunofluorescence. *teEx321* was crossed into JM139 hermaphrodites. Embryos were collected, and assayed first for GFP::SYS-1 in early embryos, then PHO-1 reporter GFP in the newly hatched larvae.

GFP::SYS-1 was analyzed both by imaging of live embryos and immunofluorescence using anti-GFP (Invitrogen) and anti-POP-1 antibodies (Lin et al., 1998). Each photograph was collected as sequential images along the Z-axis with 1.5

microns between adjacent images for a total of approximately 16 slices per specimen. All images were collected as 16-bit with the raw pixel values within the linear range of the CCD camera and processed and quantified using the ImageJ program (Lo et al., 2004; Rogers et al., 2002). In embryos which GFP::SYS-1 asymmetry is abolished, we were unable to determine whether the level of GFP::SYS-1 was elevated in anterior cells, decreased in posterior cells, or both, due to the variation in expression levels of GFP::SYS-1 from embryo to embryo.

Intestinal cells were identified by their birefringent gut-specific granules under polarized optics and staining by the monoclonal antibody, ICB4 (Kemphues et al., 1988). Pharyngeal tissues were identified based on morphology using DIC and immunofluorescence using the monoclonal antibody, 3NB12 (Priess and Thomson, 1987). Pharyngeal staining was photographed as a stack along the Z-axis to facilitate the counting of pm7 cells.

CHAPTER THREE

Deletion analysis of the POP-1 C-terminus

INTRODUCTION

The C-terminal domains of TCF proteins are highly divergent

Mammalian TCFs are highly diverse due to alternative promoter usage and extensive alternative slicing. The result is that multiple isoforms are produced from each TCF gene, and each isoform contains different combinations of domains or motifs that mediate specific protein-protein or protein-DNA interactions (Arce et al., 2006). Since each isoform contains certain domains and lacks others, the isoforms show different transcriptional activities on the regulation of target genes. Interestingly, the various activities carried out by different TCF isoforms are often not detected with TOPFLASH assays, which are the most common readout for the canonical Wnt signaling pathway. Most TCF isoforms are able to activate the expression of this luciferase reporter upon co-expression of β -catenin. Therefore, the complexity of the activities of various TCF isoforms is still poorly understood.

Unlike mammalian genomes encoding multiple TCF family genes, every species of invertebrates examined to date contains only a single TCF ortholog. POP-1 is the only clear TCF protein in *C. elegans*, and it does not seem to have alternatively spliced isoforms based on ESTs available at WormBase (www.wormbase.org). The domain of POP-1 C-terminal to HMG box consists of about one third of the POP-1 protein, and its function is poorly understood. Like other known invertebrate TCF proteins, the C-

terminus of POP-1 is most similar to the “E-tail” of mammalian TCF isoforms TCF-1E and TCF-4E. At the level of primary sequence, the tail of POP-1 is poorly conserved with that of other TCF proteins except for the Cysteine-clamp (C-clamp), which is a sequence-specific DNA-binding domain which recognizes a GC element downstream of the core TCF binding motif (Atcha et al., 2007). Questions remain as to how the tail of POP-1 may contribute to the regulation of POP-1 nuclear asymmetry and function in the switch between repression and activation functions of POP-1.

The GFP::POP-1 reporter system

To study how the nuclear asymmetry and transcriptional activities of POP-1 are regulated in live *C. elegans* early embryos, we expressed GFP::POP-1_{WT} reporters under the *med-1* promoter (*P_{med-1}gfp::pop-1_{WT}*; Figure 3.1; Maduro et al., 2002). This GFP::POP-1_{WT} fusion protein recapitulates POP-1 nuclear asymmetry between A-P sisters. The expression of the *P_{med-1}gfp::pop-1_{WT}* transgene is restricted to the EMS lineage (Maduro et al., 2001). The GFP signals are first detected in the MS and E blastomeres at the eight cell stage but GFP signals are often weak. Most of my analyses were done at the 16- to 24-cell stage when there are 4 EMS descendants (EMS4) and the differences in GFP levels between A-P nuclei are easily discernible. The GFP signals persist through several subsequent cell cycles even though the mRNA of the transgene is no longer detectable (Maduro et al., 2002). Like endogenous POP-1, the asymmetry of GFP::POP-1_{WT} is affected in many mutants of the Wnt/MAPK pathway, such as *apr-1*, *mom-2*, *mom-4*, *lit-1*, and *wrm-1*. Expression of *P_{med-1}gfp::pop-1_{WT}* in *pop-1(zu189)* embryos can rescue the extra gut phenotype of *pop-1(zu189)* and restore the posterior pharynx evident by the

specialized cuticular structure of the grinder, suggesting that GFP::POP-1_{WT} is able to repress the ectopic endoderm fate derived from MS blastomere (Maduro *et al.*, 2002). These embryos have normal amount of endoderm, suggesting that the expression of GFP::POP-1_{WT} in E is does not repress the normal endoderm fate or otherwise it would have ablated all endoderm. This provides a great platform for mutational analyses of POP-1 on the asymmetry and repression function of POP-1 in E fate specification in live embryos.

An interesting feature of GFP::POP-1_{WT} is that it forms prominent punctate structures only in the anterior nuclei but not in the nuclei of their posterior sisters. Maduro *et al.* (2002) showed that these GFP puncta represent a bona fide property of POP-1, rather than a feature specific to the GFP::POP-1 transgene. Similar punctuate structures are also detected with myc-tagged POP-1 and to a lesser extent by immunostaining of endogenous POP-1. Depleting the Wnt/MAPK signaling pathways results in the appearance of puncta in posterior nuclei. Therefore, the formation of nuclear puncta may represent a qualitative difference of POP-1 between anterior and posterior nuclei. However, the molecular nature of the puncta is not known, and the functional importance is not understood.

Domains important for GFP::POP-1 asymmetry and activity

In a deletion analysis, Maduro *et al.* showed that the β -catenin binding domain, the HMG box, and the domain extending from the HMG domain to the C-terminus of POP-1 are not required for the A-P nuclear asymmetry, whereas the region between the β -catenin

binding domain and the HMG box (the putative Groucho binding domain) is critical for A-P nuclear asymmetry (Maduro *et al.*, 2002). Lo et al. (2004) further showed that POP-1 amino acids 88-130 are essential for nuclear asymmetry. GFP::POP-1 $_{\Delta 88-130}$ exhibits equal levels between A-P nuclei and lacks repression activity as it can not repress the ectopic endoderm fate and restore the MS-derived posterior pharynx when expressed in *pop-1(zu189)*.

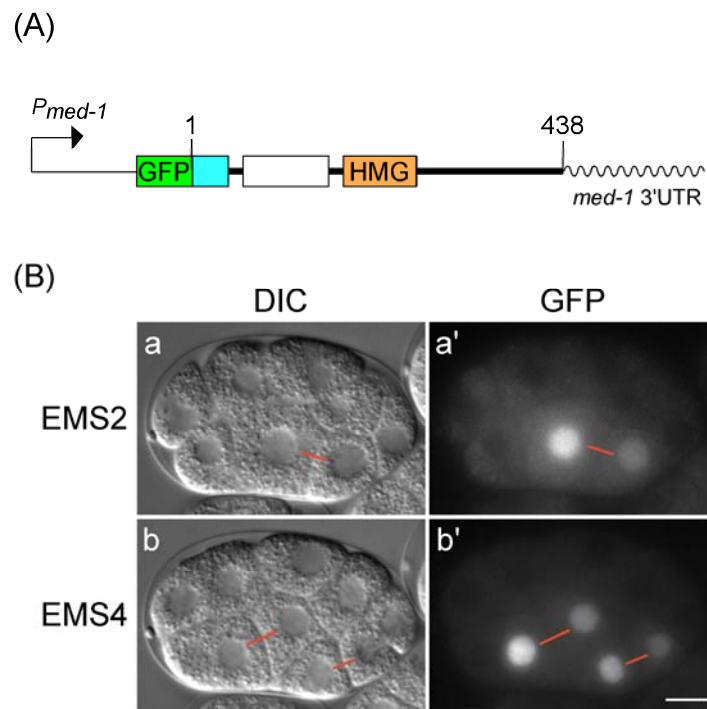


Figure 3.1. Architecture of GFP::POP-1 transgene and its expression pattern. (A)

Diagram of the GFP::POP-1_{WT} transgene expressed under the *med-1* promoter and 3'UTR. *P_{med-1}*: *med-1* promoter; green: GFP fused to the N-terminus of POP-1; cyan: β -catenin binding domain; white: repression domain; orange: HMG domain. Numbers annotate the first and last amino acids of POP-1 protein. (B) Embryos shown at stages when there are two (EMS2; a and a') or four (EMS4; b and b') cells expressing GFP. The localization of GFP::POP-1_{WT} recapitulates POP-1 nuclear asymmetry. Sister blastomeres are linked by red lines with the anterior of the embryo oriented towards the left. Note that GFP fluorescence signal is higher in the anterior nucleus of each sister blastomere pair.

There are four serines (S107/S109/S118/S127) and one threonine (T120) within this region. Lo *et al.* (2004) showed that the LIT-1/WRM-1 complex can phosphorylate at least two of the serines (S118 and S127). Mutating these four serines and the threonine either to alanines (to prevent phosphorylation) or to aspartic acids (to mimic the phosphorylated state) abolishes POP-1 asymmetry. Phosphorylation at these sites promotes the interaction between POP-1 and the 14-3-3 protein, PAR-5, and results in exportin-dependent nuclear export of POP-1 in E. Because these amino acids are important for POP-1 nuclear export, I will refer to them as the Export sites, or **Exp** sites for short. Several differences are observed between mutating the Exp sites to alanines (POP-1_{ExpA}) and mutating them to aspartic acids (POP-1_{ExpD}). First of all, GFP::POP-1_{ExpA} had GFP puncta detected in both A-P nuclei, while GFP::POP-1_{ExpD} has no detectable puncta at all. Second, GFP::POP-1_{ExpD} seems to have a slightly higher cytoplasmic signal compared to GFP::POP-1_{ExpA}. Third, GFP::POP-1_{ExpA} has strong repression activity and rescues MS fate in *pop-1(zul89)* almost completely (91%, n=32). Since it shows asymmetry, the high level of GFP::POP-1_{ExpA} even repressed the normal endoderm fate and ablated E fate in both *pop-1(zul89)* and wildtype to 62% (n=32) and 82% (n=22), respectively. Conversely, GFP::POP-1_{ExpD} only rescues MS fate in *pop-1(zul89)* to 41% (n=22) and does not cause any ablation of E fate, suggesting that mutating the Exp sites to aspartic acids weakens the repression activity.

Regarding the role POP-1 C-terminus has in POP-1 asymmetry, the only available report to date is the deletion analysis by Maduro et al. (2002). However, the most relevant construct, *Pmed-1gfp::POP-1 Δ 169-438*, deletes the HMG domain together

with the C-terminal of POP-1, resulting in mostly cytoplasmic GFP signal. Although Maduro et al. (2002) reported the GFP signal is higher in the anterior blastomere compared to its posterior sister, the conclusion may be misleading since the cytoplasmic signal would have made the analysis more difficult. Deletion analysis of domain of POP-1 C-terminal to the HMG domain is presented in this chapter.

RESULTS

The C-terminal 39 amino acids of POP-1 is required but not sufficient for GFP::POP-1 asymmetry

A previous graduate student in our lab, Miao-chia Lo, made serial deletions of POP-1 in attempt to map the *cis*-elements important for the regulation of POP-1 nuclear levels and/or activity. We found that in addition to POP-1 $_{\Delta 88-130}$, two C-terminal deletions of POP-1, POP-1 $_{\Delta 281-438}$ and POP-1 $_{\Delta 400-438}$, also exhibited no A-P asymmetry (Figure 3.2 B and C). Although all these three constructs showed equal levels between A-P nuclei, there are differences in the texture of their nuclear GFP fluorescence. GFP::POP-1_{WT} shows nuclear GFP puncta only in the anterior cells but not their posterior sisters. Both GFP::POP-1 $_{\Delta 281-438}$ (Figure 3.2.B) and GFP::POP-1 $_{\Delta 400-438}$ (Figure 3.2.C) showed puncta in both anterior and posterior nuclei, while GFP::POP-1 $_{\Delta 88-130}$ showed a homogeneous, smooth nuclear pattern (Miao-chia Lo, personal communication; data not shown). The differences in nuclear GFP puncta suggest that these transgenes are not equivalent even though they all show symmetric localization patterns.

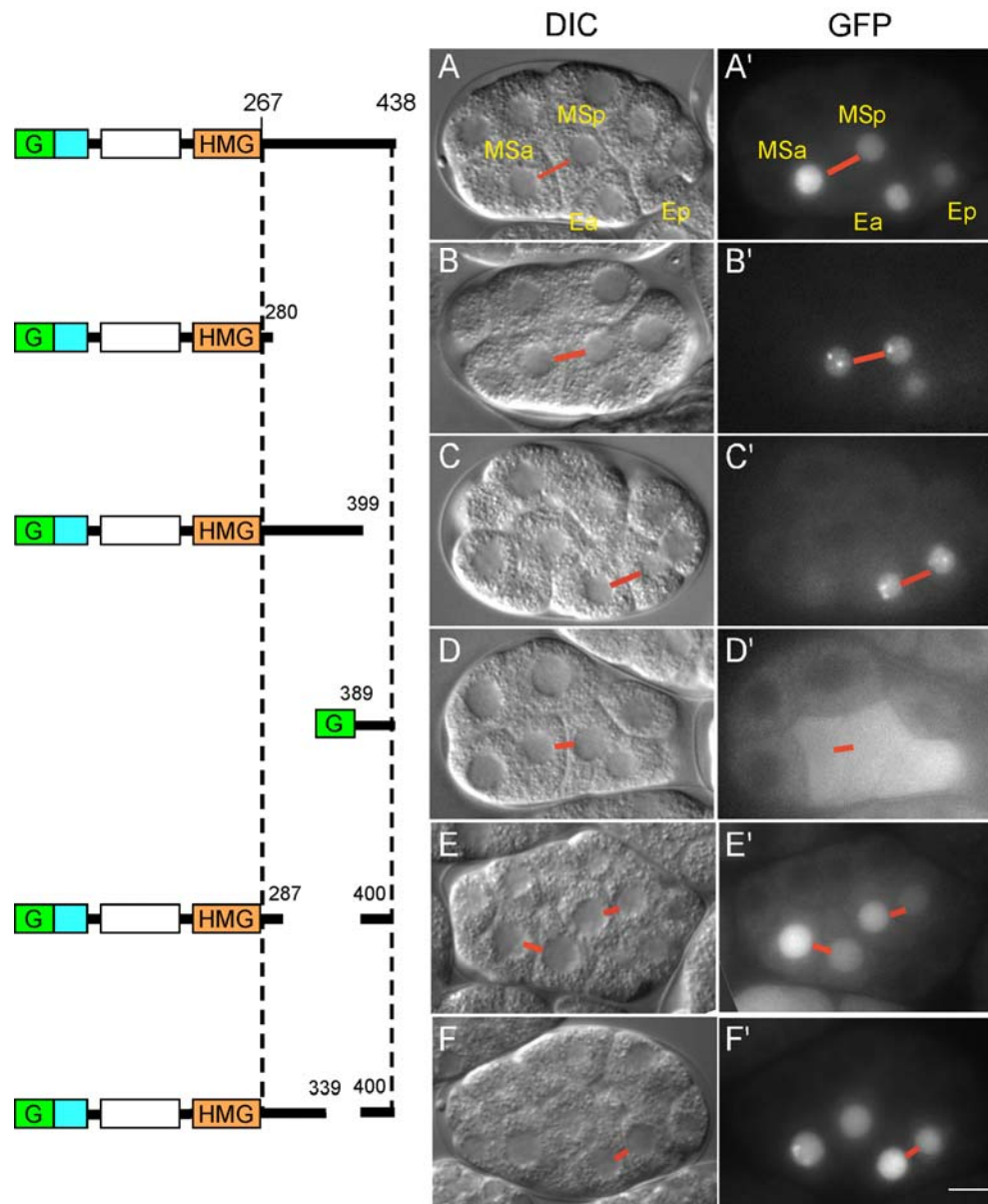


Figure 3.2. Deletion analysis of POP-1 on the domain C-terminal to the HMG box.

Schematic representation of the deletions of POP-1 and their corresponding DIC images (A-F) and GFP fluorescence (A'-F'). Embryos were shown at the stage when there were two MS and two E descendants expressing GFP. The embryos were oriented with the anterior to the left. A-P sisters that were both in focus are connected by red lines. The names of blastomeres are indicated in A and A'. G: N-terminal GFP; cyan: β -catenin binding domain; white: repression domain; HMG: high mobility group (HMG) DNA binding domain. Scale bar = 10 μ m.

To investigate if amino acids 281-399 contribute to the regulation of GFP::POP-1 nuclear asymmetry, I generated transgenic strains carrying either GFP::POP-1 $\Delta_{287-399}$ or GFP::POP-1 $\Delta_{339-399}$. Both GFP::POP-1 $\Delta_{287-399}$ and GFP::POP-1 $\Delta_{339-399}$ showed normal asymmetry in GFP levels between A-P nuclei (Figure 3.2 E and F). Therefore, POP-1 amino acids 400-438 are required for asymmetric levels of nuclear POP-1 between A-P sisters, whereas amino acids 287-399 are not. GFP::POP-1 $\Delta_{287-399}$ and GFP::POP-1 $\Delta_{339-399}$ are different in the patterns of nuclear GFP puncta. GFP::POP-1 $\Delta_{339-399}$ showed GFP puncta only in the anterior nuclei like GFP::POP-1_{WT}, but GFP::POP-1 $\Delta_{287-399}$ had no puncta at all. This result suggests that amino acids 287-338 contain motif(s) which may be important for the formation of nuclear GFP puncta. One obvious candidate is the C-clamp (POP-1 amino acids 289-312). The C-clamp has been shown to bind to double-stranded DNA. It is possible that the GFP puncta are compact DNA such as heterochromatin.

Since more analyses will be presented regarding POP-1 amino acids 400-438, to be brief, I will refer to this domain as the **PCA** domain for “POP-1 C-terminal Acidic” domain because it contains 13 acidic amino acids out of the total of 39 (Figure 3.3). I analyzed the localization of GFP::POP-1_{PCA} (amino acids 389-399 only) to test if fusing the PCA domain to GFP is sufficient to convey A-P asymmetry. GFP::POP-1_{PCA} is distributed to both the nuclear and cytoplasmic compartments and showed equal levels of GFP between A-P sister blastomeres, suggesting the PCA domain by itself is not sufficient for A-P asymmetry.

The PCA domain of POP-1 is important for the activation of endoderm genes *in vivo*

I assayed the repression function of the GFP::POP-1 fusion proteins in *pop-1(zul89)* embryos for their abilities to rescue the MS fate and restore posterior pharynx. The wildtype POP-1 was able to repress the ectopic endoderm and rescued the MS fate defect in all of the *pop-1(zul89)* embryos carrying the transgene (100%, n=31; Table 3.1) It did not repress the normal endoderm fate of E and caused no gut ablation in *pop-1(zul89)* (0%, n=31) or wildtype (0%, n>100). GFP::POP-1_{Δ281-438} rescued the MS defect in only 15% of *pop-1(zul89)* embryos (n=45; Table 3.1), suggesting it has weak repression activity. On the other hand, GFP::POP-1_{ΔPCA} not only rescued the MS defect in all *pop-1(zul89)* embryos (100%, n=28), none of these embryos made endoderm. This suggests that POP-1_{ΔPCA} behaves as a strong repressor and can not be converted to an activator in *pop-1(zul89)*. Interestingly, POP-1_{ΔPCA} only caused gut ablation in 6% of wildtype embryos carrying the transgene (Table 3.1), suggesting that although GFP::POP-1_{ΔPCA} repressed normal E fate in *pop-1(zul89)*, its presence does not interfere with the activation of E-genes by endogenous POP-1. These results suggest that amino acids 281-399 is required for repression, and the PCA domain is likely to be important for the induction of endoderm fate.





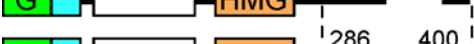
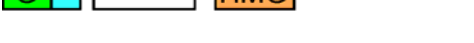


	267	438	Asy	Rescue MS in zu189	Ablate gut in zu189	Ablate gut in WT
			Y	100	0	0
			N	0	0	0
		280	N	15	4	nd
		399	N	100	100	6
		400	Y	30	0	0
		286	Y	1	0	0
			N	93	62	82
			N	41	0	nd

Table 3.1. Deletion analysis on the domain of POP-1 C-terminal to the HMG box.

Schematic representation of the deletions and relevant point mutations for comparison. G: N-terminal GFP; cyan: β -catenin binding domain; white: repression domain including the Exp sites; HMG: high mobility group DNA binding domain. Asy: GFP::POP-1 asymmetry. All numbers represent percentage of embryos expressing the transgene for ability to repress endoderm in MS in *pop-1(zu189)* (rescue MS-derived posterior pharynx), to ablate endoderm in *pop-1(zu189)*, and to ablate gut in wildtype (WT). nd: not determined.

The domain between HMG and PCA domains of POP-1 is required for the repressor activity of POP-1

When GFP::POP-1 $_{\Delta 287-399}$ was introduced into *pop-1(zu189)*, it was not able to rescue MS defect (2%, n=51; Table 3.1), suggesting that amino acids 287-399 are required for the repression activity of POP-1. On the other hand, GFP::POP-1 $_{\Delta 339-399}$ only weakly repressed endoderm fate in MS and restored posterior pharynx in 31% of *pop-1(zu189)* embryos expressing the transgene (n=48). These results suggest that, indeed, amino acids

287-399 are required for the repressor activity of POP-1. The domain required for repression can not be further narrowed down because GFP::POP-1 $_{\Delta 339-399}$ showed partial repression activity. It is possible that C-clamp of POP-1 (amino acids 289-312) plays a role in the repression function of POP-1. Deletion of the C-clamp or mutating the conserved cysteines would address this possibility.

The PCA domain is required for LIT-1/WRM-1-dependent POP-1 phosphorylation of POP-1 in HeLa cells

One possible mechanism through which the PCA domain may regulate POP-1 nuclear asymmetry is by affecting the phosphorylation of POP-1 by LIT-1 and WRM-1. I tested the effect of PCA domain deletion on LIT-1/WRM-1-dependent phosphorylation of POP-1 using a mammalian tissue culture system. It is well established that when cotransfected with WRM-1, LIT-1 kinase activity is active and can phosphorylate POP-1 in mammalian cells (Rocheleau et al., 1999). When Flag::POP-1_{WT} was transfected into HeLa cells in the absence of LIT-1/WRM-1, it migrated as a single band as detected by either the polyclonal antibody against POP-1 94I or anti-Flag antibodies in western blot analyses (Figure 3.4; data not shown). When LIT-1/WRM-1 are co-transfected, Flag::POP-1_{WT} was phosphorylated evident by the migration retardation of Flag::POP-1_{WT} on SDS-PAGE. Treating this slower migrating form of POP-1 with phosphatase reversed the migration retardation, confirming that it was caused by phosphorylation (Scott Robertson, personal communication; data not shown).

POP-1_{D9} is a conserved amino acid which is known to make a critical interaction with β -catenin. Mutating D9 to E diminishes the interaction between TCF and β -catenin, as well as between POP-1 and SYS-1 (Liu et al., 2008). Flag::POP-1_{D9E} showed migration retardation similar to that of Flag::POP-1_{WT} suggesting that the D9E mutation did not affect LIT-1/WRM-1-dependent phosphorylation of POP-1 (Figure 3.4). Flag::POP-1 _{Δ PCA} showed no change in migration upon LIT-1/WRM-1 cotransfection, i.e., Flag::POP-1 _{Δ PCA} did not have any LIT-1/WRM-1-dependent phosphorylation. Similar results were obtained in COS-7 cells (data not shown). These results show that deleting the PCA domain blocks all LIT-1/WRM-1-dependent phosphorylation of POP-1 in mammalian tissue culture systems.

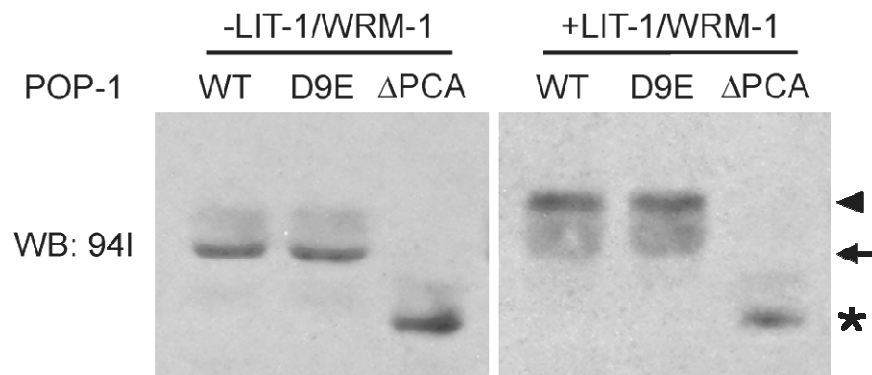


Figure 3.4. Phosphorylation of POP-1 variants in HeLa cells. Western blot detected by, 94I with HeLa cell lysates expressing variant POP-1 proteins as indicated with (right panel) or without (left panel) LIT-1/WRM-1 cotransfection. WT: wildtype; D9E: amino acid substitution at position 9 which interferes with β -catenin binding; Δ C: PCA domain deletion. All phosphorylation, which is evident by the retardation in migration, are LIT-1/WRM-1-dependent. Arrow: no LIT-1/WRM-1; arrowhead: LIT-1/WRM-1 cotransfected; *: Flag::POP-1 _{Δ PCA}. Deleting the PCA domain abolishes LIT-1/WRM-1-dependent phosphorylation.

DISCUSSION

The PCA domain affects POP-1 asymmetry by regulating LIT-1/WRM-1 phosphorylation of POP-1

The PCA domain is required for GFP::POP-1 asymmetry *in vivo*. The tissue culture experiments showed that deleting the PCA domain blocked all LIT-1/WRM-1-dependent phosphorylation of POP-1. Phosphorylation of POP-1 by LIT-1/WRM-1 at the Exp sites promotes the interaction between POP-1 and the 14-3-3 protein PAR-5, and in turn leads to the nuclear export of POP-1 and POP-1 A-P asymmetry. The lack of all LIT-1/WRM-1-dependent phosphorylation for POP-1_{ΔPCA} provides an explanation of the mechanism underlying how deleting the PCA domain results in the abolishment of GFP::POP-1 asymmetry. Although the PCA domain may control GFP::POP-1 asymmetry through mechanism(s) other than affecting LIT-1/WRM-1-dependent phosphorylation, blocking the phosphorylation at the Exp sites alone is sufficient to abolish POP-1 asymmetry.

The requirement of the PCA domain for all LIT-1/WRM-1-dependent phosphorylation may be to recruit the LIT-1/WRM-1 kinase complex. Other than direct binding with LIT-1 or WRM-1, the PCA domain may be required for a specific conformation of POP-1 which favors the interaction with LIT-1/WRM-1 complex. Or the PCA domain may bind to a scaffold protein and recruit LIT-1/WRM-1 indirectly. Alternatively, it is possible that the role of the PCA domain is to bring POP-1 to the vicinity of LIT-1 and WRM-1 by targeting POP-1 to a specific subcellular compartment.

WRM-1 has been shown to interact with POP-1, and the interaction does not require the β -catenin binding domain of POP-1. It will be interesting to find out if the PCA domain is involved in the interaction with WRM-1.

The PCA domain is important for both activation and repression activities of POP-1

POP-1 $_{\Delta PCA}$ was able to rescue the MS defect and caused gut ablation in 100% of *pop-1(zu189)* embryos expressing the transgene. This result shows that GFP::POP-1 $_{\Delta PCA}$ represses E fate in both MS and E in the absence of endogenous POP-1. This is similar to GFP::POP-1 $_{ExpA}$ which shows no POP-1 asymmetry due to lack of nuclear export. GFP::POP-1 $_{ExpA}$ caused 62% gut ablation in *pop-1(zu189)*, and the number increased to 82% in wildtype. This result suggests that when nuclear export is blocked, the increased nuclear GFP::POP-1 $_{ExpA}$ is so high that it represses the normal E fate. If endogenous POP-1 is present in addition to GFP::POP-1 $_{ExpA}$, the gut ablation phenotype is exacerbated. Compared to GFP::POP-1 $_{ExpA}$, GFP::POP-1 $_{\Delta PCA}$ caused a 100% gutless phenotype in *pop-1(zu189)*, suggesting that it may have very strong repression activity or that the PCA domain is required for the activation of endoderm genes. However, GFP::POP-1 $_{\Delta PCA}$ only showed a 6% of gut ablation phenotype when expressed in wildtype, suggesting it does not interfere with the induction of E fate by endogenous POP-1 although overall nuclear levels of POP-1 are increased similarly to that of POP-1 $_{ExpA}$. Therefore, GFP::POP-1 $_{\Delta PCA}$ is not likely to be a strong repressor and likely lacks the activation activity. There are two non-mutually exclusive possibilities to explain why POP-1 $_{\Delta PCA}$ has different activity than POP-1 $_{ExpA}$. (1) The repression activity of GFP::POP-1 $_{\Delta PCA}$ is weaker than wildtype POP-1 (e.q., reduced affinity towards

corepressors) such that it can still repress E fate in *pop-1(zul89)* but it does not interfere with the activation function of endogenous POP-1. (2) GFP::POP-1_{ΔPCA} has low activation activity. For example, it may have reduced affinity towards the limiting coactivator SYS-1. It can not activate E fate, and it does not compete with endogenous POP-1 for SYS-1 binding. Therefore even when present at high levels due to loss of asymmetry, POP-1_{ΔPCA} does not interfere with the induction of E fate by endogenous POP-1.

Two activation domains and two repression domains

POP-1 contains two domains functioning in endoderm repression, amino acids 88-130 and amino acids 287-399. Deleting either amino acids 88-130 or amino acids 287-399 abolishes ability of POP-1 to repress endoderm fate almost completely (Table 3.1). It is known that POP amino acids 88-130 regulate POP-1 asymmetry and is important for repression likely by mediating the interaction with corepressor Groucho/UNC-37. My results showed that amino acids 287-399 are not required for POP-1 asymmetry but is required for the repression activity of POP-1. The only conserved domain in this region is the C-clamp. It is worth noting that although the C-clamp has been associated with activation of Wnt target genes (Atcha et al., 2003; Hecht and Stemmler, 2003), the C-clamp of POP-1 (amino acids 289-312) may be important for the repression activity in early *C. elegans* embryos. It is possible that amino acids 287-399 are also involved in binding corepressors such as Groucho or HDAC. Some mammalian TCF E-tails contain CtBP binding motifs that are not found in the POP-1 C-terminus (Waterman, 2004). It may be that a diverged CtBP binding motif in this region interacts with CtBP and

therefore is important for repression. Or it is possible that amino acids 287-399 contain a *cis*-regulatory element which regulates the binding of UNC-37 to amino acids 88-130.

For activation, the β -catenin binding domain is required because of its direct requirement for the interaction with SYS-1. The repression assay suggests that the PCA domain may be required not only for POP-1 asymmetry but also for its activation function. The PCA domain contains many acidic residues and may activate target genes by interacting with the basal transcription machinery in a way that is similar to other well-known acidic activation domains, e.g., VP16 (Xiao et al., 1994). Alternatively, because the PCA domain is required for all LIT-1/WRM-1-dependent phosphorylation, it is possible that phosphorylation by LIT-1/WRM-1 changes the activity of POP-1 (further discussed in Chapter Four). The rescue assay used here only tests the repression activities of GFP::POP-1 transgenes in embryos, i.e., the abilities to repress ectopic and/or normal endoderm fate. The assay is further complicated because many of the mutations have loss of nuclear POP-1 asymmetry. We have shown that the nuclear level of POP-1 has to be lowered for it to function as an activator (Shetty et al., 2005), making it difficult to assay activation by POP-1 mutants with no asymmetry. We are in the process of developing a strategy to test the activation activity of the POP-1 mutants *in vivo*.

Nuclear GFP puncta and qualitative differences of POP-1 between A-P sister nuclei

The molecular structure of the GFP puncta is not known. For all the GFP::POP-1 constructs I examined, the presence of nuclear GFP puncta does not correlate with POP-1

asymmetry or cell fate. Instead, nuclear GFP puncta appear in both anterior and posterior nuclei when the Exp sites remain unphosphorylated and are missing when the Exp sites are phosphorylated. In POP-1_{ExpA} and all constructs that lack the PCA domain, GFP puncta are detected in both anterior and posterior nuclei. Deleting the PCA domain blocks all LIT-1/WRM-1-dependent phosphorylation including at the Exp sites. It is possible that the presence of GFP puncta is linked to the unphosphorylated state of Exp sites. The only possible exception is POP-1_{Δ287-399}, which has the PCA domain but does not show any puncta. The LIT-1/WRM-1-dependent phosphorylation profiles of this construct should be examined, and POP-1_{Δ287-399} can be combined with ExpA or ExpD to determine if the Exp sites are phosphorylated in POP-1_{Δ287-399} and if the Exp sites are epistatic to POP-1_{Δ287-399} in terms of the formation of nuclear GFP puncta. Also, GFP::POP-1_{WT} should be combined with markers, such as H3K9 methylation for heterochromatin (Cui and Han, 2007), to identify the nature of the GFP::POP-1 puncta.

MATERIALS AND METHODS

Strains

N2 was used as the wildtype strain. Genetic markers: LGI, *pop-1(zul89)*, *dpy-5(e61)*, *teIs3[P_{med-1gfp}::pop-1]*, *hT1(I;V)*; LGIII, *unc-119(ed3)*; LGIV, *him-3(e1147)*. TX352 *teEx72[P_{med-1gfp}::pop-1]*, TX589 *teEx218[P_{med-1gfp}::pop-1_{Δ281-438}]*, and TX616 *teEx243[P_{med-1gfp}::pop-1_{Δ400-438}]* were generated by M-c Lo. TX1167 *teEx563[P_{med-1gfp}::pop-1_{Δ289-399}]*, TX1169 *teEx565[P_{med-1gfp}::pop-1_{Δ389-399}]*, and TX1178 *teEx572[P_{med-}*

gfp::pop-I₃₈₉₋₄₃₈] were generated by injecting *unc-119(ed3) III* worms with pRL2199, pRL2215, and pRL2706, respectively, together with pDPmm016 (*unc-119+*) and pCF-115 (*[P_{ttx-3::rfp}]*, neuronal marker) at a concentration of 100 µg/ml for each.

Plasmid Construction

All expression clones were constructed using the Gateway cloning technology (Invitrogen) (Lo *et al.*, 2004; Robertson *et al.*, 2004). Deletions were generated either with the QuikChange Site-Directed Mutagenesis kit (Stratagene) or by PCR using Phusion polymerase (New England Biolabs, Inc.) followed by DpnI digestion at 37°C for 1hour. Entry clones were verified by sequencing with RLOLG349 and RLOLG350. Expression clones were then made by LR reactions between entry clones and the destination vector pRL707 to generate N-terminal GFP fused POP-1 under the *med-1* promoter for expression in early *C. elegans* embryos.

All clones expressed in HeLa cells were driven by the CMV promoter in pcDNA-based Gateway vectors. LIT-1(pRL1684), and WRM-1(pRL1530) both have N-terminal FLAG tags. All POP-1 constructs were generated by LR reactions between POP-1 entry clones and the destination vector pRL1312 and have N-terminal Flag tags. SYS-1(pRL2722) construct was made by LR reaction between the destination vector pRL1313 (N-terminal c-Myc tag) and the SYS-1 entry clone pRL2687.

Analysis of Embryos and Imaging

Imaging of live embryos was performed using an Axioplan microscope equipped with epifluorescence and differential interference contrast (DIC) optics, and a MicroMax-512EBFT CCD camera controlled by the Metamorph acquisition software (Molecular Devices, Inc.). 4-D microscopy was performed on live embryos mounted on 3% agarose pads sealed with Vaseline to prevent over-drying. At each time point of live imaging, GFP fluorescence and DIC images were collected either as stacked images or from a selected focal plane to follow particular anteroposterior sister pairs. Stacked images were collected as sequential images along the z-axis with 8 slices per embryo (~3 microns between adjacent images). Consecutive time points were 3-5 min apart. All images were collected as 16-bit with the raw pixel values within the linear range of the CCD camera and processed and quantified using the ImageJ program (Lo et al., 2004; Rogers et al., 2002).

Assay for POP-1 Repressor Activity

Various *Pmed-1gfp::pop-1* transgenes were introduced into *pop-1(zu189)* mutant embryos by mating males carrying the transgenes with hermaphrodites homozygous for *pop-1(zu189)* at 20°C for 24 hours. The embryos were collected on 3% agar pads, checked for the presence of GFP using fluorescence microscopy, and allowed to develop at 16°C for 18 hours. The developed embryos were checked with differential interference contrast (DIC) optics for the production of posterior pharynx judged by the size of pharyngeal tissue and the presence of the grinder. Intestinal cells were identified by their birefringent gut granules under polarized light optics.

Transfection assay

HeLa cells were cultured in 100mm Petri dishes in Dulbecco's modified Eagle's medium (DMEM) with 10% FBS. Cells were transfected at ~70% confluency with 12 μ g of total DNA using Turbofect *in vitro* transfection reagent (Fermentas). Twenty-four hours post-transfection, the cells were harvested in CellLytic M cell lysis reagent (Sigma) supplemented with Halt Protease and Phosphatase Inhibitor Cocktail (Pierce) and centrifuged at ~16,000g for 10 minutes. The resulting supernatants were boiled in SDS sample buffer. Cell lysates were resolved by 10% SDS-polyacrylamide gel electrophoresis (SDS-PAGE) followed by Western blot analysis. Primary antibodies used include: 94I (rabbit polyclonal antibody against POP-1) at 1:2,000, mabRL2 (monoclonal antibody against POP-1, also known as P4G4) at 1:100, α -c-Myc (9E10, Santa Cruz Biotechnology) at 1:5,000, and α -FLAG (M2, Sigma) at 1:2,000. Secondary antibodies used were: ECL anti-rabbit-IgG, HRP-linked whole antibody (GE Healthcare), and goat anti-mouse IgG1-HRP (Santa Cruz Biotechnology, Inc), both at 1:10,000.

CHAPTER FOUR

Mutational analysis within the PCA domain of POP-1

INTRODUCTION

In this chapter, I describe a mutational analysis within the PCA domain of POP-1. Amino acid residues that are probable post-translational modification sites were mutated to amino acids that mimic the non-modified form or the constitutively modified form. The resulting POP-1 mutant proteins were expressed in *C. elegans* embryos and were analyzed for their effects on A-P nuclear asymmetries, repressor activities, and LIT-1/WRM-1-dependent phosphorylation using the experimental setup presented in Chapter Three.

Putative phosphorylation sites

Within the PCA domain, there are four serines and three threonines. Among these, S404/S406/S408 and T426 are predicted to be probable phosphorylation sites by online prediction programs NetPhos 2.0 (<http://www.cbs.dtu.dk/services/NetPhos/>) (Blom et al., 1999) and Scansite (<http://scansite.mit.edu/>) (Obenauer et al., 2003). S404/406/408 are candidate sites to be phosphorylated by Casein Kinase II (CKII). CKII has been shown to be a positive regulator in the Wnt signaling pathway and phosphorylation of LEF1 by CKII enhances LEF1/ β -catenin binding (Hammerlein et al., 2005). T426 is a candidate site for Calmodulin-dependent Kinase II (CamKII) phosphorylation. CamKII plays a role in the non-canonical Wnt/Calcium pathway. It has been shown to block the Wnt/ β -catenin pathway downstream of β -catenin, possibly by directly or indirectly

phosphorylating LEF-1 in *Xenopus* (Kuhl et al., 2001). Moreover, CamKII can activate the TAK-1/NLK MAPK cascade (Ishitani et al., 2003). Phosphorylation of TCF by NLK inhibits the interaction of the β -catenin-TCF complex with DNA and antagonizes the canonical Wnt signaling pathway (Ishitani et al., 1999). Therefore, CamKII negatively regulates the canonical Wnt pathway.

In addition, S434 is predicted with medium stringency by the Group-based Phosphorylation Scoring Method (GPS; <http://gps.biocuckoo.org/1.1/index.php>, (Zhou et al., 2004)) to be a putative phosphorylation site. I mutated S404/406/408, T426, or S434 into either alanine to make them unable to be phosphorylated, or to aspartic acid to mimic the phosphorylated state. Similar to the deletion analyses presented in Chapter Three, these mutant proteins were expressed in the EMS lineage under the *med-1* promoter as N-terminal GFP fusion proteins and analyzed for asymmetric localization and their ability to repress the endoderm fate.

C436S

In addition to the probable phosphorylation sites, cysteine436 also deserves attention. There are only five cysteines in POP-1. Four of the five are located in the C-clamp domain located C-terminal to the HMG box, and C436 is the fifth. C436 may be involved in disulfide bond formation with one of the cysteines in the C-clamp. The C-clamp is just C-terminal to the HMG domain and NLS, and it has been shown to bind to GC-rich motifs downstream of the typical TCF binding site. If C436 does form a

disulfide bond with a cysteine in the C-clamp, it might bring the acidic PCA domain near the HMG DNA-binding domain, thus affecting the transcriptional activity of POP-1.

The C436 of POP-1 is a predicted palmitoylation site by the program CSS-Palm (<http://csspalm.biocuckoo.org/>) (Zhou et al., 2006). Palmitoylation is the covalent addition of a 16-carbon palmitate group to a cysteine residue of a protein substrate. Palmitoylation enhances the hydrophobicity of a protein and regulates protein sorting, membrane association, protein-protein interaction, and protein trafficking. Unlike prenylation or myristoylation, palmitoylation is a reversible posttranslational modification and allows for dynamic regulation of intracellular localization of specific proteins. Another intriguing feature of palmitoylation is that many palmitoylated proteins are insoluble in cold non-ionic detergent, and have therefore been proposed to localize to lipid rafts. To test the potential role of C436, I mutated it to serine, an amino acid which has the most similar side chain to cysteine, and analyzed its effect on GFP::POP-1 asymmetry and the repression of endoderm fate.

RESULTS

Mutating T426 to aspartic acid, but not alanine, abolishes GFP::POP-1 nuclear asymmetry

I mutated threonine426 to either alanine or aspartic acid and made N-terminal GFP fusion proteins driven by the *med-1* promoter. GFP::POP-1_{T426A} showed nuclear localization

with clear A-P asymmetry (Figure 4.1.B). The only deviation from the GFP::POP-1_{WT} pattern is that GFP puncta are detected in the posterior nuclei. These GFP puncta are normally restricted to the anterior nuclei and not observed in the posterior nuclei. On the other hand, GFP::POP-1_{T426D} showed no detectable A-P asymmetry and had prominent GFP puncta in both A/P nuclei. There are two features of aspartic acid that are similar to a phosphate group. An aspartic acid has a bulky side chain which is similar to a phosphate group in size, and an aspartic acid is negatively charged like a phosphate group. It is possible that T424D is simply too bulky and caused structural changes that affects POP-1 asymmetry. I mutated T426 to asparagine (N), which is an

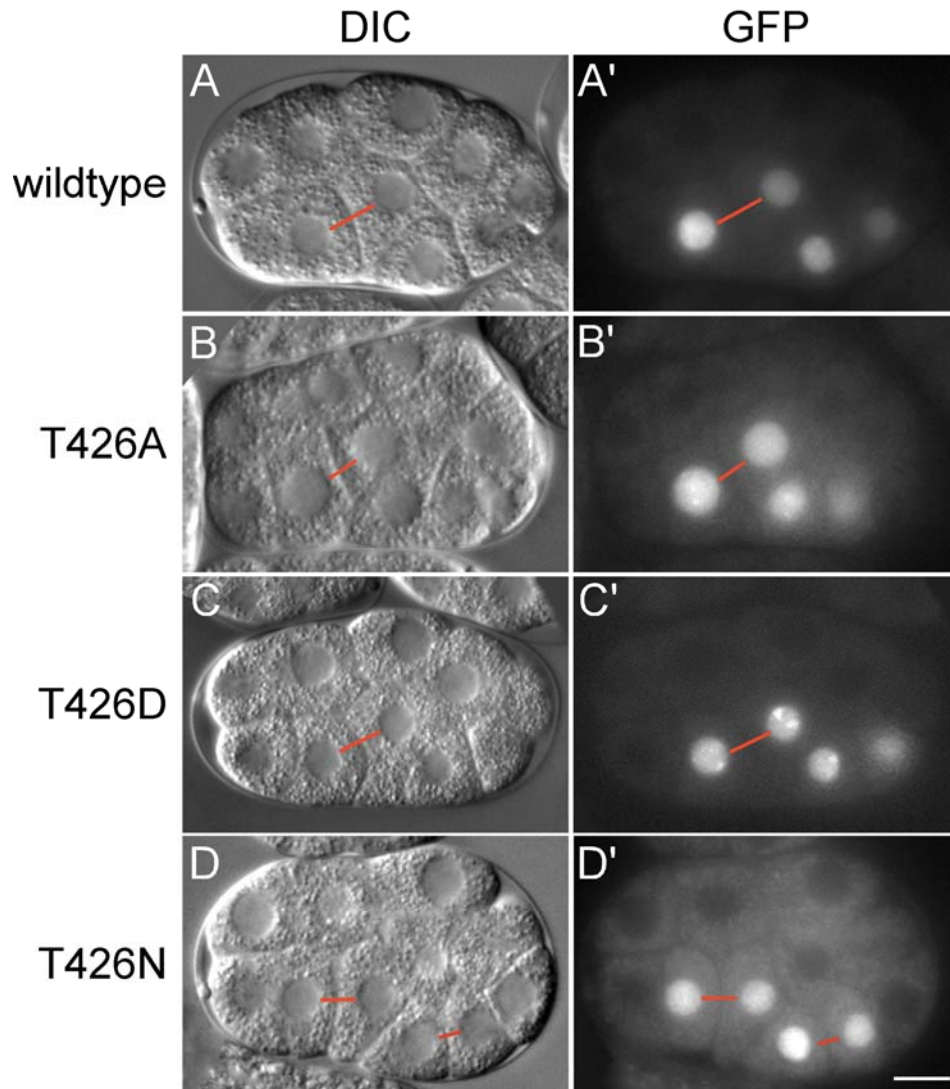


Figure 4.1. The effects of T426 mutations on GFP::POP-1 nuclear asymmetry.

Micrographs of *C. elegans* embryos carrying the *P_{med-1gfp}::pop-1* transgenes encoding wildtype POP-1 or POP-1 with threonine426 mutated to alanine (T426A), aspartic acid (T426D), or asparagine (T426N). Embryos are shown at the stage when there are two MS and two E descendants expressing GFP as DIC (A-D) and corresponding GFP fluorescence (A'-D') images. The embryos are oriented with the anterior to the left. A-P sisters that were both in focus are connected by red lines. GFP signals were asymmetric in B'. POP-1 nuclear asymmetry is abolished in C', and both A-P nuclei have GFP puncta. The A-P nuclear asymmetry is affected variably in T426N and this particular example shows MSa/p having similar GFP levels (D'). Scale bar = 10 μ m.

amino acid similar to an aspartic acid or a phosphate group in its size, but it has a neutrally charged side chain. GFP::POP-1_{T426N} showed variable effects on POP-1 asymmetry (Figure 4.1.D), suggesting that both the size and the charge of an aspartic acid are likely to contribute to abolishing the asymmetry of GFP::POP-1_{T426D}.

I introduced GFP::POP-1_{T426A} and GFP::POP-1_{T426D} into the *pop-1(zu189)* background to test their abilities to repress E fate in MS and rescue the posterior pharynx. GFP::POP-1_{T426A} was able to rescue MS fate in *pop-1(zu189)* (97%, n=37). Although GFP::POP-1_{T426A} had clear A-P asymmetry, it caused 43% gut ablation (n=37) in *pop-1(zu189)*, suggesting T426 is important for the activity of POP-1 and GFP::POP-1_{T426A} is a stronger repressor than wildtype. As to GFP::POP-1_{T426D}, it rescued MS fate to 78% (n=27) in *pop-1(zu189)*. Compared to POP-1_{WT}, which rescued MS fate to 100%, this result suggests that T426D weakened the repression activity. Expression of GFP::POP-1_{T426D} caused 96% gutless (n=27) in *pop-1(zu189)* and 8% E fate ablation (n=71) in wildtype background. These results are similar to those of GFP::POP-1_{ΔPCA} (Table 4.1), suggesting that even though GFP::POP-1_{T426D} showed no asymmetry and repressed normal endoderm fate in *pop-1(zu189)*, it did not interfere with the function of endogenous POP-1 in the wildtype background. It caused a low level of gut ablation in wildtype background, even though the overall nuclear level of POP-1 would have been even higher with endogenous POP-1 plus the transgenic GFP::POP-1_{T426D}.

	Asy	Rescue MS in <i>zu189</i>	Ablate gut in <i>zu189</i>	Ablate gut in WT
	Y	100	0	0
	N	15	4	nd
	N	100	100	6
	N	93	36	37
	N	41	0	nd
	Y	100	43	nd
	N	78	96	8
	N	74	63	4
	N	100	89	8
	N	42	0	0
	N	43	5	0

Table 4.1. Epistasis analysis of POP-1 T426 and the Exp sites. Schematic representation of point mutations used in this analysis. G: N-terminal GFP; cyan: β -catenin binding domain; HMG: high mobility group DNA binding domain. The numbers of As or Ds in the white box represent the number of amino acids mutated to A or D in the Exp sites, i.e., S107, S109, S117, T120, and S127. Asy: GFP::POP-1 asymmetry. All numbers represent percentage of embryos expressing the transgene for ability to repress endoderm in MS in *pop-1(zu189)* (rescue MS-derived posterior pharynx), to ablate endoderm in *pop-1(zu189)*, and to ablate gut in wildtype (WT). nd: not determined.

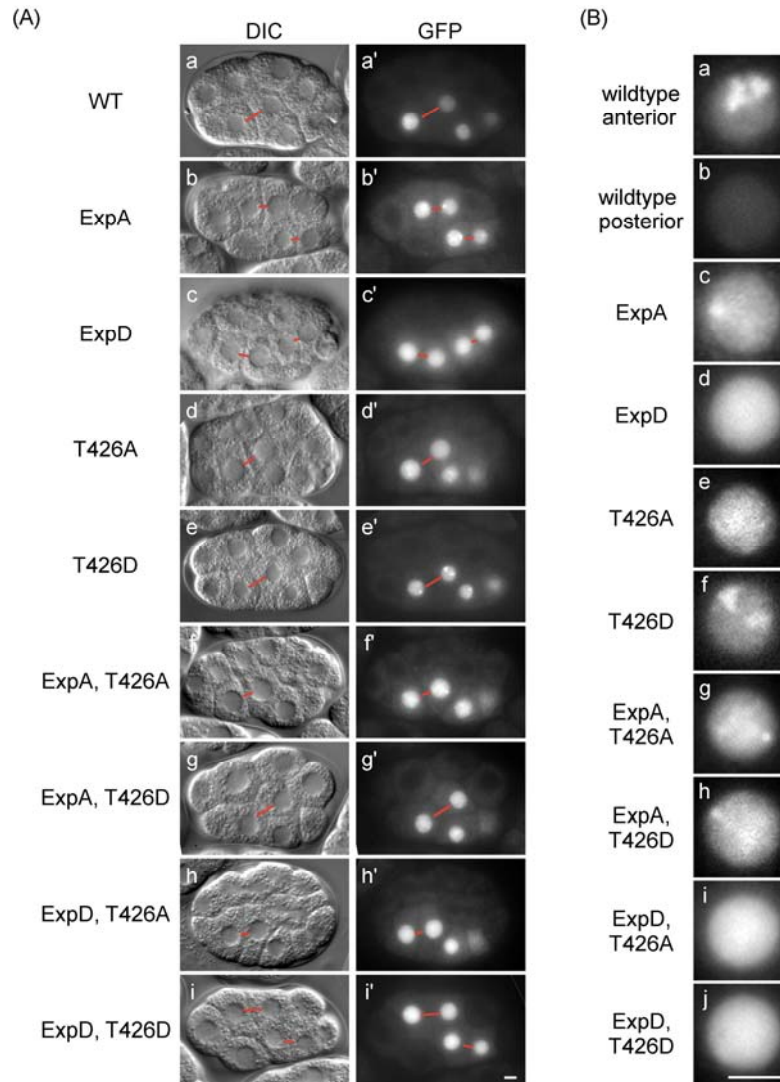


Figure 4.2. The epistasis of Exp sites and T426 on GFP::POP-1 nuclear asymmetry.

(A) Micrographs of *C. elegans* embryos carrying *P_{med-1}::gfp::pop-1* transgenes encoding wildtype POP-1 or POP-1 with mutations as labeled on the left. Embryos are shown at the stage when there were two MS and two E descendants expressing GFP as DIC (a-i) and corresponding GFP fluorescence (a'-i') images. The embryos are oriented with the anterior to the left. A-P sisters that were both in focus are connected by red lines. GFP signals were asymmetric in (b'). POP-1 nuclear asymmetry is abolished in (c') – (i'). (B) Enlarged excerpts of nuclei expressing indicated POP-1 variants. Note that ExpD (d) does not have the GFP puncta normally detected in wildtype anterior nuclei (a), and this phenotype is epistatic to T426D (i and j). Scale bars = 5 μ m.

The Export sites are epistatic to T426 for the nuclear asymmetry and the repression activity of POP-1

One mechanism to lower the nuclear level of POP-1 is LIT-1-dependent phosphorylation of POP-1, which ultimately leads to the nuclear export of POP-1. To test if T426 and the Exp sites function through a single mechanism (nuclear export) or if they have parallel inputs in the regulation of POP-1 asymmetry, I generated transgenes carrying combined mutations of Exp sites and T426 to either A or D. I examined GFP::POP-1 asymmetry, the repression activity in terms of the rescue of MS fate in *pop-1(zul89)* and the ablation of E fate in *pop-1(zul89)* and wildtype. None of the combined mutants had GFP asymmetry (Figure 4.2). Neither GFP::POP-1_{ExpD,T426A}, nor GFP::POP-1_{ExpD,T426D} had nuclear puncta (Figure 4.2.B i and j), which is similar to GFP::POP-1_{ExpD} (Figure 4.2.B.d), but not to GFP::POP-1_{T426A} or GFP::POP-1_{T426D} (Figure 4.2.B e and f). In terms of repression activity, both GFP::POP-1_{ExpD,T426A} and GFP::POP-1_{ExpD,T426D} behaved similarly to GFP::POP-1_{ExpD} alone (Table 4.1). These results suggest that the ExpD mutation is epistatic to T426A or T426D. Both GFP::POP-1_{ExpA} and GFP::POP-1_{T426A} have nuclear puncta (Figure 4.2.B c and e) and similar repression activities. However, GFP::POP-1_{T426A} showed clear asymmetry, and GFP::POP-1_{ExpA} and GFP::POP-1_{ExpA,T426A} did not (Figure 4.2.A b', d', and f'). Therefore, in terms of asymmetry, T426A did not suppress the asymmetry defect of GFP::POP-1_{ExpA}.

S404/406/408 have variable effects on GFP::POP-1 nuclear asymmetry

When S404/406/408 were mutated to alanines, GFP::POP-1_{S404/406/408A} showed a partial defect in asymmetry, which was abolished or less obvious between A-P sisters in some

embryos (Figure 4.3.B) but not others. When the transgene is introduced into *pop-1(zul89)*, the MS fate defect was rescued in most of the embryos expressing GFP::POP-1_{S404/406/408A} (88%, n = 65; Table 4.2). Five percent of the wildtype (n = 22) and 35% of the *pop-1(zul89)* (n = 65) embryos expressing GFP::POP-1_{S404/406/408A} failed to make any endoderm, suggesting that the endoderm fate was repressed in both MS and E (Table 4.2).

When S404/406/408 are mutated to aspartic acids, GFP::POP-1_{S404/406/408D} showed normal nuclear asymmetry (Figure 4.3.C). GFP::POP-1_{S404/406/408D} rescued the MS fate defect in 91% of embryos and caused 11% endoderm ablation in *pop-1(zul89)* expressing the transgene (n=45; Table 4.2). These results suggest that S404/406/408 to A mutations affect POP-1 nuclear asymmetry, but that S404/406/408D do not. Furthermore, changing S404/406/408 to either A or D did not affect the repression activity of POP-1.

Mutating S434 has no effect on GFP::POP-1 asymmetry or the repression activity

GFP::POP-1_{S434A} and GFP::POP-1_{S434D} both showed normal nuclear asymmetry (Figure 4.3 D and E). When the GFP::POP-1_{S434A} transgene was introduced into *pop-1(zul89)*, the MS fate defect was rescued in 100% of the embryos expressing (n = 10; Table 4.2). Ten percent of the *pop-1(zul89)* (n = 10) embryos expressing GFP::POP-1_{S434A} failed to make endoderm. Expressing GFP::POP-1_{S434D} in *pop-1(zul89)* rescued the MS fate defect in 89% of embryos and caused 11% endoderm ablation expressing the transgene (n=27; Table 4.2). There was no gut ablation in the wildtype background for either the

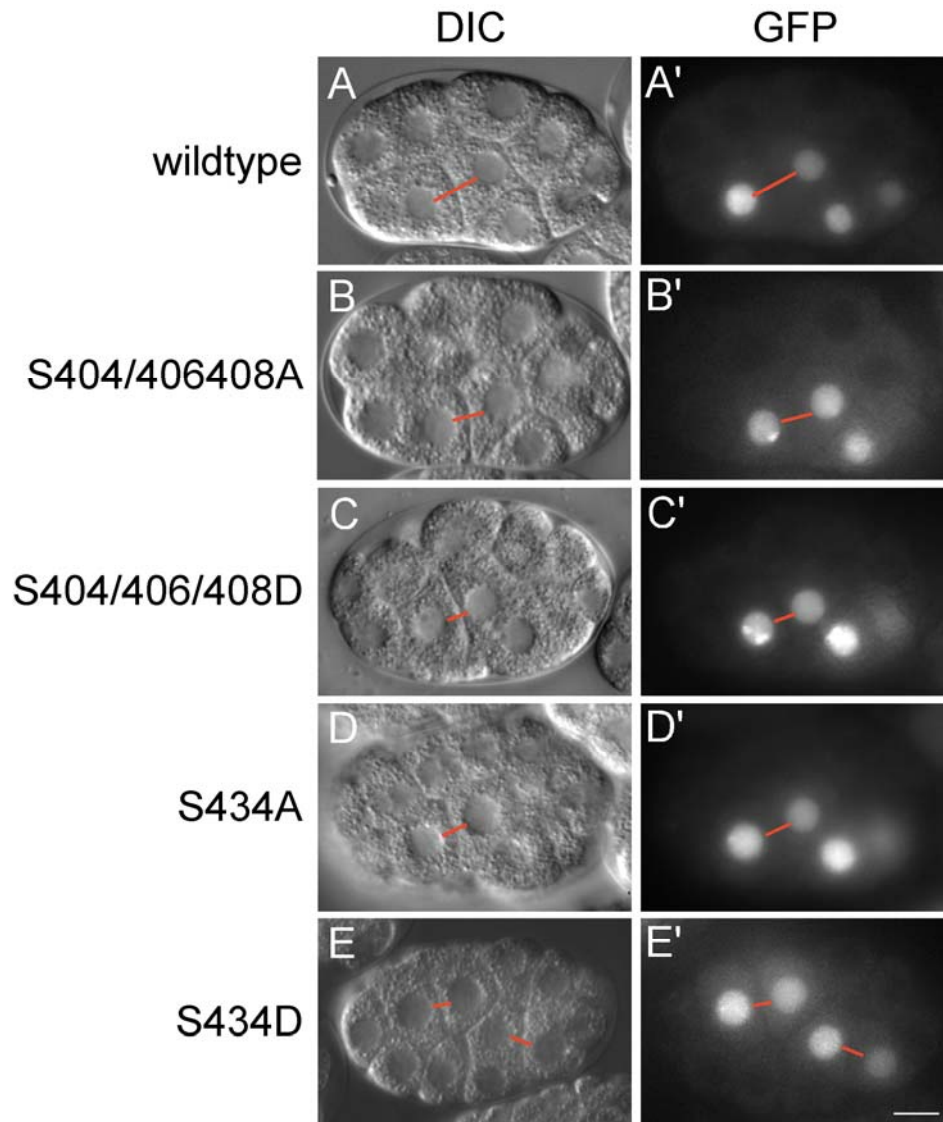


Figure 4.3. The effects of mutations within the PCA domain on GFP::POP-1 nuclear asymmetry. Micrographs of *C. elegans* embryos carrying the *P_{med-1gfp}::pop-1* transgenes encoding wildtype POP-1 or POP-1 with serines 404/406/408 mutated to alanine (S404/406/408A) or aspartic acid (S404/406/408D), or serine 434 mutated to alanine (S434A) or aspartic acid (S434D). Embryos are shown at the stage when there were two MS and two E descendants expressing GFP as DIC (A-E) and corresponding GFP fluorescence (A'-E') images. The embryos are oriented with anterior to the left. A-P sisters that were both in focus are connected by red lines. The A-P nuclear asymmetry is affected variably in S404/406/408A, and this particular example shows MSa/p having similar GFP levels (D'). GFP signals were normal in C', D', and E'. Scale bar = 10 μ m.

		267	438	Asy	Rescue MS in <i>zu189</i>	Ablate gut in <i>zu189</i>	Ablate gut in WT
Full-length				Y	100	0	0
Δ PCA			399	N	100	100	6
ExpA				N	91	62	82
ExpD				N	41	0	nd
T426A			426	Y	100	43	nd
T426D			426	N	78	96	8
S404/406/408A				V	88	35	5
S404/406/408D				Y	91	11	nd
S434A			434	Y	100	10	0
S434D			434	Y	89	11	0
C436S(1)			436	V	96	15	0
C436S(2)			436	V	86	0	0
C436S(3)			436	V	100	0	0

Table 4.2. Mutational analysis of the PCA domain of POP-1. Schematic representation of the point mutations used in this analysis. G: N-terminal GFP; cyan: β -catenin binding domain; white: repression domain including the Exp sites; HMG: high mobility group DNA binding domain. Asy: GFP::POP-1 asymmetry. All numbers represent percentage of embryos expressing the transgene for ability to repress endoderm in MS in *pop-1(zu189)* (rescue MS-derived posterior pharynx), to ablate endoderm in *pop-1(zu189)*, and to ablate gut in wildtype (WT). Numbers for three independent lines of the C436S mutation are showed. nd: not determined.

GFP::POP-1_{S434A} or GFP::POP-1_{S434D} transgenes (n = 23 and n = 44, respectively). These results suggest that S434 does not play a significant role in the regulation of POP-1 nuclear asymmetry or its repression activity.

C436S is more important for GFP::POP-1 nuclear asymmetry in MS and E than in later divisions

GFP::POP-1_{C436S} showed an interesting asymmetry defect. At first glance, many embryos showed clear GFP asymmetry at the EMS4 stage. However, with a closer look, many embryos in fact had little difference in GFP intensities between A-P nuclei in the MSa/p sister pair while having clearly asymmetric GFP in Ea/p sisters (Figure 4.4.D; compare to wildtype pattern in B). Moreover, GFP asymmetry at EMS2 stage is almost completely abolished in these embryos (Figure 4.4.C; compare to wildtype in A). This phenotype is similar to that of *mom-2*. Compared to the differences of POP-1 levels detected by mabRL2 in wildtype embryos, POP-1 asymmetry is lost in most of *mom-2(or42)* embryos at EMS2 stage (Figure 4.4.G, compared to wildtype in E) and often the MSa/p sisters but not affected as much in Ea/p (Figure 4.4.H; compare to wildtype in F). This observation suggests that POP-1_{C436S} may be regulated by Wnt/*mom-2*.

I introduced GFP::POP-1_{C436S} into *pop-1(zul89)* to test whether the transgene can repress E fate. For the three lines I tested, all rescued MS fate in >85% of embryos (n=69 total, see Table 4.2 for detail), and only one line had 15% gut ablation (line 1, n=26) while the other two lines had no gut ablation (line 2 and line 3, n=29 and 14, respectively). The differences may be due to the variable defects in GFP asymmetry at different stages. None of the three lines showed any gut ablation in wildtype background.

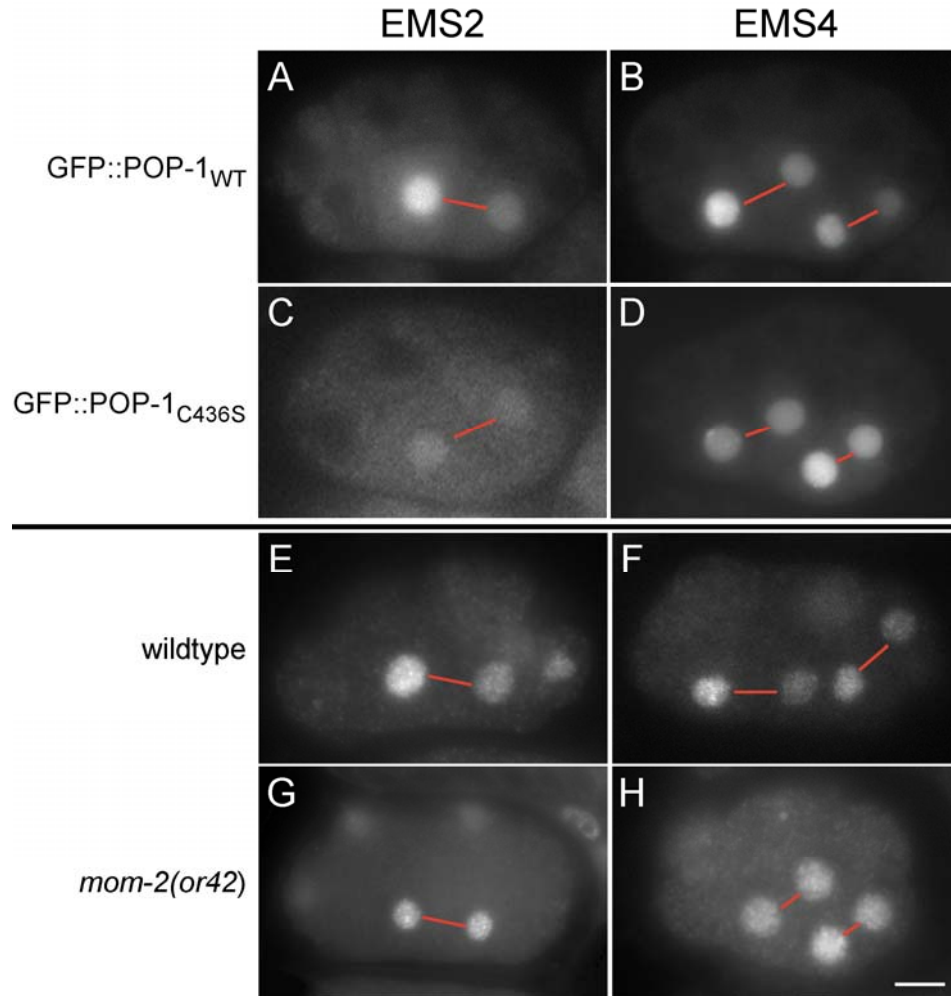


Figure 4.4. The effects of the C436S mutation on GFP::POP-1 nuclear asymmetry compared to endogenous POP-1 asymmetry in *mom-2(or42)*. (A-D) GFP fluorescence micrographs of *C. elegans* embryos carrying *P_{med-1gfp}::pop-1* transgenes encoding for wildtype POP-1 or POP-1_{C436S}. Embryos are shown at the stage at stages when there were MS and E (A and C), or two MS and two E descendants (B and D) expressing GFP. The A-P nuclear asymmetry was lost in C436S in (C), and in many embryos was also lost in MSa/p as shown in (D). (E-H) Immunofluorescence micrographs of wildtype or *mom-2(or42)* embryos stained with mabRL2 against endogenous POP-1. Embryos are shown at the stage at stages when there were MS and E (E and G), or two MS and two E descendants (F and H). The A-P nuclear asymmetry was lost in *mom-2(or42)* as shown in (G), and in most embryos it was also lost in MSa/p as shown in (H). The embryos are oriented the anterior to the left. A-P sisters that were both in focus are connected by red lines. Scale bar = 10 μ m.

Mutating T426 to aspartic acid blocks LIT-1/WRM-1–dependent phosphorylation of POP-1

I made Flag::POP-1 constructs with the amino acid mutations described above and tested their phosphorylation profiles by LIT-1/WRM-1 cotransfection in HeLa cells. I found that Flag::POP-1_{T426D} showed no sign of LIT-1/WRM-1-dependent phosphorylation (Figure 4.5), the same effect as deleting the whole PCA domain. Flag::POP-1_{T426A} was phosphorylated by LIT-1/WRM-1 and showed migration retardation similar to Flag::POP-1_{WT}. Upon LIT-1/WRM-1 cotransfection, Flag::POP-1_{ExpA} and Flag::POP-1_{Exp5D} both showed migration retardation (Figure 4.5), suggesting the presence of LIT-1/WRM-1-dependent phosphorylation sites other than the Exp sites. In fact, Flag::POP-1_{ExpA} appeared to have more slow-migrating POP-1 upon LIT-1/WRM-1 cotransfection than Flag::POP-1_{WT}, suggesting that ExpA may promote LIT-1/WRM-1-dependent phosphorylation at sites other than the Exp sites. ExpA did not suppress the effect of T426D so that Flag::POP-1_{ExpA, T426D} had little or no phosphorylation by LIT-1/WRM-1 complex (Figure 4.5). These results showed that T426D has the same phenotype as deleting the PCA domain, and T426D is epistatic to ExpA for further LIT-1/WRM-1-dependent phosphorylation. The combination of ExpD, T426D was excluded from this analysis due to a cloning error and is under construction currently.

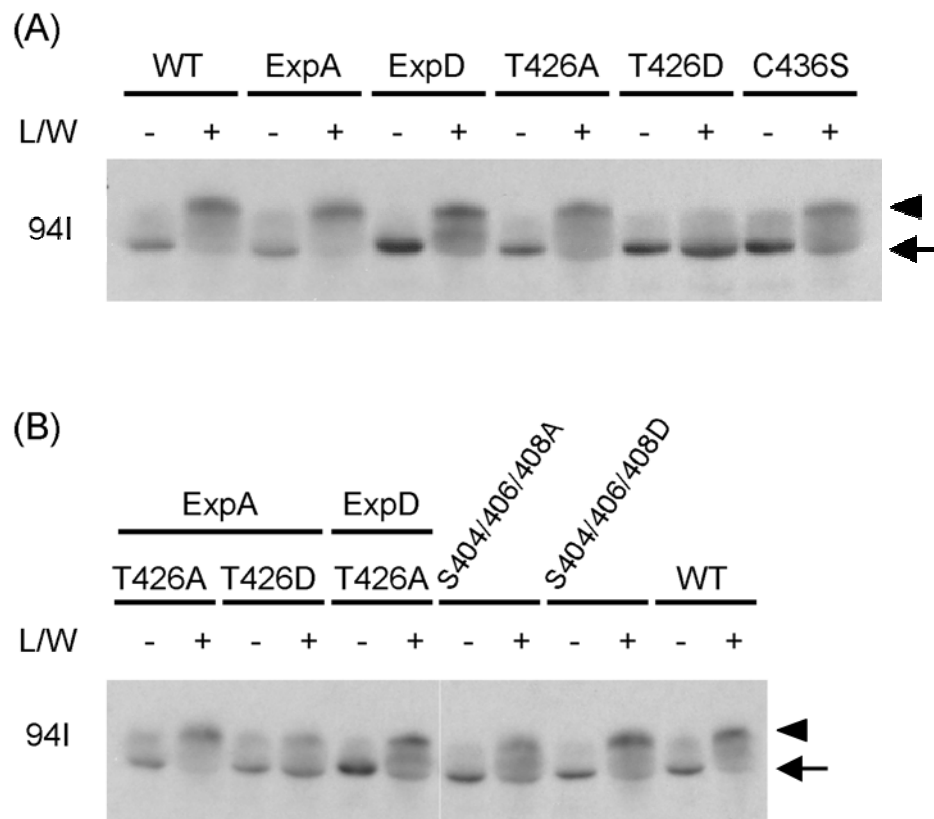


Figure 4.5. Phosphorylation of POP-1 variants in HeLa cells. Western blot probed with, 94I of HeLa cell lysates expressing POP-1 protein variants as indicated with (L/W +) or without (L/W -) LIT-1/WRM-1 cotransfection. WT: wildtype. All phosphorylation, which is evident by the retardation in migration, is LIT-1/WRM-1-dependent. Arrow: unphosphorylated; arrowhead: LIT-1/WRM-1 phosphorylated. T426D mutation abolished all LIT-1/WRM-1-dependent phosphorylation (A), and ExpA, T426D mutant can not be phosphorylated (B).

Other mutations I tested include Flag::POP-1_{S404/406/408A}, Flag::POP-1_{S404/406/408D}, and Flag::POP-1_{C436S}. Mutating these sites had mild or no effects on the overall LIT-1/WRM-1-dependent phosphorylation levels (Figure 4.5).

DISCUSSION

The T426D mutation has similar phenotypes to the deletion of the PCA domain

The T426D mutation is the first example of a single amino acid change which abolishes GFP::POP-1 asymmetry. POP-1_{T426D} shares many phenotypes with POP-1_{ΔPCA}. Both GFP::POP-1_{T426D} and GFP::POP-1_{ΔPCA} abolished asymmetry and showed nuclear puncta in both A-P nuclei. Both mutants showed strong gut ablation in *pop-1(zu189)* (96%, n=27 and 100%, n=28, respectively) but not in the wildtype background (8%, n=71 and 6%, n=34, respectively; see Table 4.1 for detail). And, in a mammalian tissue culture system, both mutations block all LIT-1/WRM-1-dependent phosphorylation of POP-1.

It is interesting that putative phosphorylation of T426, an amino acid within the PCA domain, would cause similar phenotypes to deleting the whole domain. The simplest explanation is that deleting the PCA domain abolishes the interaction between POP-1 and WRM-1 or LIT-1, and that T426D also blocks this interaction. Or phosphorylation may be the signal for another modification in the PCA domain and block the interaction indirectly (see Chapter Five).

It is not true that any mutation at the C-terminus of POP-1 results in defect. S434 provides an example of a putative phosphorylation site in the PCA domain, and did not cause any defects in POP-1 asymmetry or repression activity when mutated to either alanine or aspartic acid. This result further augments confidence that the phenotypes I

observed with the other mutations are specific and real, not just general effects due to change in the overall structure of the PCA domain.

Epistasis between the Exp sites and T426

In HeLa cells, T426D blocks most, if not all, of the LIT-1/WRM-1-dependent phosphorylation of POP-1_{ExpA}. Both POP-1_{ExpA} and POP-1_{ExpD} showed LIT-1/WRM-1-dependent phosphorylation, suggesting there are LIT-1/WRM-1 phosphorylation sites other than the Exp sites. Indeed, there are other strong MAPK sites predicted by phosphorylation prediction programs, NetPhosK and Scansite. In fact, POP-1_{ExpA}, which mimics the unphosphorylated state of the Exp sites, seems to promote LIT-1/WRM-1-dependent phosphorylation at sites other than the Exp sites because POP-1_{ExpA} was more highly phosphorylated POP-1 than POP-1_{WT}. In addition, it appears that the phosphorylation of POP-1_{ExpA} was blocked when T426 is in the phosphorylated state. That is to say, T426D blocks most, if not all, LIT-1/WRM-1-dependent phosphorylation in POP-1_{ExpA}, while T426A allows phosphorylation to occur.

Mutating the Exp sites to aspartic acids suppresses the effects of T426 mutations on GFP::POP-1 nuclear puncta and activity in *C. elegans* embryos. Because the T426D mutation blocks all LIT-1/WRM-1-dependent phosphorylation of POP-1, these results in embryos suggest that the phosphorylation at the Exp sites is downstream of the regulation by T426. Efforts are underway to test if Flag::POP-1_{ExpD, T426D} can be phosphorylated by LIT-1/WRM-1 in HeLa cells

LIT-1/WRM-1 phosphorylation may regulate the transcription activity of POP-1

LIT-1/WRM-1 not only regulates POP-1 asymmetry but may also promote the switch of POP-1 from a repressor to an activator for endoderm fate. Although the actual mechanism is not known, theoretically this may be achieved by lowering the affinity of POP-1 for the corepressors (e.g., UNC-37 or HDA-1, increasing the affinity of POP-1 for the coactivator (e.g., SYS-1), or both. Because the activation of endoderm genes requires that the nuclear level of POP-1 to be lowered while that of SYS-1 increases, it would be counterproductive if phosphorylation at the Exp sites, which facilitates nuclear export of POP-1, enhances the binding with SYS-1. An attractive model is that besides the Exp sites, there are other LIT-1/WRM-1-dependent phosphorylation sites that promote activation, possibly by increasing the affinity for SYS-1 when phosphorylated. These sites will be referred to as **Act** sites because phosphorylation at these sites favors activation. Phosphorylation at these Act sites is likely to be mutually exclusive with phosphorylation at the Exp sites. The population of POP-1 with phosphorylation at the Act sites is likely to remain in the nucleus and bound to SYS-1 since the Exp sites are not phosphorylated. The population of POP-1 with phosphorylation at the Exp sites is exported from the nucleus and has lower affinity for SYS-1. Since the PCA domain is required for activation, it is possible that the Act sites are located near or within the PCA domain.

Candidate Act sites should fit the following criteria. (1) If the sites are mutated to aspartic acid (ActD), the mutant protein would exhibit no asymmetry because the Exp sites can not be phosphorylated. ActD would increase the affinity for SYS-1 and cause

mild or no gut ablation phenotypes even with no asymmetry. (2) Mutating the Act sites to alanine may not affect asymmetry, but the mutant is predicted to have strong repression activity and cause gutless phenotypes in wildtype and *pop-1(zul89)*. Based on this model, T426 does not fit the criteria and is not a good candidate for the Act site because GFP::POP-1_{T426D} caused almost complete ablation of endoderm in *pop-1(zul89)*. A better candidate may be S404/406/408. GFP::POP-1_{S404/406/408A} caused variable effects on asymmetry, but it caused 35% gut ablation in *pop-1(zul89)*. Further experiments are needed to screen for mutations that affect the affinity between POP-1 and SYS-1 for possible Act sites.

The C436S phenotype is similar to that of *mom-2*

The POP-1 asymmetry defect of GFP::POP-1_{C436S} is similar to that seen in *mom-2(or42)*. Both GFP::POP-1_{C436S} and *mom-2(or42)* showed stronger defects in POP-1 asymmetry at the EMS2 stage than the EMS4 stage. Also, at the EMS4 stage, MSa/p sister blastomeres have less GFP asymmetry compared to Ea/p sister pair. POP-1 asymmetry is reestablished in *mom-2(or42)* as the embryo develops further (Huang et al., 2007; Park and Priess, 2003). These results suggest that C436 and *mom-2(+)* activity are required for POP-1 asymmetry at the EMS2 stage, but not so much at later stages.

C436 is a predicted site for palmitoylation. It is possible that the role of C436 in POP-1 asymmetry is to change the subcellular localization of POP-1 or the interaction between POP-1 and other cofactor(s) by palmitoylation. Alternatively, C436 may be involved in disulfide bond formation with a cysteine in the C-clamp. Because mutating

C436 showed similar phenotype to *mom-2(or42)*, it is possible that the modification of C436 is regulated by MOM-2. Further experiments are needed to show if C436 is palmitoylated or forms a disulfide bond and if these processes are dependent on MOM-2.

MATERIALS AND METHODS

Strains

N2 was used as the wildtype strain. Genetic markers: LGI, *pop-1(zu189)*, *dpy-5(e61)*, *hT1(I;V)*; LGIII, *unc-119(ed3)*; LGIV, *him-3(e1147)*. TX352 *teEx72[P_{med-1gfp}::pop-1]*, TX498 *teEx160[P_{med-1gfp}::pop-1(S109/118/T120/S127A)]*, TX629 *teEx248[P_{med-1gfp}::pop-1(S107/109/118/T120/S127D)]*, and TX722 *teEx283[P_{med-1gfp}::pop-1_{S404/406/408A}]* were generated by M-c Lo. TX839 *teEx337[P_{med-1gfp}::pop-1(T426A)]*, TX851 *teEx349[P_{med-1gfp}::pop-1(S404/406/408D)]* were generated by injecting TX576 *unc-119(ed3)III*; *him-3(e1147)IV* worms with pRL1819 and pRL1723, respectively, together with pDPmm016 (*unc-119+*) at a concentration of 100 µg/ml for each. TX874 *teEx365[P_{med-1gfp}::pop-1(T426D)]*, TX1094 *teEx512[P_{med-1gfp}::pop-1(S434A)]*, TX1095 *teEx513[P_{med-1gfp}::pop-1(S434D)]* were generated by injecting *unc-119(ed3)III* worms with pRL1867, pRL2445, and pRL2447, respectively, together with pDPmm016 (*unc-119+*) at a concentration of 100 µg/ml for each. TX1096 *teEx514[P_{med-1gfp}::pop-1(S107/118/S127A, T426A)]*, TX1098 *teEx516[P_{med-1gfp}::pop-1(S107/118/S127A, T426D)]*, TX1100 *teEx518[P_{med-1gfp}::pop-1(S107/109/118/T120/S127D, T426A)]*, and TX1102 *teEx520[P_{med-1gfp}::pop-1(S107/109/118/T120/S127D, T426D)]* were generated

by injecting *unc-119(ed3)III* worms with pRL2562, pRL2563, pRL2564, pRL2565, respectively, together with pDPmm016 (*unc-119+*) and pCF-115 ($[P_{\text{ttx-3}}::rfp]$, neuronal marker) at a concentration of 100 µg/ml for each. TX1164 *teEx560*[$P_{\text{med-1gfp}}::pop-1(C436S)$ line 1], TX1165 *teEx561*[$P_{\text{med-1gfp}}::pop-1(C436S)$ line 2], and TX1166 *teEx562*[$P_{\text{med-1gfp}}::pop-1(C436S)$ line 3] were three lines generated by injecting *unc-119(ed3)III* worms with pRL2669, together with pDPmm016 (*unc-119+*) and pCF-115 ($[P_{\text{ttx-3}}::rfp]$, neuronal marker) at a concentration of 100 µg/ml for each.

Plasmid Construction

All expression clones were constructed using the Gateway cloning technology (Invitrogen) (Lo *et al.*, 2004; Robertson *et al.*, 2004). Mutations were generated either with the QuikChange Site-Directed Mutagenesis kit (Stratagene) or by PCR using Phusion polymerase (New England Biolabs, Inc.). Entry clones were verified by sequencing with RLOLG349 and RLOLG350. Expression clones were then generated by LR reactions between entry clones and the destination vector pRL707 to generate N-terminal GFP fused POP-1 under control of the *med-1* promoter for expression in early *C. elegans* embryos.

All clones expressed in HeLa cells were driven by the CMV promoter in pcDNA-based Gateway vectors. LIT-1(pRL1684), and WRM-1(pRL1530) both have N-terminal FLAG tags. All POP-1 constructs were generated by LR reactions between POP-1 entry clones and the destination vector pRL1312 and have N-terminal Flag tags.

The SYS-1 construct, pRL2722, was made by LR reaction between the destination vector pRL1313 (N-terminal c-Myc tag) and the SYS-1 entry clone pRL2687.

Analysis of Embryos and Imaging

Imaging of live embryos was performed using an Axioplan microscope equipped with epifluorescence and differential interference contrast (DIC) optics, and a MicroMax-512EBFT CCD camera controlled by the Metamorph acquisition software (Molecular Devices, Inc.). 4-D microscopy was performed on live embryos mounted on 3% agarose pads sealed with Vaseline to prevent over-drying. At each time point of live imaging, GFP fluorescence and DIC images were collected either as stacked images or from a selected focal plane to follow particular anteroposterior sister pairs. Stacked images were collected as sequential images along the z-axis with 8 slices per embryo (~3 microns between adjacent images). Consecutive time points were 3 or 4 min apart. All images were collected as 16-bit with the raw pixel values within the linear range of the CCD camera, and were processed and quantified using the ImageJ program (Lo et al., 2004; Rogers et al., 2002).

Assay for POP-1 Repressor Activity

Various *gfp::pop-1* transgenes were introduced into *pop-1(zu189)* mutant embryos by mating males carrying the transgenes with hermaphrodites homozygous for the *pop-1(zu189)* mutation at 20°C for 24 hours. The embryos were collected onto 3% agar pads, checked for the presence of GFP using fluorescence microscopy, and allowed to develop at 16°C for 18 hours. Then the embryos were checked with differential interference

contrast (DIC) optics for the production of posterior pharynx and scored as rescued if they produced the wildtype amount of posterior pharyngeal tissues. Intestinal cells were identified by their birefringent gut granules under polarized optics.

Transfection assay

HeLa cells were cultured in 100mm Petri dishes in Dulbecco's modified Eagle's medium (DMEM) with 10% FBS. Cells were transfected at ~70% confluency with 12 μ g of total DNA using Turbofect *in vitro* transfection reagent (Fermentas). Twenty-four hours post-transfection, the cells were harvested in CelLytic M cell lysis reagent (Sigma) supplemented with Halt Protease and Phosphatase Inhibitor Cocktail (Pierce) and centrifuged at ~16,000g for 10 minutes. The resulting supernatants were boiled in SDS sample buffer. Cell lysates were resolved by 10% SDS-polyacrylamide gel electrophoresis (SDS-PAGE) and subjected to Western blot analysis. Primary antibodies used include: 94I (rabbit polyclonal antibody against POP-1) at 1:2,000, mabRL2 (monoclonal antibody against POP-1, also known as P4G4) at 1:100, α -c-Myc (9E10, Santa Cruz Biotechnology) at 1:5,000, and α -FLAG (M2, Sigma) at 1:2,000. Secondary antibodies used were: ECL anti-rabbit-IgG, HRP-linked whole antibody (GE Healthcare), and goat anti-mouse IgG1-HRP (Santa Cruz Biotechnology, Inc), both at 1:10,000.

CHAPTER FIVE

Differential presentation of mabRL2 epitope *in vivo*

INTRODUCTION

POP-1 is not only quantitatively but also qualitatively different between MS and E

Many lines of evidence suggest that LIT-1/WRM-1 does not simply down-regulate nuclear POP-1 level in E but also causes qualitative changes in POP-1 and alters its activity. First, MS and E nuclei exhibit morphological differences. GFP::POP-1 and, to a lesser degree, endogenous POP-1, form nuclear punctate structures that are associated with the repression activity of POP-1 and the anterior fate (discussed in detail in Chapter Three). Second, the nuclear levels of POP-1 are uncoupled from the repression of E fate in certain mutants. For example, although POP-1 asymmetry is lost in *lit-1(t1534)*, the mutant embryos are able to produce endoderm (Maduro et al. 2002). Another example is that in *mom-2(ne874)*, WRM-1 nuclear levels are reduced or abolished in the E nucleus (Nakamura et al., 2005). The gutless phenotype of *mom-2(ne874)* is partially suppressed by depleting the exportin *xpo-1* by RNAi, which raises the nuclear level of WRM-1 (Nakamura et al, 2005). Since *xpo-1* is also required for the nuclear export of POP-1 (Lo et al., 2004), this experiment suggests that the high level of nuclear POP-1 in *xpo-1(RNAi)* embryo does not result in the repression of endoderm fate. Moreover, I showed that a *P_{med-1gfp}::pop-1*-carrying strain is sensitive to the manipulation of SYS-1 level (Huang et al., 2007). Increasing SYS-1 levels in almost all *mom* mutants results in the suppression of gutless phenotypes, except for *wrm-1(RNAi)* and *lit-1(t1512ts)*. Collectively, these results suggest that the level of POP-1 is important but not sufficient

to explain the cell fate difference between MS and E. POP-1 is likely to be qualitatively modified by LIT-1/WRM-1, possibly by changing the transcriptional activity of POP-1.

Differential presentation of the mabRL2 epitope

One qualitative difference we detect is the differential presentation of the mabRL2 epitope in wildtype. The monoclonal antibody mabRL2 was generated by injecting mice with a recombinant POP-1 protein with the HMG domain deleted to minimize cross-reactivity with other HMG-type proteins. Sera from injected mice were screened by ELISA and immunofluorescence for antibodies that work the best in detecting POP-1 asymmetry. A hybridoma line was then produced from the selected mouse and the monoclonal antibody was collected from the culture supernatant. The polyclonal antibody to POP-1, 94I, was raised in rabbit against the same recombinant POP-1 protein. By western blot analysis, 94I detects all forms of POP-1 we have tested to date, including truncation and mutations, no matter if they are expressed in worms, mammalian cells, or bacteria. On the other hand, the monoclonal antibody mabRL2 does not recognize the hyperphosphorylated POP-1 present in wildtype embryo extracts, but can only recognize the hypo- and un-phosphorylated POP-1. The differential recognition of the mabRL2 epitope may represent a qualitative difference between the hyper- and hypo-phosphorylated POP-1 *in vivo*. Together, the polyclonal and monoclonal antibodies allow us to test how the differential presentation of mabRL2 epitope is regulated and its possible functional significance.

In this chapter, I describe my efforts to map the mabRL2 epitope and the to test the different possibilities for the underlying molecular basis of the differential epitope presentation.

RESULTS

Mapping the epitope for mabRL2

The epitope of mabRL2 has been previously mapped to the PCA domain of POP-1 (Miao-chia Lo, personal communication; data not shown). I designed five constructs 20-amino-acid-long peptides to map the epitope. The first peptide contained the most C-terminus twenty amino acids. The following peptides each contained twenty amino acids that are shifted two amino acids toward the N-terminus compared to the previous construct (see Figure 5.1.A). I expressed these peptides in *E. coli* and tested if they can be recognized by the polyclonal antibody 94I and the monoclonal antibody mabRL2 by Western blot analysis. 94I recognized all five peptides similarly (left panel of Figure 5.1.B). Moving two amino acids from the C-terminal end had no effect on mabRL2 recognition (construct B in the right panel of Figure 5.1.B). The recognition by mabRL2 was greatly diminished when the last four amino acids were excluded (construct C in the right panel of Figure 5.1.B). Considering that the average length of an epitope is approximately 10 amino acids, we estimate the epitope for mabRL2 to be at ~amino acids 427 - 436 of POP-1.

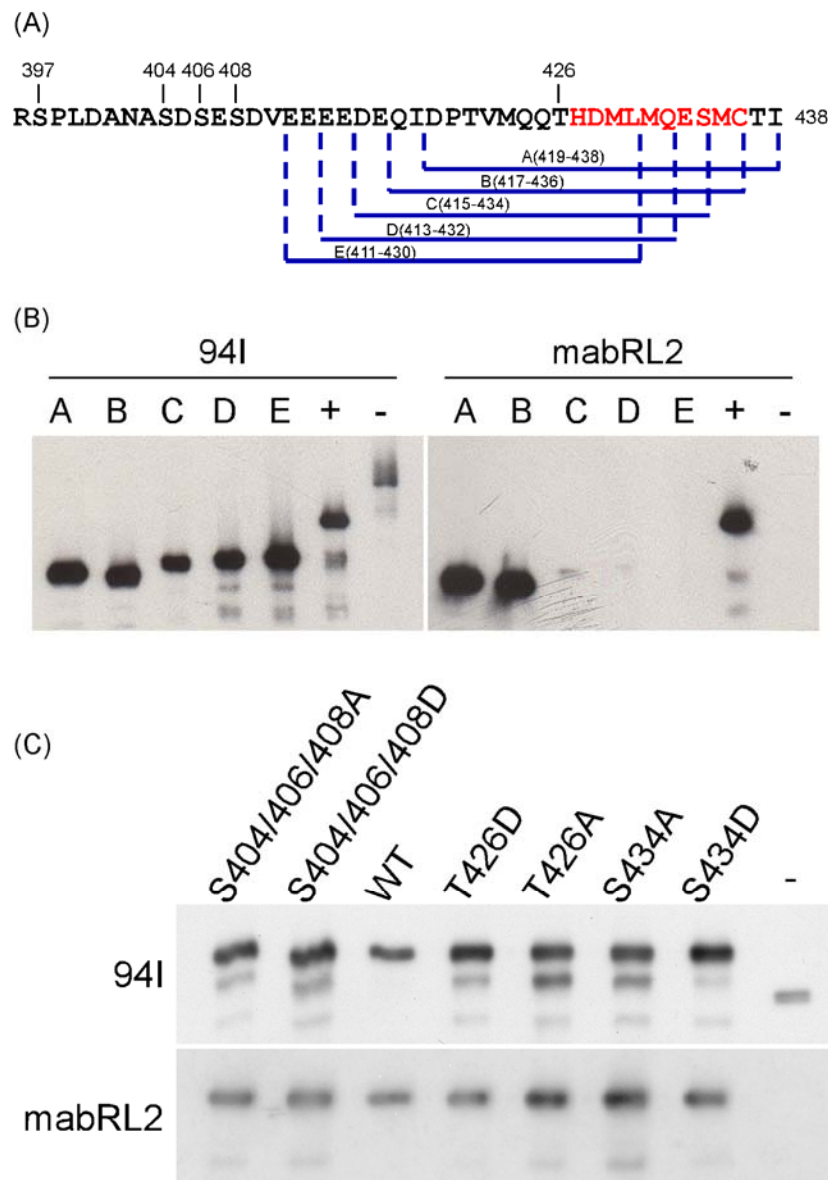


Figure 5.1. Mapping the mabRL2 epitope. (A) C-terminal sequence of POP-1 showing the 20-amino acid fragments used to map the mabRL2 epitope (highlighted in red). Amino acids that are tested by mutational analysis are marked. (B) Western blot analysis of the 20-amino acid fragments, positive control (+), and negative control (-) as detected by the polyclonal antibody 94I and the monoclonal mabRL2. (C) Western blot analysis of bacterially expressed POP-1 variants as detected by 94I and mabRL2. Top bands are POP-1; lower bands are degradation products. The negative control (-) is smaller in size.

Hyperphosphorylated POP-1 in wildtype embryos is not detected by mabRL2

Previously we have shown that POP-1 is highly phosphorylated in wildtype embryo extracts, and the phosphorylation of POP-1 is reduced in embryo extracts obtained from *lit-1(t1512ts)* mutants (Figure 5.2; Lo et al., 2004). This is evident by the mobility retardation of POP-1 proteins on SDS-PAGE, and the collapse of the slower migrating forms into a faster migrating band upon phosphatase treatment (Figure 5.2.A). I found that the hyperphosphorylated POP-1 was enriched in embryo extracts generated by gentle sonication of wildtype embryos. In fact, when I lysed wildtype embryos directly in SDS sample buffer by freeze-thaw cycles (“freeze-thawed lysates,” see Materials and Methods for detail), I found that the amount of POP-1 protein released was much greater and POP-1 was not as hyperphosphorylated compared to the sonicated embryo extract from wildtype (Figure 5.4.B). One possibility is that the hyperphosphorylated POP-1 in wildtype embryos is enriched in a certain cellular compartment and was preferentially released by sonication.

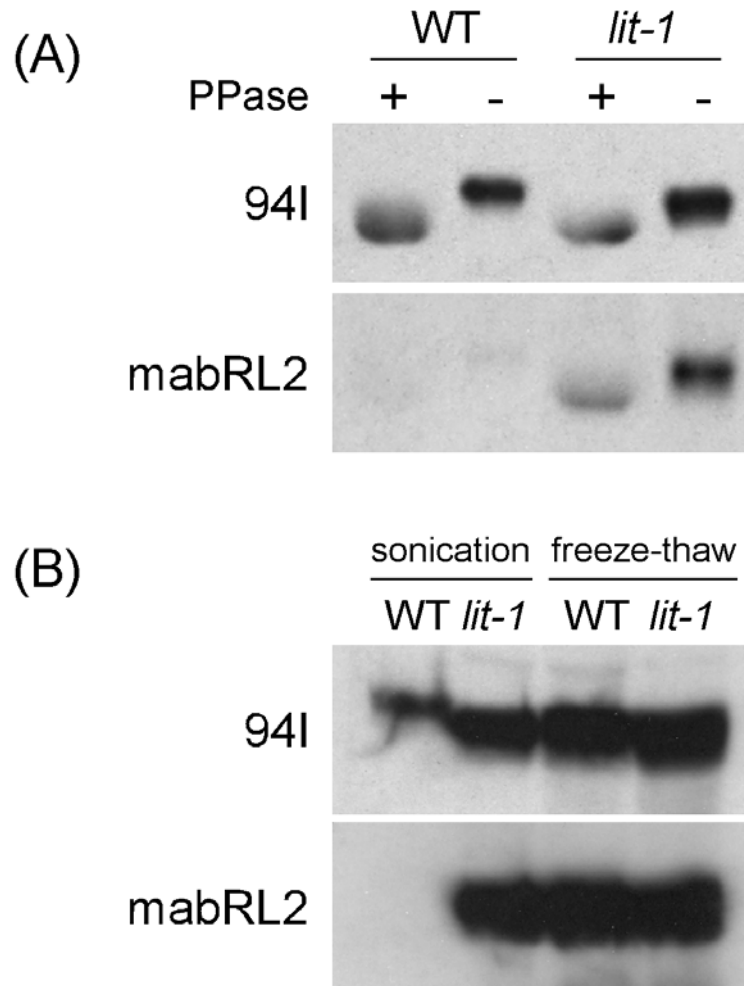


Figure 5.2. Hyperphosphorylated POP-1 in wildtype embryos is not detected by mabRL2 and is sensitive to the methods of embryo extract preparation. (A) Western blot analysis of sonicated wildtype and *lit-1(t1512ts)* embryo extracts as detected by 94I and mabRL2 with and without phosphatase treatment. POP-1 in wildtype embryo extracts migrated slower than that in *lit-1(t1512ts)*. The hyperphosphorylated POP-1 in wildtype is not detected by mabRL2, and the recognition is not enhanced after phosphatase treatment. (B) Western blot analysis of sonicated and freeze-thawed wildtype and *lit-1(t1512ts)* embryo extracts as detected by 94I and mabRL2. POP-1 is hyperphosphorylated in sonicated wildtype embryo extract but not in sonicated *lit-1(t1512ts)* extracts. By freeze-thaw lysis, POP-1 in wildtype extract was still slightly more phosphorylated than that of *lit-1(t1512ts)*, but not as high as the wildtype sonicated embryo extract.

To study the hyperphosphorylated population of POP-1 that is not recognized by mabRL2, I prepared embryo extracts by dounce homogenization followed by differential centrifugation to fractionate the embryo extracts into crude debris, nuclear, and soluble cytoplasmic fractions. I was able to enrich the hyperphosphorylated population of POP-1 further in the debris fraction by a low-speed spin of 2,000xg for 2 minutes (Figure 5.3), and it was very weakly detected by mabRL2. It is interesting that the hyperphosphorylated, mabRL2-epitope-lacking POP-1 was in the soluble supernatant of the sonicated embryo extracts, but it was identified in the debris fraction using dounce homogenization. One possible explanation is proposed in detail in the discussions of this chapter.

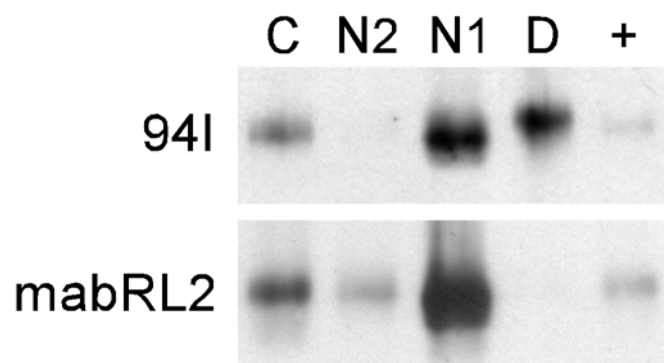


Figure 5.3. Western blot analysis of dounced wildtype embryo extracts as detected by 94I and mabRL2. Embryo extract was subjected to differential centrifugation to obtain the debris fraction (D), two nuclear fractions (N1 and N2; two consecutive spins at the same speed to ensure the cytoplasmic fraction is cleared), and the cytoplasmic (soluble) fraction (C). The debris fraction was enriched with hyperphosphorylated POP-1 which was not detected by mabRL2. +: sonicated *lit-1(t1512ts)* embryo extract as positive control.

The recognition of mabRL2 is sensitive to protein fusion to the C terminus of POP-1

One possible explanation of the mabRL2 epitope being undetectable in the hyperphosphorylated POP-1 is that the C-terminus of hyperphosphorylated POP-1 is proteolytically cleaved, deleting a part or all of the mabRL2 epitope. However, from western blotting analyses we do not detect any bands with the polyclonal antibody 94I that would suggest cleavage products of POP-1. If there are any cleavage products, they are likely to be short peptides and small in sizes that may become unstable. To test this hypothesis, I made a construct of POP-1 with GFP fused to the C-terminus (POP-1_{WT}::GFP) expressed under the *med-1* promoter, and detected if there were any cleaved products from the GFP-tagged C-terminus of POP-1.

The localization of POP-1_{WT}::GFP was variable. While many embryos still showed asymmetrical GFP distribution between A-P nuclei, some pairs had very subtle differences between A-P nuclei compared to POP-1 with GFP tagged at the N terminus (GFP::POP-1_{WT}; shown in Figure 5.4.2 B'). These observations suggest that fusing GFP to the C terminus of POP-1 interferes with POP-1 nuclear asymmetry. Moreover, the level of GFP detected in the nuclei of the Ea/p pair was often higher than that in the MSa/p pair. This is different from GFP::POP-1_{WT}, which is usually detected at higher levels in the MSa/p pair than in the Ea/p pair (Figure 5.4.2 A'), if the two pairs show any differences in their intensities at all.

I assayed the repression function of POP-1_{WT}::GFP fusion protein in *pop-1 (zu189)* mutant embryos by the rescue of MS-derived endoderm and the formation of the posterior pharynx. POP-1_{WT}::GFP did not cause gut ablation in either wildtype or *pop-1*

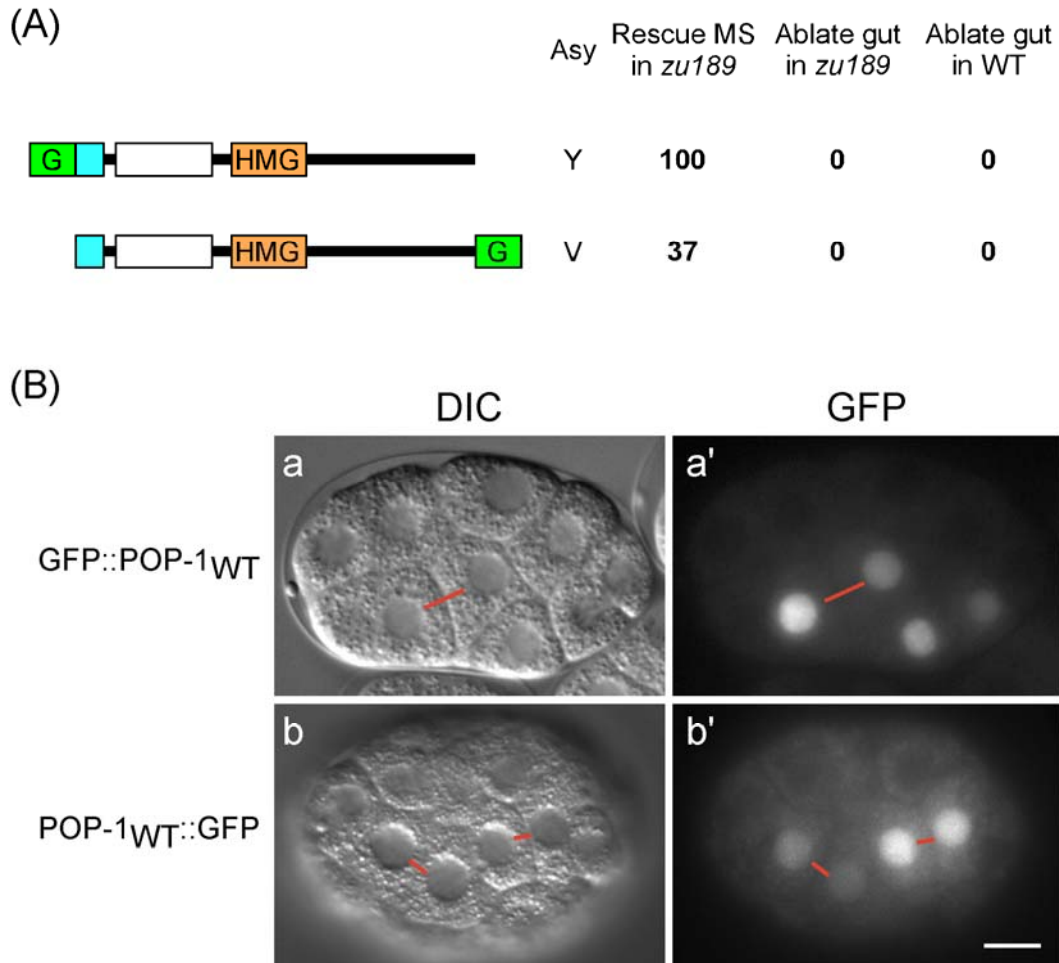


Figure 5.4. Comparison between N-terminal and C-terminal GFP fusion transgenes of POP-1. (A) Schematic representation of the transgenes used in this analysis. G: GFP; cyan: β -catenin binding domain; white: repression domain; HMG: high mobility group DNA binding domain. Asy: GFP::POP-1 asymmetry. All numbers represent percentages of embryos expressing the transgene for ability to repress endoderm in MS in *pop-1(zu189)* (rescue MS-derived posterior pharynx), to ablate endoderm in *pop-1(zu189)*, and to ablate gut in wildtype (WT). (B) Micrographs of *C. elegans* embryos carrying the transgenes. Embryos are shown at the stage when there were two MS and two E descendants expressing GFP as DIC (A and B) and corresponding GFP fluorescence (A' and B') images. The embryos are oriented with the anterior to the left. A-P sisters that are both in focus are connected by red lines. The A-P nuclear asymmetry is affected variably in C-terminal GFP fused POP-1, and this particular example shows both MSa/p and Ea/p having subtle differences in their GFP levels (B'). Scale bar = 10 μ m.

(*zul89*), but it rescued the MS defect in only 37% of *pop-1(zul89)* embryos (n=51), suggesting that fusing GFP to the C-terminus affected the repression activity of POP-1.

I analyzed the ability of mabRL2 to recognize POP-1 with GFP fused to the N-terminus (GFP::POP-1_{WT}) vs. C-terminus (POP-1_{WT}::GFP) by western blotting of embryos carrying the respective transgenes lysed in SDS sample buffer by the freeze-thaw method (Figure 5.5.A). With this method, endogenous POP-1 is mostly hypophosphorylated and GFP::POP-1_{WT} is well detected by both the polyclonal antibody 94I and the monoclonal antibody mabRL2. Both N- and C-terminal GFP fusions of POP-1 are present at similar levels as detected by the polyclonal antibody 94I on western blot. Interestingly, under the conditions in which GFP::POP-1_{WT} was well detected by mabRL2, POP-1_{WT}::GFP could not be detected at all (Figure 5.5.A). Since the western blots were performed under denaturing conditions, the lack of detection is not due to the steric obstruction of mabRL2 epitope by the GFP tag. One possible explanation is that the epitope recognition by mabRL2 requires the free carboxyl group (-COOH) and is therefore sensitive to any protein fusion at the C terminus. Or, there could be a posttranslational modification that occurs at or near the epitope and blocks the recognition by mabRL2. It is possible that for endogenous POP-1, the same modification only occurs in the hyperphosphorylated population of POP-1, but POP-1_{WT}::GFP is constitutively modified.

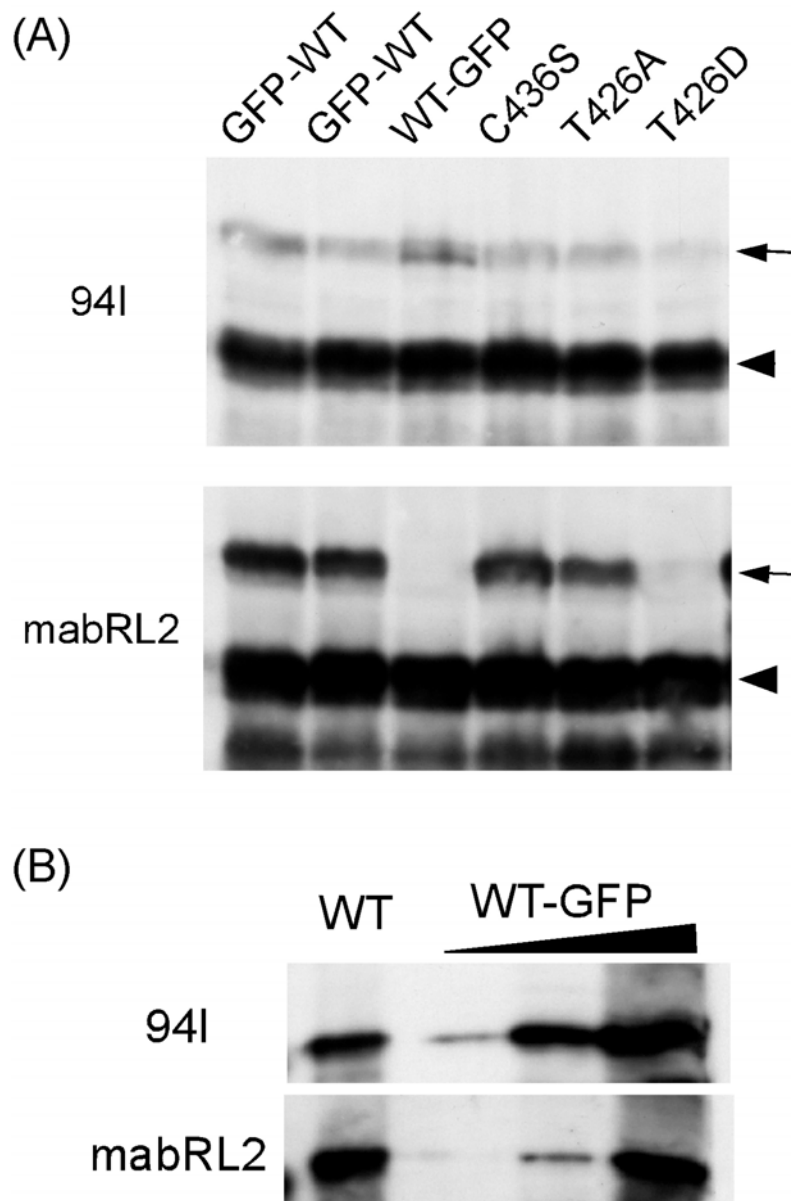


Figure 5.5. Western blot analysis of GFP::POP-1 variants as detected by 94I and mabRL2. (A) Freeze-thawed embryo extracts expressing transgenes. Note that POP-1_{WT}::GFP in embryo extract could not be detected by mabRL2. T426D may have weakened detection by mabRL2, but its expression level is also lower as revealed by 94I. (B) 6xHis::POP-1_{WT} (first lane on the left) and increasing amounts of POP-1_{WT}::GFP(exon 1) (labeled: WT-GFP) expressed in *E. coli*. Fusing GFP exon 1 to the C-terminus of POP-1 weakened but did not abolish the recognition by mabRL2.

To distinguish between these two possibilities, I made bacterially expressed full-length POP-1 with GFP exon 1 fused to the C-terminus, which does not have any of the posttranslational modifications seen in eukaryotes. Using the N-terminally 6xHis-tagged POP-1 as a standard, the POP-1::GFP(exon 1) signal probed with mabRL2 is ~10-fold reduced (Figure 5.5.B). However, this level of difference is not sufficient to explain the complete lack of detection of POP-1_{WT}::GFP expressed in worms. Therefore, although the free carboxyl group (-COOH) at the C terminus may contribute to the mabRL2 epitope, the mabRL2 epitope is likely blocked by a constitutive modification at or near the mabRL2 epitope in POP-1_{WT}::GFP.

Possible phosphorylation of the mabRL2 epitope does not account for the lack of reactivity of mabRL2 towards hyperphosphorylated POP-1

If it is phosphorylation of the epitope that is blocking mabRL2 recognition, removing it by phosphatase treatment should reverse the obstruction and allow mabRL2 recognition. For this experiment I compared sonicated embryo extracts of wildtype to those of *lit-1*. Under the sample preparation conditions, the wildtype embryo extracts were enriched for mostly hyperphosphorylated POP-1, while the *lit-1* embryo extracts contain mainly hypophosphorylated POP-1 (Figure 5.6). With the level of total POP-1 detected by 94I being similar for wildtype and *lit-1* extracts, mabRL2 could recognize the hypophosphorylated POP-1 in *lit-1* extracts, but the detection of POP-1 in wildtype embryo extracts is minimal. Phosphatase treatment of embryo extracts with increasing incubation time resulted in bands shifting towards faster migrating forms on western blots, suggesting the removal of phosphate groups from POP-1. However, there was little

difference in mabRL2 recognition before and after treating hyperphosphorylated POP-1 with phosphatase (Figure 5.6). This result suggests that phosphorylation does not account for the lack of mabRL2 recognition of the hyperphosphorylated POP-1.

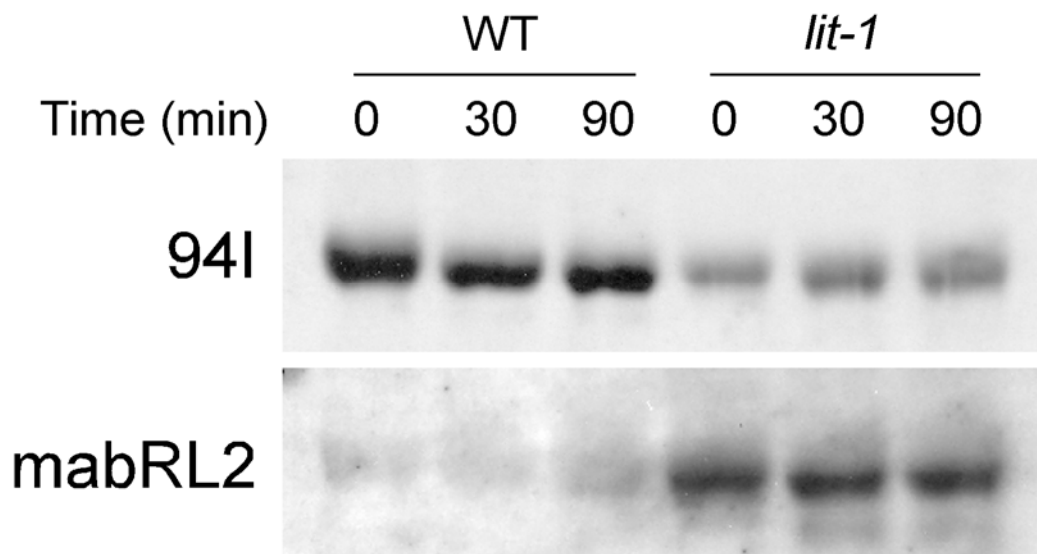


Figure 5.6. Time course analysis of wildtype and *lit-1(t1512ts)* embryo extracts treated with phosphatase. Embryo extracts were obtained by sonication so that POP-1 was mostly hyperphosphorylated and was poorly detected by mabRL2. Bands collapse towards a faster migrating, sharper band through time indicating the successful removal of phosphate groups by phosphatase treatment. Recognition of POP-1 in this wildtype embryo extract is not enhanced by phosphatase treatment.

I tested bacterially expressed POP-1 with various mutations mimicking the phosphorylated or unphosphorylated state of amino acid(s) within the PCA domain to assess their roles in mabRL2 epitope recognition (Figure 5.1.C). None of the mutations I tested, including S404/406/408A, S404/406/408D, T426A, T426D, S434A, and S434D, had any detectable effect on mabRL2 epitope recognition compared to wildtype. It is possible that none of these amino acids is important for mabRL2 epitope. It is also likely

that a combination of phosphorylation and/or other type(s) of modifications occurs on the hyperphosphorylated POP-1 in *C. elegans* embryos, and, together, these modifications contribute to the blocking of mabRL2 recognition. Expressing these mutant proteins in *E. coli* did not allow other modifications to occur, and therefore resulted in no detectable change in epitope recognition.

I tested if the mutations T426A, T426D, S434A, and S434D affect the recognition by mabRL2 when expressed in *C. elegans* embryos (Figure 5.5.A). The GFP localization patterns and repression assays are described in Chapter Four. I collected embryos from these transgenic lines and dissolved the embryos in SDS sample buffer by the freeze-thaw method. It was clear that T426A, S434A, and S434D did not block the mabRL2 epitope, and these GFP fusion POP-1 proteins were detected by 94I and mabRL2 similarly to GFP::POP-1_{WT}. The T426D mutation may have weakened the recognition by mabRL2. However, this result needs to be repeated because the GFP::POP-1_{T426D} level was quite low compared to other transgenes as detected by 94I (upper panel of Figure 5.5.A).

Possible disulfide bond formation does not account for the weak reactivity of mabRL2 towards hyperphosphorylated POP-1

It is possible that C436 forms a disulfide bond with one of the cysteines in the C-clamp (Figure 5.7) in hyperphosphorylated POP-1 so that the epitope becomes inaccessible to the mabRL2 antibody. Although the lysis buffer and the SDS sample buffer contain DTT and 2-mercaptoethanol (2-ME) respectively, these reducing agents are known to be very

labile and are themselves susceptible to both oxidation and disulfide formation. Therefore, I treated hyperphosphorylated POP-1 in sonicated wildtype embryo extracts with high concentrations of reducing agents, i.e., 20%(v/v) 2-mercaptoethanol (2-ME), 200mM dithiothreitol (DTT). Typical working concentrations for disulfide reduction are 100mM for DTT and 5% (or 700mM) for 2-ME, since DTT is a more potent reducing agent. If the formation of a disulfide bond accounts for why mabRL2 fails to detect the hyperphosphorylated POP-1, reducing the disulfide bond with high 2-ME or DTT should expose the epitope and allow mabRL2 detection. I used sonicated embryo extracts from *lit-1(t1512ts)* as my control. POP-1 is mostly hypophosphorylated in the control embryo extracts and is well detected by mabRL2 (Figure 5.8.A).

2-ME treatment caused significant improvement in mabRL2 recognition for both hyperphosphorylated POP-1 in wildtype embryo extracts and hypophosphorylated POP-1 in *lit-1(t1512ts)* embryo extracts. However, even at the highest 2-ME concentration (20%), the detection of hyperphosphorylated POP-1 by mabRL2 was still quite poor compared to the untreated hypophosphorylated POP-1 in *lit-1(t1512ts)* embryo extracts (Figure 5.8.A). DTT treatment produced an even weaker effect (Figure 5.8.B), likely due to the lower concentration used in the assay compared to 2-ME (20% = ~2.84M), or to the quality of reagent.

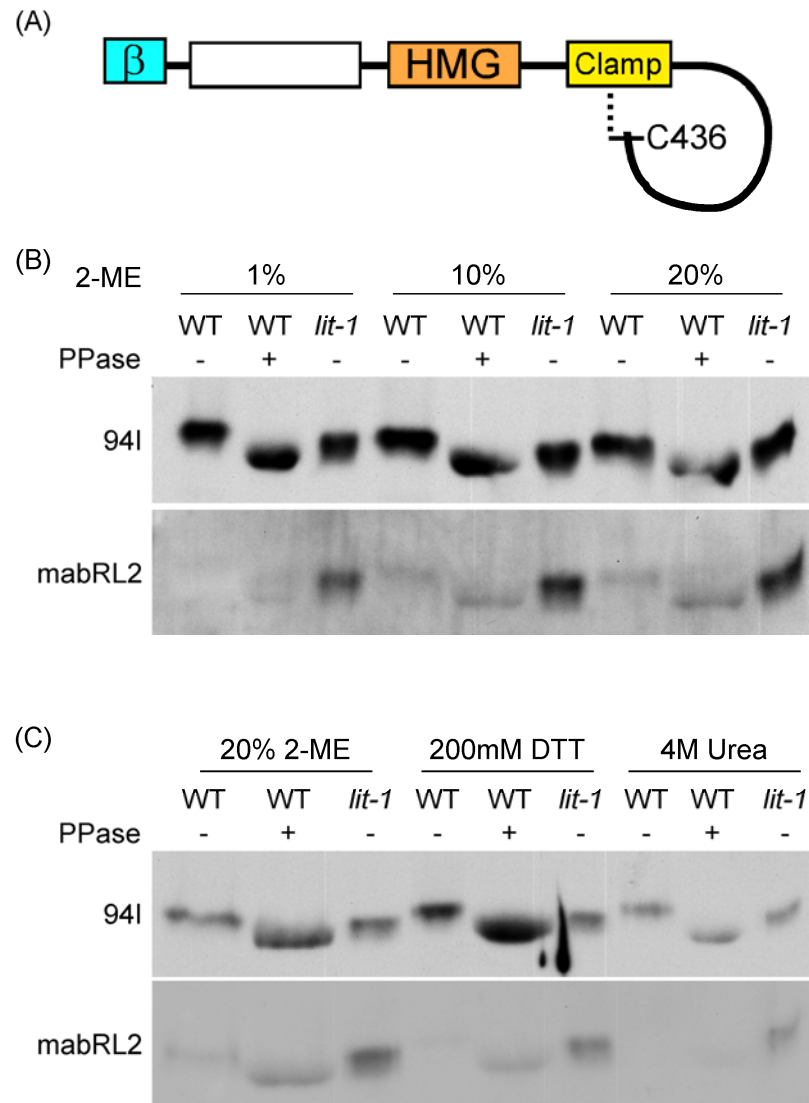


Figure 5.8. Western blot analysis of POP-1 treated with various reducing agents.

(A) Schematic view of disulfide bond formation between C436 and the C-clamp. (B) WT (+/- phosphatase treatment) and *lit-1* sonicated embryo extracts treated with 1%, 10%, and 20%(v/v) of 2-mercaptoethanol. Note that signals were enhanced overall but even with 20% 2-ME treatment, POP-1 in wildtype embryo extract was still poorly recognized by mabRL2. (C) WT (+/- phosphatase treatment) and *lit-1* sonicated embryo extracts treated with 2-ME, DTT, or Urea. Note that the signals in mabRL2 are stronger for the *lit-1* embryo extracts due to exposure. Considering that POP-1 in *lit-1* embryo extracts showed stronger signals in mabRL2 blots, the recognition of POP-1 wildtype embryo extracts are slightly enhanced in the 20% 2-ME treatment but still significantly weaker than the *lit-1* embryo extracts.

It is possible that boiling in SDS sample buffer was not sufficient to denature POP-1 completely. I treated sonicated embryo extracts with urea to a final concentration of 4M to see if the recognition of hyperphosphorylated POP-1 by mabRL2 can be enhanced. As shown in Figure 5.7.B, adding urea did not make any difference compared to control. This result suggests that either POP-1 was already fully denatured in SDS sample buffer and the mabRL2 epitope is blocked by some other factor(s), or 4M urea is still not sufficient to resolve the tertiary structure of hyperphosphorylated POP-1 and allow mabRL1 recognition.

DISCUSSION

Differences in mabRL2 epitope presentation are sensitive to the method of sample preparation

The different methods for enriching the hyperphosphorylated, mabRL2 epitope-lacking POP-1 have hinted at where this population of POP-1 might be present *in vivo*. For sonicated embryo extracts, this population of POP-1 is in the soluble portion. For the dounced embryo extracts, it appears in the debris fraction. I will discuss these two methods in detail to speculate on how hyperphosphorylated POP-1 purified by these two different methods ends up in different fractions.

First of all, for embryo extracts, embryos were collected by dissolving away adult hermaphrodites in hypochlorite solution. The embryos are protected by eggshells and

can survive the hypochlorite treatment. The eggshell contains three layers, an outer vitelline layer, middle chitinous layer, and an inner lipid layer (Bird, 1991). The vitelline layer is removed after the hypochlorite treatment, but the chitinous layer is still able to provide structural integrity to the eggshell (Bird, 1991). Therefore, the hypochlorite-treated embryos have weakened eggshells.

Dounce homogenization involves forcing samples through a narrow space between a pestle and an outer tube, thereby shearing the cell membranes. For embryos with weakened eggshells from hypochlorite treatment, one can imagine them as large water balloons (eggshells) with small water balloons (cells and organelles) inside. When these liquid-filled membranes are pushed through a narrow space, the balloons burst and contents leak out, while the layers of membrane may stay together. Therefore, this method will favor the release of all subcellular POP-1 - nuclear and cytoplasmic - into solution, but the population of POP-1 associated with membrane will be spun down and go to the debris fraction. Under DIC, the debris fraction contained unbroken or partially broken embryos, unidentifiable small particles, and a significant amount of membranous structures.

Sonication is a way to disrupt embryos by agitation with ultrasonic waves. The embryos have weak eggshells from the hypochlorite treatment, and sonication was considered complete when <10% intact embryos were left. At this point, many large chunks of fragmented embryos were still observed, suggesting the sonication was far from homogeneous and many subcellular structures are likely to be left intact. The

extracts were then centrifuged at ~16000g to remove insoluble debris including unbroken and large fragments of embryos. It is possible that this method partially damages embryos and allows cytoplasmic POP-1 to leak out into solution. The majority of POP-1 remained in other cellular compartments (such as nuclear POP-1) and was removed as insoluble debris. Another feature of the sonication method is that lipids tend to form small vesicles after sonication. When the lipids in cell membranes are released during sonication, lipid vesicles may form and stay in the soluble fraction. If a population of POP-1 is associated with the lipids in cell membranes, it is possible that it can stay in solution, too.

Considering the physics behind these two methods, it is most likely that hyperphosphorylated, mabRL2-epitope-lacking POP-1 is associated with the membrane. Two lines of evidence support this notion. First, there is membrane staining detected in wildtype embryos with the polyclonal antibody 94I but not with the monoclonal antibody mabRL2 (data not shown). Second, the hyperphosphorylated, mabRL2-epitope-lacking POP-1 in the dounced debris from can not be extracted by non-ionic detergents such as Triton X-100 (Scott Robertson, personal communication; data not shown). These supports that the hyperphosphorylated POP-1 which lacks mabRL2 epitope may be associated with detergent-resistant membrane. Further analysis with markers and better fractionation techniques may help identify the subcellular localization of hyperphosphorylated POP-1.

The importance of the C-terminus of the POP-1 protein

There are a couple of previous reports suggesting that POP-1 with GFP fused to the C terminus has abnormal localization. Maduro et al. (2002) reported that reporters with GFP fused to the C terminus of POP-1 do not recapitulate POP-1 asymmetry, although there were no actual data shown. Siegfried et al (2004) showed that a POP-1::GFP construct including ~3.5 kb of sequence upstream of the *pop-1* gene, introns 1 and 2, and GFP fused at the C terminus does not show different nuclear levels between sister cells in any tissues. However, from the description of how the reporter was constructed, it seems like the C-terminal most ~12 amino acids of POP-1 are deleted in the final construct. From my analysis, fusing a tag to the C terminus affects POP-1 nuclear asymmetry. Therefore, all evidence suggests that the region near the very C-terminus of POP-1 contains an important regulatory element for POP-1 asymmetry.

The observation that for endogenous POP-1, mabRL2 epitope recognition is only blocked in the hyperphosphorylated population suggests that this is a regulated event. If the lack of mabRL2 epitope is due to a posttranslational modification at or near the epitope, this modification only occurs in the hyperphosphorylated POP-1. When a tag is fused to the C terminus, this modification becomes constitutive and results in the blocking of mabRL2 epitope in all POP-1_{WT}::GFP. It is possible that in wildtype, phosphorylation at certain site(s) is required to allow the unknown modification to occur, maybe by opening up the three dimensional structure locally. When a tag is fused to the C-terminus, the presence of tag makes the local structure more open, so that the modification becomes constitutive.

A possible molecular basis for the masking of mabRL2 epitope in hyperphosphorylated POP-1

I tested two hypotheses for why the hyperphosphorylated POP-1 in wildtype embryo extracts is not recognized by mabRL2 on western blot analysis: (1) phosphorylation; and (2) disulfide bond formation. Unfortunately, my results do not seem to support or rule out either one at this point. Mutations changing putative phosphorylation sites to alanines or aspartic acids do not have significant effects on mabRL2 recognition, although it is possible that aspartic acids may not mimic the phosphorylated state. Meanwhile, phosphatase treatment did not restore the mabRL2 epitope in hyperphosphorylated POP-1. These results suggest that phosphorylation is not likely to be the main reason why mabRL2 fails to detect hyperphosphorylated POP-1.

Treating hyperphosphorylated POP-1 with 2-ME at concentrations as high as 20% did enhance mabRL2 detection on western blot to some extent. It is possible that a disulfide bond does form between POP-1_{C436} and one of the cysteines in the C-clamp and contributes to the blocking of the mabRL2 epitope. It is also possible that hyperphosphorylated POP-1 becomes more accessible to mabRL2 in a reducing environment. However, this does not have a major impact on the mabRL2 epitope because the signal was still quite weak compared to the signal seen with hypophosphorylated POP-1. I concluded that phosphorylation and/or disulfide bond formation may contribute partially to the blocking of mabRL2 epitope in hyperphosphorylated POP-1. Other possibilities include an unidentified posttranslational modification at or near the mabRL2 epitope, or proteolytic cleavage of the C-terminus in

hyperphosphorylated POP-1. The most definitive way to answer this question is to purify hyperphosphorylated POP-1 and use mass spectrometry to determine the molecular basis for the blocking of mabRL2 epitope.

MATERIALS AND METHODS

Strains

N2 was used as the wildtype strain. Genetic markers: LGI, *pop-1(zu189)*, *dpy-5(e61)*, *teIs3[P_{med-1gfp}::pop-1]*, *hT1(I;V)*; LGIII, *unc-119(ed3)*; LGIV, *him-3(e1147)*. TX352 *teEx72[P_{med-1gfp}::pop-1]*, TX498 *teEx160[P_{med-1gfp}::pop-1(S109/118/T120/S127A)]*, and TX629 *teEx248[P_{med-1gfp}::pop-1(S107/109/118/T120/S127D)]* were generated by M-c Lo. TX839 *teEx337[P_{med-1gfp}::pop-1(T426A)]*, TX874 *teEx365[P_{med-1gfp}::pop-1(T426D)]*, TX1094 *teEx512[P_{med-1gfp}::pop-1(S434A)]*, TX1095 *teEx513[P_{med-1gfp}::pop-1(S434D)]*, and TX1164 *teEx560[P_{med-1gfp}::pop-1(C436S)]* were described in previous chapters.

Protein expression in *E. coli*

DNA sequences encoding 20 amino acid fragments spanning from the C terminus of POP-1 with each construct shifting two amino acids away from the C terminus were cloned by “one-tube” protocol to put *attB*-PCR products directly into the destination vector pDEST15 (N-terminal GST tag) for epitope mapping. Wildtype and mutant POP-1 entry clones were used for LR reactions with the destination vector pDEST17 (N-

terminal 6xHis tag). Expression in *E. coli* was induced by IPTG at 0.5mM for 3 hours at room temperature. Bacteria were sonicated in co-IP buffer (Calvo *et al.*, 2001) at setting 3 for 3 times of 15-second sonication pulses with 10-second intervals between each round of sonication, and centrifuged at ~16,000g at 4 degrees for 30 minutes. SDS sample buffer was added to the resulting supernatant and boiled. The boiled solution was then analyzed by Western blot analysis.

***C. elegans* embryo extracts preparation methods and treatments**

Sonication

Embryos were collected from synchronized gravid adults by hypochlorite treatment. Embryo pellets were resuspended in 3X pellet volume of co-IP buffer (Calvo *et al.*, 2001), sonicated on ice for the total of ~15 times of 15-second per sonication pulses with 10-second intervals between each round of sonication, until <10% intact embryos remained when viewed under dissecting scope. Sonicated embryo lysates were then centrifuged for 10 minutes at ~16000g, and the resulting supernatants were collected as sonicated embryo extracts. TX150 *lit-1(t1512)* mutant animals were shifted to 25°C at the L3 stage and embryos were collected at 25°C.

Dounce homogenization

Embryos were collected from synchronized gravid adults by hypochlorite treatment and resuspended in 3X pellet volume of co-IP buffer (Calvo *et al.*, 2001). Embryo suspensions were then homogenized on ice in a 5ml Dounce homogenizer until <10% intact embryos remained. For fractionation experiments, dounced embryo

suspension was centrifuged at 2,000g for 2 minute to collect “debris.” The resulting supernatant was centrifuged twice at ~16,000g for 10 minutes. Both pellets were pooled together into the “nuclear” fraction, and the final supernatant is “cytosol.” “Debris” and “nuclear” fractions were washed one time with 500µl co-IP buffer (Figure 5.9).

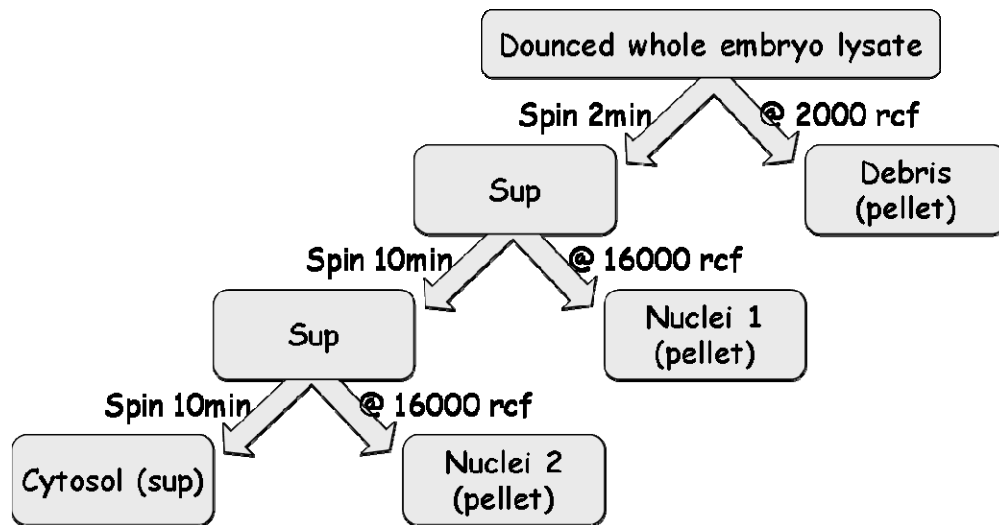


Figure 5.9. Flow chart of the fractionation of embryo extract after douncing. At the end of douncing, the crude embryo lysate was subjected to three rounds of centrifugation at the speeds indicated. All steps were performed at 4°C.

Freeze-thaw lysis

Embryos were collected from synchronized gravid adults by hypochlorite treatment. After the final wash with M9 buffer, embryo pellets were mixed with equal volumes of 2XSDS sample buffer and processed through 3 cycles of boiling (4 minutes) and freezing (1 minute in a dry ice/ethanol bath). After the last boiling, the soluble portion of each sample was collected and subjected to Western blot analysis.

Phosphatase treatment

For phosphatase treatments, 20 µg of embryo extracts were incubated with 20 U of calf intestinal alkaline phosphatase (NEB) at 37°C for 1.5 hours prior to boiling in SDS sample buffer.

Treatments with reducing agents

Sonicated embryo extracts were mixed with 2X SDS sample buffer containing 2%, 20%, or 40% 2-Mercaptoethanol, or 400mM dithiothreitol (DTT) and incubated at room temperature for 15 minutes before boiling. For urea treatment, sonicated embryo extracts were mixed with SDS sample buffer containing 2% 2-mercaptoethanol, boiled, and cooled to room temperature. Urea was added to 4M final concentration and the sample incubated at room temperature for 15 minutes before it was subjected to SDS-PAGE and Western blot analysis.

Analysis of Embryos and Imaging

Imaging of live embryos was performed using an Axioplan microscope equipped with epifluorescence and differential interference contrast (DIC) optics, and a MicroMax-512EBFT CCD camera controlled by the Metamorph acquisition software (Molecular Devices, Inc.). 4-D microscopy was performed on live embryos mounted on 3% agarose pads sealed with Vaseline to prevent over-drying. At each time point of live imaging, GFP fluorescence and DIC images were collected either as stacked images or from a selected focal plane to follow particular anteroposterior sister pairs. Stacked images were collected as sequential images along the z-axis with 8 slices per embryo (~3 microns

between adjacent images). Consecutive time points were 3 or 4 min apart. All images were collected as 16-bit with the raw pixel values within the linear range of the CCD camera and processed and quantified using the ImageJ program (Lo et al., 2004; Rogers et al., 2002).

Assay for POP-1 Repressor Activity

Various *gfp::pop-1* transgenes were introduced into *pop-1(zu189)* mutant embryos by mating males carrying the transgenes with hermaphrodites homozygous for the *pop-1(zu189)* mutation at 20°C for 24 hours. The embryos were collected onto 3% agar pads, checked for the presence of GFP using fluorescence microscopy, and allowed to develop at 16°C for 18 hours. Then the embryos were checked with differential interference contrast (DIC) optics for the production of posterior pharynx and scored as rescued if they produced the wildtype amount of posterior pharyngeal tissues. Intestinal cells were identified by their birefringent gut granules under polarized optics.

CHAPTER SIX

Regulation of the interaction between POP-1 and its coactivator SYS-1

INTRODUCTION

Interactions between POP-1 and *C. elegans* β -catenin homologs

There is only one β -catenin and multiple TCF isoforms in the vertebrates. The single β -catenin functions both in cell adhesion by associating with cadherins at cell junctions, and as a transcriptional coactivator in the canonical Wnt pathway (also called the Wnt/ β -catenin pathway) by interacting with the downstream transcription factor, TCF. The differences in the outcomes of canonical Wnt signaling are thought to be determined by the TCF isoforms expressed in the specific tissue at a certain time. In *C. elegans*, there are four β -catenins, BAR-1, HMP-2, WRM-1, and SYS-1, each with distinct functions, and only one TCF protein, POP-1. HMP-2 binds to cadherin and functions in cell adhesion, and it does not interact with POP-1. BAR-1 binds to POP-1 and functions in processes regulated by the canonical Wnt pathway. WRM-1 binds to the Nemo-like kinase LIT-1 and activates its kinase activity. WRM-1 interacts with POP-1 very weakly and the interaction does not require the β -catenin binding domain of POP-1. WRM-1 is required for the phosphorylation of POP-1 by LIT-1 and the subsequent lowering of the nuclear level of POP-1.

SYS-1 is a recently discovered β -catenin homolog identified not by sequence similarities but based on its function. SYS-1 can rescue a *bar-1* mutant when expressed

under the *bar-1* promoter, and it functions as a coactivator of POP-1 in tissue culture reporter assay (Kidd et al., 2005). SYS-1 has been shown to interact with POP-1 directly through the β -catenin interacting domain of POP-1, although the strength of the interaction is weaker compared to that between POP-1 and BAR-1 (Kidd et al., 2005). We and others showed that SYS-1 is required for the expression of POP-1-dependent genes and cell fates (also see Chapter Two) (Huang et al., 2007; Phillips et al., 2007) and it functions together with WRM-1 in what has been termed the “Wnt/ β -catenin asymmetry pathway” (Mizumoto and Sawa, 2007).

Crystal structure of POP-1/SYS-1 complex

SYS-1 has only ~10% sequence identity to canonical β -catenins (Kidd et al., 2005). Although it functions as a β -catenin, it was reported to have only three armadillo repeats (Kidd et al., 2005). Liu et al. (2008) solved the crystal structure of the SYS-1 by itself and in a complex with the β -catenin binding domain of POP-1. Surprisingly, although the primary sequence of SYS-1 is highly divergent, structurally it is very similar to the canonical β -catenins and possesses 12 armadillo repeats. Canonical β -catenins have extended C-terminal domains, which are important for transcriptional activation. The C-terminal domain of SYS-1 has only 16 amino acids, significantly shorter than that of canonical β -catenins at >100 residues. This suggests that SYS-1 may use alternative mechanisms to activate downstream target genes.

To determine the crystal structure of the SYS-1/POP-1 complex, the armadillo repeat of SYS-1 was crystallized with POP-1₁₋₂₀₀ (Liu et al., 2008). Although the first two hundred amino acids of POP-1 were included in the crystals, electron density was only observed for POP-1 amino acids 7-14. This shows that the primary SYS-1-interacting domain of POP-1 is small, and the rest of the POP-1₁₋₂₀₀ peptide does not adapt a stable folded structure in the crystal and may not make any significant contribution to the SYS-1/POP-1 binding. Within POP-1 amino acids 7-14, POP-1 amino acid D9 is a conserved aspartic acid which forms a crucial salt bridge critical for the interaction between TCF and β -catenin (Graham et al., 2000), including POP-1/SYS-1 binding (Liu et al., 2008). Mutating D9 to glutamic acid has been shown to diminish the interaction between TCF and β -catenin. One caveat of this structural study is that it only used less than half of the POP-1 protein and it did not take into consideration any posttranslational modifications of POP-1.

In this chapter, I investigate whether the binding between POP-1 and SYS-1 is regulated in the context of full-length proteins. I tested if mutations of the amino acids I characterized in Chapters Four and Five affect the ability of POP-1 to be coimmunoprecipitated with SYS-1 both in the presence and in the absence of LIT-1/WRM-1 in the mammalian cell culture system. Wildtype or mutant POP-1 proteins were expressed in HeLa cells. A duplicate set of HeLa cells were transfected with the same set of constructs together with plasmids expressing LIT-1 and WRM-1. The amount of POP-1 expressed in each lysate was determined by western blot with the polyclonal antibody 94I, and the result was used to normalize the input levels of POP-1

protein for immunoprecipitation. Myc-tagged SYS-1 was expressed separately in HeLa cells either with or without LIT-1/WRM-1 cotransfection. SYS-1 in HeLa cell lysate was immunoprecipitated by anti-Myc agarose beads and the same amount of SYS-1-bound beads were mixed with the normalized POP-1-containing lysates for immunoprecipitation. The amount of POP-1 brought down in each immunoprecipitation was analyzed by SDS-PAGE, followed by western blot using the polyclonal antibody against POP-1, 94I. The results are described below.

RESULTS

Interaction of POP-1 with SYS-1 is weakened upon LIT-1/WRM-1 cotransfection

Compared to POP-1_{WT}, the level of the negative control POP-1_{D9E} was reduced upon coimmunoprecipitation with SYS-1 (Figure 6.1). POP-1_{ΔN}, which had the β-catenin binding domain deleted, was tested as a negative control as it may provide a more complete abolishment of POP-1/SYS-1 interaction. However, POP-1_{ΔN} was either not expressed or not stable and could not be detected, preventing any further analysis. Under the assay conditions, the interaction between POP-1_{D9E} and SYS-1 was not abolished but greatly reduced in the absence of LIT-1/WRM-1, suggesting the assay condition was not very stringent.

Under these conditions, the interaction between POP-1 and SYS-1 was weakened upon LIT-1/WRM-1 co-transfection based on the following evidence. (1) In the case of

POP-1_{WT}, with similar input levels (upper panels of Figure 6.1), the amount of POP-1_{WT} coimmunoprecipitated was reduced upon LIT-1/WRM-1 cotransfection (lower panels of Figure 6.1). (2) Upon LIT-1/WRM-1 cotransfection, POP-1_{WT} showed a slower migrating population of phosphorylated POP-1. However, the POP-1_{WT} coimmunoprecipitated with SYS-1 showed more of a faster migrating band corresponding to the position of the unphosphorylated form of POP-1 in the absence of LIT-1/WRM-1 (Figure 6.1). This result suggests that the phosphorylated POP-1_{WT} did not bind to SYS-1 as well as the unphosphorylated form. Therefore, when there are mixed populations of phosphorylated and unphosphorylated POP-1, the unphosphorylated POP-1 is preferentially immunoprecipitated with SYS-1. (3) The

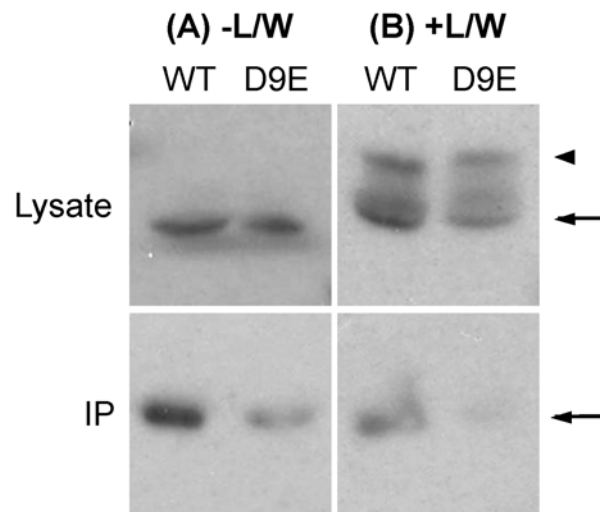


Figure 6.1. Coimmunoprecipitation of POP-1_{WT} and POP-1_{D9E} with SYS-1. Western blot probed with 94I of HeLa cell lysate inputs (upper panels) and the corresponding immunoprecipitation with anti-Myc to pull down Myc::SYS-1 (lower panels) in the presence (B) or absence (A) of LIT-1/WRM-1. The POP-1 variants expressed are indicated on top. Input loading is ~7% of IP. L/W: LIT-1/WRM-1; arrow: unphosphorylated POP-1; arrowhead: phosphorylated POP-1.

binding between SYS-1 and POP-1_{D9E} became weaker upon LIT-1/WRM-1 cotransfection (compare to Figure 6.1), suggesting that LIT-1/WRM-1 cotransfection further weakened the binding between SYS-1 and POP-1_{D9E}.

POP-1_{ΔPCA} showed weakened binding toward SYS-1

POP-1_{ΔPCA} also showed reduced interaction with SYS-1 (Figure 6.2). I showed in Chapter Three that deleting the PCA domain blocks all LIT-1/WRM-1-dependent phosphorylation of POP-1; therefore, POP-1_{ΔPCA} is not phosphorylated at the Exp sites. If only phosphorylation at the Exp sites weakens POP-1/SYS-1 binding, POP-1_{ΔPCA} would not be predicted to have reduced interaction with SYS-1. This result strongly suggests that the PCA domain participates in the interaction between POP-1 and SYS-1, independent of the phosphorylation by LIT-1/WRM-1. Although POP-1_{T426D} showed similar phenotypes to POP-1_{ΔPCA} in its effect on POP-1 asymmetry, the ability to repress endoderm fate, and LIT-1/WRM-1-dependent phosphorylation, it had very little, if any, effect on the interaction with SYS-1 (Figure 6.2).

The differences between POP-1_{WT} and POP-1_{ΔPCA} seemed less dramatic in Figure 6.2.B compared to 6.2.A. Since POP-1_{ΔPCA} is not phosphorylated by LIT-1/WRM-1 (see Chapter Three, Figure 3.4), the amount of POP-1_{ΔPCA} is not expected to change upon LIT-1/WRM-1 cotransfection. When the level of POP-1_{WT} being brought down decreased in the presence of LIT-1/WRM-1, and the amount of POP-1_{ΔPCA}

coimmunoprecipitated did not decrease further, the difference between POP-1_{WT} and POP-1_{ΔPCA} is reduced.

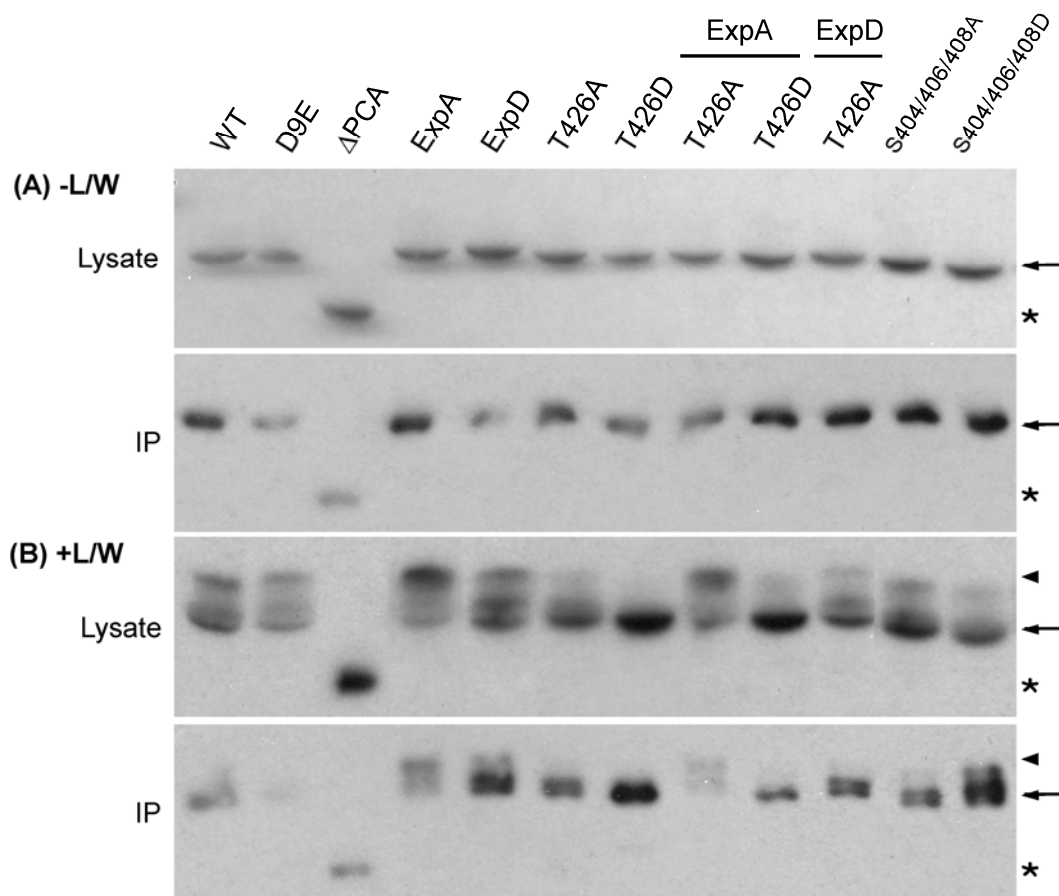


Figure 6.2. Coimmunoprecipitation of POP-1 variants with SYS-1. Western blot probed with 94I of HeLa cell lysate inputs (upper panels in A and B) and the corresponding immunoprecipitation with anti-Myc to pull down Myc::SYS-1 (lower panels) in the presence (B) or absence (A) of LIT-1/WRM-1. The POP-1 variants expressed are indicated on top. Input loading is ~7% of IP. L/W: LIT-1/WRM-1; arrow: unphosphorylated POP-1; arrowhead: phosphorylated POP-1; *: Δ PCA, which is not phosphorylated upon LIT-1/WRM-1 cotransfection.

ExpD reduced the interaction between POP-1 and SYS-1

POP-1_{ExpD} also showed significant reduction in the amount of POP-1 being brought down with SYS-1, suggesting that acidification of POP-1 at the Exp sites weakened the interaction between POP-1 and SYS-1. When LIT-1 and WRM-1 were cotransfected, the amount of POP-1_{ExpD} may have been higher than that of POP-1_{WT}. However, POP-1_{WT} and POP-1_{ExpD} migrated differently in the presence of LIT-1/WRM-1 (upper panel of Figure 6.2.B), making it impossible to compare fairly the relative amounts being brought down with SYS-1.

ExpA and T426

Both POP-1_{ExpA,T426A} and POP-1_{ExpA,T426D} had reduced coimmunoprecipitation with SYS-1 upon LIT-1/WRM-1 cotransfection (Figure 6.2.B). There was no obvious reduction for POP-1_{ExpA}, POP-1_{T426A}, or POP-1_{T426D}. Since POP-1_{ExpA,T426A} and POP-1_{ExpA,T426D} showed very different phosphorylation profiles upon LIT-1/WRM-1 cotransfection (upper panel of Figure 6.2.B), it is curious that both of them showed reduced binding towards SYS-1. Since POP-1_{ExpA} is highly phosphorylated by LIT-1/WRM-1 and POP-1_{T426D} was not phosphorylated at all, the difference in the amount of POP-1_{ExpA} brought down with SYS-1 is hard to compare to POP-1_{WT}. It is possible that the single mutations alone caused slight reductions in POP-1/SYS-1 interaction, but the differences were too mild under the low stringency of this experiment. Only when ExpA was combined with T426 mutations and further reduced the binding between POP-1 and SYS-1 did it show detectable differences.

Others

Because POP-1 variants were phosphorylated to different degrees upon LIT-1/WRM-1 cotransfection, it is hard to determine if the input levels of POP-1 are equal, and if there are differences between the total amount of POP-1 being coimmunoprecipitated with SYS-1 (Figure 6.2.B). It is therefore difficult to determine whether the mutations affected POP-1/SYS-1 interaction upon LIT-1/WRM-1 phosphorylation in this set of experiments. In order to better distinguish the amounts of POP-1 being brought down, in the future, the normalization of POP-1 expression levels and the quantification after immunoprecipitation should be done by resolving the lysates briefly by SDS-PAGE so that all POP-1 migrates together and forms sharp bands despite their levels of phosphorylation.

DISCUSSION

Phosphorylation of POP-1 by LIT-1/WRM-1 affects the binding affinity of POP-1/SYS-1 activation complex

My results show that the binding between POP-1_{WT} and SYS-1 is weakened upon LIT-1/WRM-1 cotransfection, and POP-1_{ExpD} showed weaker interaction with SYS-1 than POP-1_{WT} did, independent of LIT-1/WRM-1. Since LIT-1/WRM-1 phosphorylates POP-1 at the Exp sites and leads to the nuclear export of POP-1, it makes sense that the phosphorylated POP-1 would have reduced affinity towards SYS-1. Otherwise, the nuclear export of POP-1 would lead to lowering of nuclear SYS-1 as well. In the E blastomere, which has higher nuclear levels of LIT-1 and WRM-1 than its anterior sister

MS, the nuclear level of SYS-1 is also higher, suggesting that SYS-1 nuclear level is not reduced with the nuclear export of POP-1. Phosphorylation at the Exp sites may cause allosteric changes in the β -catenin domain and affect the interaction with SYS-1. Alternatively, in tertiary structure, the Exp sites may be located in the vicinity of the β -catenin domain and participate in β -catenin binding directly.

POP-1 contains LIT-1/WRM-1-dependent phosphorylation sites other than the Exp sites (e.g., the model of the Act sites as mentioned in Chapter Four). None of the other POP-1 variants mutating putative phosphorylation sites shows significant changes in its ability to bind to SYS-1 in this analysis. Further analysis is required to elucidate how phosphorylation at these other sites contributes to the interaction between POP-1 and SYS-1.

The PCA domain of POP-1 is important for POP-1/SYS-1 interaction

The interaction between POP-1 and SYS-1 requires the β -catenin binding domain. However, my observation that deleting the PCA domain weakens the interaction between POP-1 and SYS-1 suggests that the C-terminal region of POP-1 may contribute to POP-1/SYS-1 binding. The effect of deleting the PCA domain is not through affecting the LIT-1/WRM-1-dependent phosphorylation of POP-1. The simplest model is that the PCA domain participates in SYS-1 binding directly. There is no precedent suggesting domain(s) other than the β -catenin interacting domain of TCF family protein are involved in the interaction with β -catenin. However, the PCA domain is unique to POP-1 and was

not included in the structural analysis or other binding assays with SYS-1 (Kidd et al., 2005; Liu et al., 2008). It is possible that in the tertiary structure of the POP-1/SYS-1 complex, the PCA domain contributes to the interaction between POP-1 and SYS-1 either through direct interaction with SYS-1, or by indirectly stabilizing the binding of SYS-1 to the β -catenin binding domain of POP-1.

Regarding the possible interaction between SYS-1 and the PCA domain of POP-1, it is worth mentioning again that the PCA domain may interact with another β -catenin, WRM-1 (see discussions in Chapter Three). An attractive model is that the PCA domain may be regulated in an unknown way which determines whether it interacts with SYS-1 or WRM-1. If the PCA domain interacts with SYS-1, POP-1/SYS-1 complex functions in the activation of endoderm fate. If the PCA domain interacts with WRM-1, then LIT-1 is recruited and results in the phosphorylation of the Exp sites and nuclear export of POP-1.

It should be noted that in some other trials, POP-1_{WT} was so highly phosphorylated upon LIT-1/WRM-1 cotransfection that no or very little unphosphorylated POP-1 was detected (e.g., Figure 4.5). This is clearly not the case for the experiments shown in this chapter, suggesting that the phosphorylation by LIT-1/WRM-1 was far from effective. Since the unphosphorylated POP-1 has higher affinity toward SYS-1, ineffective phosphorylation would mask potential differences between the POP-1 variants tested in their abilities to bind to SYS-1. The experiment should be

repeated to achieve higher levels of phosphorylation to reveal any potential effect on POP-1/SYS-1 interaction.

MATERIALS AND METHODS

Plasmid Construction

All clones expressed in HeLa cells were driven by the CMV promoter in pcDNA-based Gateway vectors. LIT-1(pRL1684), and WRM-1(pRL1530) both have N-terminal FLAG tags. All POP-1 constructs were tagged N-terminally with FLAG (destination vector pRL1312). SYS-1(pRL2722) construct was made by LR reaction between the destination vector pRL1313 (N-terminal c-Myc tag) and the SYS-1 entry clone pRL2687.

Transfection assay

HeLa cells were cultured in 100mm Petri dishes in Dulbecco's modified Eagle's medium (DMEM) with 10% FBS. Cells were transfected at ~70% confluency with 12µg of total DNA using Turbofect *in vitro* transfection reagent (Fermentas). Twenty-four hours post-transfection, the cells were harvested in 0.75ml CelLytic M cell lysis reagent (Sigma) supplemented with Halt Protease and Phosphatase Inhibitor Cocktail (Pierce) and centrifuged at ~16,000g for 10 minutes. The resulting cell lysates were kept on ice. For all transfections of POP-1 variants with or without LIT-1/WRM-1 cotransfection, 50µl of each lysate was set aside and boiled in SDS sample buffer. The boiled solution was resolved by 10% SDS-polyacrylamide gel electrophoresis (SDS-PAGE) and detected

with the Snap i.d. Protein Detection System (Millipore). The primary antibody used was 94I (rabbit polyclonal antibody against POP-1) at 1:500. The secondary antibody used was ECL anti-rabbit-IgG, HRP-linked whole antibody (GE Healthcare) at 1:5,000. The expression levels of POP-1 variants were determined and adjusted with mock transfection HeLa cell lysate to the final volume of 700 μ l so that the input levels of POP-1 variants were equal for each immunoprecipitation. Before proceeding to immunoprecipitation, 50 μ l of each equilibrated lysate was set aside, boiled in SDS sample buffer, and saved as a reference for input levels.

Immunoprecipitation

A total of eight 100mm dishes of HeLa cells were transfected with SYS-1 with or without LIT-1/WRM-1 cotransfection. Lysates with the same plasmids transfected were pooled together, and split into 8 x 750 μ l aliquots. , 40 μ l α -c-Myc agarose (9E10, Santa Cruz Biotechnology) was added to each tube, and the tubes were rotate at room temperature for 2 hours then shifted to 4°C for 2 more hours. At the end of the incubation, beads were combined and centrifuged at 16,000rcf for 30 sec and washed 3 times with cold PBS. After the last centrifugation, the beads were resuspended into a total volume of 250 μ l and kept on ice.

For each equilibrated HeLa cell lysate, 15 μ l of SYS-1-coupled 1 α -c-Myc agarose was used for immunoprecipitation at 4°C overnight. Agarose beads were spun down by centrifugation at 16,000rcf for 30 seconds and washed two times in cold, high-salt PBS (PBS supplemented with NaCl so that total salt concentration was 500mM). After the

second wash, the beads were washed one more time in regular PBS. The pelleted beads were then resuspended into a final of 50 μ l with PBS, boiled in SDS sample buffer, and subjected to Western blot analysis.

CHAPTER SEVEN

Conclusions

This study focuses on how the TCF protein POP-1 is regulated both quantitatively and qualitatively for the specification of endoderm fate in early *C. elegans* embryos. It has been known for a long time that the nuclear level of POP-1 is lowered in all posterior cells in the A-P divisions in response to the Wnt and MAPK signaling pathways. Not until recently has it become clear that the lowering of nuclear POP-1 is required for the activation of endoderm genes. I show in Chapter Two that the reason why nuclear POP-1 level has to be lowered for the induction of endoderm fate is because of the limiting β -catenin coactivator SYS-1. Similar to POP-1, SYS-1 exhibits reiterated asymmetry, but its asymmetry is reciprocal to that of POP-1. It is not the absolute quantity of either SYS-1 or POP-1 but the SYS-1-to-POP-1 ratio that is critical for the specification of anterior and posterior cell fates. A high ratio drives posterior cell fates whereas a low ratio drives anterior cell fates in multiple A-P divisions throughout development.

The specification of endoderm fate in *C. elegans* embryos requires the Wnt and MAPK pathways. It has remained in question why mutations affecting one pathway cause incomplete gutless phenotypes, whereas mutations affecting both pathways are fully penetrant. I show that SYS-1 asymmetry is regulated solely by the MOM-2/MOM-5/APC-1 pathway. In the absence of signaling, SYS-1 is targeted for proteasomal degradation, similar to β -catenin in the canonical Wnt pathway. On the other hand, POP-1 asymmetry is primarily regulated by the MOM-4/LIT-1/WRM-1 pathway. The two

pathways work together to robustly elevate the SYS-1-to-POP-1 ratio, ensuring the activation of endoderm genes and the specification of E fate.

My discovery that SYS-1 is a limiting coactivator provides an explanation for the requirement for lowering the nuclear level of POP-1 in response to signaling. The relative levels of SYS-1 to POP-1 in MS and E cells could account for the OFF and ON switch of E-specific genes. However, since the corepressors are shown to be present ubiquitously in the early embryo (Calvo et al., 2001), the model of limiting coactivators also suggests that POP-1 would bind with higher affinity to SYS-1 than to corepressors in a signal-dependent manner. This aspect of the model should be further tested in the future. In addition, several circumstantial observations suggest that POP-1 might be qualitatively different between MS and E.

Chapters Three to Six aimed at investigating possible mechanisms by which POP-1 activity could be modified in E, most likely, but not necessarily, by LIT-1/WRM-1. A large part of the analysis focuses on the PCA domain. I show that the PCA domain is required for POP-1 nuclear asymmetry and possibly for the activation of endoderm fate. On the other hand, the domain between the HMG and PCA domains of POP-1 is not required for asymmetry but is required for the repression activity of POP-1. Deleting the PCA domain blocks all LIT-1/WRM-1-dependent phosphorylation of POP-1 in mammalian tissue culture cells. Mutating POP-1_{T426} to aspartic acid, but not alanine, shows phenotypes similar to that of POP-1_{ΔPCA}. It is possible that the PCA domain is involved in recruiting the LIT-1/WRM-1 complex.

The *in vivo* rescue assay only tests the repression activities of various POP-1 transgenes because in the absence of POP-1, basal expression of the endoderm genes allows the formation of extra endoderm. Therefore, I tested the ability of these POP-1 variants in the coimmunoprecipitation analysis to show that deleting the PCA domain reduces the amount of POP-1 bound to SYS-1 compared to wildtype, suggesting that the PCA domain is involved in the interaction between POP-1 and SYS-1. It will be interesting in the future if the PCA domain directly interacts with WRM-1, SYS-1, or both. This result is the first example suggesting that the C-terminal tail of a TCF protein is involved in interacting with β -catenin. Since SYS-1 differs from a typical β -catenin and lacks the C-terminal domain which is important for transactivation, it is possible that the unique C-terminal acidic domain of POP-1 provides the activation activity that is missing in SYS-1.

POP-1 is not only quantitatively but also qualitatively changed between MS and E by the Wnt and MAPK pathways. My work supports the qualitative difference of POP-1 in the following aspects:

- (1) LIT-1/WRM-1-dependent phosphorylation of POP-1 reduces its binding to the coactivator SYS-1.
- (2) Phosphorylation by LIT-1/WRM-1 might affect or be affected by the accessibility of the C-terminal domain to mabRL2.

I showed that LIT-1/WRM-1-dependent phosphorylation of POP-1 reduces its binding to the coactivator SYS-1. LIT-1 and WRM-1 phosphorylate POP-1 at the Exp sites and

target POP-1 for nuclear export. POP-1 and SYS-1 asymmetries are regulated independently, and my result further suggests that SYS-1 nuclear level is not likely to be affected by the nuclear export of POP-1. This result suggests that there are likely at least two populations of POP-1 in E. One population is the Exp sites-phosphorylated POP-1 which has reduced affinity towards SYS-1 and is exported from the nucleus, and the other population is the unphosphorylated POP-1 which remains in the nucleus and functions in a complex with SYS-1 to activate endoderm genes.

One detectable qualitative difference is the differential presentation of mabRL2 epitope. The monoclonal antibody against POP-1, mabRL2, detects the hypo- or unphosphorylated POP-1, but not the hyperphosphorylated POP-1. The epitope of mabRL2 is mapped to a region near the C-terminus of POP-1. Protein fusion at the C-terminus of POP-1 interferes with POP-1 nuclear asymmetry and blocks recognition by mabRL2. My results suggest that the masking of mabRL2 in the hyperphosphorylated POP-1 is likely due to an unknown modification, and the hyperphosphorylated POP-1 may have enriched cortical localization. The hyperphosphorylated POP-1 should be purified for mass spectrometry to elucidate the molecular nature of the qualitative difference(s) of POP-1. More work should be done to understand how these qualitative modifications are regulated and the relationship of these modifications with respect to phosphorylation at the Exp sites and T426.

This study greatly advanced the understanding of how the Wnt and MAPK pathways converge on the TCF protein POP-1, both quantitatively and qualitatively

regulating its nuclear asymmetry and transcriptional activity, to specify the MS and E fates in early *C. elegans* embryos. This study also provides a new way of thinking about how transcription activation can be achieved by two well-studied, conserved signaling pathways. Although the similarity between the POP-1 C-terminus and that of other TCF proteins is low at the level of primary sequences, functionally it is still possible for them to play similar roles or carry out similar interactions, with SYS-1 being the best example of conservation in function but not in sequence homology. It is worth looking into whether similar regulatory mechanisms are conserved for TCF proteins in higher organisms.

BIBLIOGRAPHY

- Albertson, D. G. and Thomson, J. N.** (1976). The pharynx of *Caenorhabditis elegans*. *Philos Trans R Soc Lond B Biol Sci* **275**, 299-325.
- Arce, L., Yokoyama, N. N. and Waterman, M. L.** (2006). Diversity of LEF/TCF action in development and disease. *Oncogene* **25**, 7492-504.
- Asally, M. and Yoneda, Y.** (2005). Beta-catenin can act as a nuclear import receptor for its partner transcription factor, lymphocyte enhancer factor-1 (lef-1). *Exp Cell Res* **308**, 357-63.
- Atcha, F. A., Munguia, J. E., Li, T. W., Hovanes, K. and Waterman, M. L.** (2003). A new beta-catenin-dependent activation domain in T cell factor. *J Biol Chem* **278**, 16169-75.
- Atcha, F. A., Syed, A., Wu, B., Hoverter, N. P., Yokoyama, N. N., Ting, J. H., Munguia, J. E., Mangalam, H. J., Marsh, J. L. and Waterman, M. L.** (2007). A unique DNA binding domain converts T-cell factors into strong Wnt effectors. *Mol Cell Biol* **27**, 8352-63.
- Barolo, S. and Posakony, J. W.** (2002). Three habits of highly effective signaling pathways: principles of transcriptional control by developmental cell signaling. *Genes Dev* **16**, 1167-81.
- Bei, Y., Hogan, J., Berkowitz, L. A., Soto, M., Rocheleau, C. E., Pang, K. M., Collins, J. and Mello, C. C.** (2002). SRC-1 and Wnt signaling act together to specify endoderm and to control cleavage orientation in early *C. elegans* embryos. *Dev Cell* **3**, 113-25.
- Berkowitz, L. A. and Strome, S.** (2000). MES-1, a protein required for unequal divisions of the germline in early *C. elegans* embryos, resembles receptor tyrosine kinases and is localized to the boundary between the germline and gut cells. *Development* **127**, 4419-31.
- Bird, A. F., Bird, J.** (1991). *The structure of nematodes*: Academic Press, Inc.
- Blom, N., Gammeltoft, S. and Brunak, S.** (1999). Sequence and structure-based prediction of eukaryotic protein phosphorylation sites. *J Mol Biol* **294**, 1351-62.
- Bowerman, B., Draper, B. W., Mello, C. C. and Priess, J. R.** (1993). The maternal gene *skn-1* encodes a protein that is distributed unequally in early *C. elegans* embryos. *Cell* **74**, 443-52.
- Bowerman, B., Eaton, B. A. and Priess, J. R.** (1992). *skn-1*, a maternally expressed gene required to specify the fate of ventral blastomeres in the early *C. elegans* embryo. *Cell* **68**, 1061-75.
- Broitman-Maduro, G., Maduro, M. F. and Rothman, J. H.** (2005). The noncanonical binding site of the MED-1 GATA factor defines differentially regulated target genes in the *C. elegans* mesendoderm. *Dev Cell* **8**, 427-33.

- Cadigan, K. M. and Nusse, R.** (1997). Wnt signaling: a common theme in animal development. *Genes Dev* **11**, 3286-305.
- Calvo, D., Victor, M., Gay, F., Sui, G., Luke, M. P., Dufourcq, P., Wen, G., Maduro, M., Rothman, J. and Shi, Y.** (2001). A POP-1 repressor complex restricts inappropriate cell type-specific gene transcription during *Caenorhabditis elegans* embryogenesis. *EMBO J* **20**, 7197-208.
- Cavallo, R. A., Cox, R. T., Moline, M. M., Roose, J., Polevoy, G. A., Clevers, H., Peifer, M. and Bejsovec, A.** (1998). *Drosophila* Tcf and Groucho interact to repress Wingless signalling activity. *Nature* **395**, 604-8.
- Costa, M., Raich, W., Agbunag, C., Leung, B., Hardin, J. and Priess, J. R.** (1998). A putative catenin-cadherin system mediates morphogenesis of the *Caenorhabditis elegans* embryo. *J Cell Biol* **141**, 297-308.
- Cui, M. and Han, M.** (2007). Roles of chromatin factors in *C. elegans* development. *WormBook*, 1-16.
- DeRenzo, C., Reese, K. J. and Seydoux, G.** (2003). Exclusion of germ plasm proteins from somatic lineages by cullin-dependent degradation. *Nature* **424**, 685-9.
- Eisenmann, D. M., Maloof, J. N., Simske, J. S., Kenyon, C. and Kim, S. K.** (1998). The beta-catenin homolog BAR-1 and LET-60 Ras coordinately regulate the Hox gene *lin-39* during *Caenorhabditis elegans* vulval development. *Development* **125**, 3667-80.
- Fagotto, F., Gluck, U. and Gumbiner, B. M.** (1998). Nuclear localization signal-independent and importin/karyopherin-independent nuclear import of beta-catenin. *Curr Biol* **8**, 181-90.
- Fukushige, T., Goszczynski, B., Yan, J. and McGhee, J. D.** (2005). Transcriptional control and patterning of the *pho-1* gene, an essential acid phosphatase expressed in the *C. elegans* intestine. *Dev Biol* **279**, 446-61.
- Gerhart, J.** (1999). 1998 Warkany lecture: signaling pathways in development. *Teratology* **60**, 226-39.
- Giese, K., Cox, J. and Grosschedl, R.** (1992). The HMG domain of lymphoid enhancer factor 1 bends DNA and facilitates assembly of functional nucleoprotein structures. *Cell* **69**, 185-95.
- Giles, R. H., van Es, J. H. and Clevers, H.** (2003). Caught up in a Wnt storm: Wnt signaling in cancer. *Biochim Biophys Acta* **1653**, 1-24.
- Goldstein, B.** (1992). Induction of gut in *Caenorhabditis elegans* embryos. *Nature* **357**, 255-7.
- Gonczy, P. and Rose, L. S.** (2005). Asymmetric cell division and axis formation in the embryo. *WormBook*, 1-20.
- Gordon, M. D. and Nusse, R.** (2006). Wnt signaling: multiple pathways, multiple receptors, and multiple transcription factors. *J Biol Chem* **281**, 22429-33.

- Graham, T. A., Weaver, C., Mao, F., Kimelman, D. and Xu, W.** (2000). Crystal structure of a beta-catenin/Tcf complex. *Cell* **103**, 885-96.
- Hammerlein, A., Weiske, J. and Huber, O.** (2005). A second protein kinase CK1-mediated step negatively regulates Wnt signalling by disrupting the lymphocyte enhancer factor-1/beta-catenin complex. *Cell Mol Life Sci* **62**, 606-18.
- Hawkins, N. C., Ellis, G. C., Bowerman, B. and Garriga, G.** (2005). MOM-5 frizzled regulates the distribution of DSH-2 to control *C. elegans* asymmetric neuroblast divisions. *Dev Biol* **284**, 246-59.
- Hecht, A. and Stemmler, M. P.** (2003). Identification of a promoter-specific transcriptional activation domain at the C terminus of the Wnt effector protein T-cell factor 4. *J Biol Chem* **278**, 3776-85.
- Herman, M.** (2001). *C. elegans* POP-1/TCF functions in a canonical Wnt pathway that controls cell migration and in a noncanonical Wnt pathway that controls cell polarity. *Development* **128**, 581-90.
- Hoppler, S. and Kavanagh, C. L.** (2007). Wnt signalling: variety at the core. *J Cell Sci* **120**, 385-93.
- Hsu, H. T., Liu, P. C., Ku, S. Y., Jung, K. C., Hong, Y. R., Kao, C. and Wang, C.** (2006). Beta-catenin control of T-cell transcription factor 4 (Tcf4) importation from the cytoplasm to the nucleus contributes to Tcf4-mediated transcription in 293 cells. *Biochem Biophys Res Commun* **343**, 893-8.
- Huang, S., Shetty, P., Robertson, S. M. and Lin, R.** (2007). Binary cell fate specification during *C. elegans* embryogenesis driven by reiterated reciprocal asymmetry of TCF POP-1 and its coactivator beta-catenin SYS-1. *Development* **134**, 2685-95.
- Hunter, C. P. and Kenyon, C.** (1996). Spatial and temporal controls target pal-1 blastomere-specification activity to a single blastomere lineage in *C. elegans* embryos. *Cell* **87**, 217-26.
- Ishitani, T., Kishida, S., Hyodo-Miura, J., Ueno, N., Yasuda, J., Waterman, M., Shibuya, H., Moon, R. T., Ninomiya-Tsuji, J. and Matsumoto, K.** (2003). The TAK1-NLK mitogen-activated protein kinase cascade functions in the Wnt-5a/Ca(2+) pathway to antagonize Wnt/beta-catenin signaling. *Mol Cell Biol* **23**, 131-9.
- Ishitani, T., Ninomiya-Tsuji, J., Nagai, S., Nishita, M., Meneghini, M., Barker, N., Waterman, M., Bowerman, B., Clevers, H., Shibuya, H. et al.** (1999). The TAK1-NLK-MAPK-related pathway antagonizes signalling between beta-catenin and transcription factor TCF. *Nature* **399**, 798-802.
- Kaletta, T., Schnabel, H. and Schnabel, R.** (1997). Binary specification of the embryonic lineage in *Caenorhabditis elegans*. *Nature* **390**, 294-8.

- Kemphues, K. J., Priess, J. R., Morton, D. G. and Cheng, N. S.** (1988). Identification of genes required for cytoplasmic localization in early *C. elegans* embryos. *Cell* **52**, 311-20.
- Kemphues, K. J. and Strome, S.** (1997). Fertilization and establishment of polarity in the embryo. In *C. elegans II*, (ed. D. L. Riddle T. Blumenthal B. J. Meyer and J. R. Priess), pp. 335-360. Plainview, NY: Cold Spring Harbor Laboratory Press.
- Kestler, H. A. and Kuhl, M.** (2008). From individual Wnt pathways towards a Wnt signalling network. *Philos Trans R Soc Lond B Biol Sci* **363**, 1333-47.
- Kidd, A. R., 3rd, Miskowski, J. A., Siegfried, K. R., Sawa, H. and Kimble, J.** (2005). A beta-catenin identified by functional rather than sequence criteria and its role in Wnt/MAPK signaling. *Cell* **121**, 761-72.
- Klaus, A. and Birchmeier, W.** (2008). Wnt signalling and its impact on development and cancer. *Nat Rev Cancer* **8**, 387-98.
- Kohn, A. D. and Moon, R. T.** (2005). Wnt and calcium signaling: beta-catenin-independent pathways. *Cell Calcium* **38**, 439-46.
- Korswagen, H. C., Herman, M. A. and Clevers, H. C.** (2000). Distinct beta-catenins mediate adhesion and signalling functions in *C. elegans*. *Nature* **406**, 527-32.
- Krieghoff, E., Behrens, J. and Mayr, B.** (2006). Nucleo-cytoplasmic distribution of beta-catenin is regulated by retention. *J Cell Sci* **119**, 1453-63.
- Kuhl, M., Geis, K., Sheldahl, L. C., Pukrop, T., Moon, R. T. and Wedlich, D.** (2001). Antagonistic regulation of convergent extension movements in *Xenopus* by Wnt/beta-catenin and Wnt/Ca²⁺ signaling. *Mech Dev* **106**, 61-76.
- Lee, P. N., Pang, K., Matus, D. Q. and Martindale, M. Q.** (2006). A WNT of things to come: evolution of Wnt signaling and polarity in cnidarians. *Semin Cell Dev Biol* **17**, 157-67.
- Lin, R., Hill, R. J. and Priess, J. R.** (1998). POP-1 and anterior-posterior fate decisions in *C. elegans* embryos. *Cell* **92**, 229-39.
- Lin, R., Thompson, S. and Priess, J. R.** (1995). pop-1 encodes an HMG box protein required for the specification of a mesoderm precursor in early *C. elegans* embryos. *Cell* **83**, 599-609.
- Liu, J., Phillips, B. T., Amaya, M. F., Kimble, J. and Xu, W.** (2008). The *C. elegans* SYS-1 protein is a bona fide beta-catenin. *Dev Cell* **14**, 751-61.
- Lo, M. C., Gay, F., Odom, R., Shi, Y. and Lin, R.** (2004). Phosphorylation by the beta-catenin/MAPK complex promotes 14-3-3-mediated nuclear export of TCF/POP-1 in signal-responsive cells in *C. elegans*. *Cell* **117**, 95-106.
- Maduro, M. F.** (2008). Structure and evolution of the *C. elegans* embryonic endomesoderm network. *Biochim Biophys Acta*.

- Maduro, M. F., Broitman-Maduro, G., Mengarelli, I. and Rothman, J. H.** (2007). Maternal deployment of the embryonic SKN-1-->MED-1,2 cell specification pathway in *C. elegans*. *Dev Biol* **301**, 590-601.
- Maduro, M. F., Hill, R. J., Heid, P. J., Newman-Smith, E. D., Zhu, J., Priess, J. R. and Rothman, J. H.** (2005a). Genetic redundancy in endoderm specification within the genus *Caenorhabditis*. *Dev Biol* **284**, 509-22.
- Maduro, M. F., Kasmir, J. J., Zhu, J. and Rothman, J. H.** (2005b). The Wnt effector POP-1 and the PAL-1/Caudal homeoprotein collaborate with SKN-1 to activate *C. elegans* endoderm development. *Dev Biol* **285**, 510-23.
- Maduro, M. F., Lin, R. and Rothman, J. H.** (2002). Dynamics of a developmental switch: recursive intracellular and intranuclear redistribution of *Caenorhabditis elegans* POP-1 parallels Wnt-inhibited transcriptional repression. *Dev Biol* **248**, 128-42.
- Maduro, M. F., Meneghini, M. D., Bowerman, B., Broitman-Maduro, G. and Rothman, J. H.** (2001). Restriction of mesendoderm to a single blastomere by the combined action of SKN-1 and a GSK-3beta homolog is mediated by MED-1 and -2 in *C. elegans*. *Mol Cell* **7**, 475-85.
- Maloof, J. N., Whangbo, J., Harris, J. M., Jongeward, G. D. and Kenyon, C.** (1999). A Wnt signaling pathway controls hox gene expression and neuroblast migration in *C. elegans*. *Development* **126**, 37-49.
- Mello, C. C., Draper, B. W., Krause, M., Weintraub, H. and Priess, J. R.** (1992). The pie-1 and mex-1 genes and maternal control of blastomere identity in early *C. elegans* embryos. *Cell* **70**, 163-76.
- Mello, C. C., Schubert, C., Draper, B., Zhang, W., Lobel, R. and Priess, J. R.** (1996). The PIE-1 protein and germline specification in *C. elegans* embryos. *Nature* **382**, 710-2.
- Meneghini, M. D., Ishitani, T., Carter, J. C., Hisamoto, N., Ninomiya-Tsuji, J., Thorpe, C. J., Hamill, D. R., Matsumoto, K. and Bowerman, B.** (1999). MAP kinase and Wnt pathways converge to downregulate an HMG-domain repressor in *Caenorhabditis elegans*. *Nature* **399**, 793-7.
- Miskowski, J., Li, Y. and Kimble, J.** (2001). The sys-1 gene and sexual dimorphism during gonadogenesis in *Caenorhabditis elegans*. *Dev Biol* **230**, 61-73.
- Mizumoto, K. and Sawa, H.** (2007). Two betas or not two betas: regulation of asymmetric division by beta-catenin. *Trends Cell Biol* **17**, 465-73.
- Nakamura, K., Kim, S., Ishidate, T., Bei, Y., Pang, K., Shirayama, M., Trzepacz, C., Brownell, D. R. and Mello, C. C.** (2005). Wnt signaling drives WRM-1/beta-catenin asymmetries in early *C. elegans* embryos. *Genes Dev* **19**, 1749-54.
- Natarajan, L., Witwer, N. E. and Eisenmann, D. M.** (2001). The divergent *Caenorhabditis elegans* beta-catenin proteins BAR-1, WRM-1 and HMP-2

- make distinct protein interactions but retain functional redundancy in vivo. *Genetics* **159**, 159-72.
- Ninomiya-Tsuji, J., Kishimoto, K., Hiyama, A., Inoue, J., Cao, Z. and Matsumoto, K.** (1999). The kinase TAK1 can activate the NIK-I kappaB as well as the MAP kinase cascade in the IL-1 signalling pathway. *Nature* **398**, 252-6.
- Nusse, R.** (2008). Wnt signaling and stem cell control. *Cell Res* **18**, 523-7.
- Nusse, R. and Varmus, H. E.** (1982). Many tumors induced by the mouse mammary tumor virus contain a provirus integrated in the same region of the host genome. *Cell* **31**, 99-109.
- Obenauer, J. C., Cantley, L. C. and Yaffe, M. B.** (2003). Scansite 2.0: Proteome-wide prediction of cell signaling interactions using short sequence motifs. *Nucleic Acids Res* **31**, 3635-41.
- Oosterveen, T., Coudreuse, D. Y., Yang, P. T., Fraser, E., Bergsma, J., Dale, T. C. and Korswagen, H. C.** (2007). Two functionally distinct Axin-like proteins regulate canonical Wnt signaling in *C. elegans*. *Dev Biol* **308**, 438-48.
- Park, F. D. and Priess, J. R.** (2003). Establishment of POP-1 asymmetry in early *C. elegans* embryos. *Development* **130**, 3547-56.
- Pflugrad, A., Meir, J. Y., Barnes, T. M. and Miller, D. M., 3rd.** (1997). The Groucho-like transcription factor UNC-37 functions with the neural specificity gene *unc-4* to govern motor neuron identity in *C. elegans*. *Development* **124**, 1699-709.
- Phillips, B. T., Kidd, A. R., 3rd, King, R., Hardin, J. and Kimble, J.** (2007). Reciprocal asymmetry of SYS-1/beta-catenin and POP-1/TCF controls asymmetric divisions in *Caenorhabditis elegans*. *Proc Natl Acad Sci U S A* **104**, 3231-6.
- Pires-daSilva, A. and Sommer, R. J.** (2003). The evolution of signalling pathways in animal development. *Nat Rev Genet* **4**, 39-49.
- Polakis, P.** (2000). Wnt signaling and cancer. *Genes Dev* **14**, 1837-51.
- Praitis, V., Casey, E., Collar, D. and Austin, J.** (2001). Creation of low-copy integrated transgenic lines in *Caenorhabditis elegans*. *Genetics* **157**, 1217-26.
- Priess, J. R. and Thomson, J. N.** (1987). Cellular interactions in early *C. elegans* embryos. *Cell* **48**, 241-50.
- Robertson, S. M., Shetty, P. and Lin, R.** (2004). Identification of lineage-specific zygotic transcripts in early *Caenorhabditis elegans* embryos. *Dev Biol* **276**, 493-507.
- Rocheleau, C. E., Downs, W. D., Lin, R., Wittmann, C., Bei, Y., Cha, Y. H., Ali, M., Priess, J. R. and Mello, C. C.** (1997). Wnt signaling and an APC-related gene specify endoderm in early *C. elegans* embryos. *Cell* **90**, 707-16.
- Rocheleau, C. E., Yasuda, J., Shin, T. H., Lin, R., Sawa, H., Okano, H., Priess, J. R., Davis, R. J. and Mello, C. C.** (1999). WRM-1 activates the

- LIT-1 protein kinase to transduce anterior/posterior polarity signals in *C. elegans*. *Cell* **97**, 717-26.
- Rogers, E., Bishop, J. D., Waddle, J. A., Schumacher, J. M. and Lin, R.** (2002). The aurora kinase AIR-2 functions in the release of chromosome cohesion in *Caenorhabditis elegans* meiosis. *J Cell Biol* **157**, 219-29.
- Schnabel, H. and Priess, J. R.** (1997). Specification of cell fates in the early embryo. In *C. elegans II*, (ed. D. L. Riddle T. Blumenthal B. J. Meyer and J. R. Priess), pp. 361-382. Plainview, NY: Cold Spring Harbor Laboratory Press.
- Schroeder, D. F. and McGhee, J. D.** (1998). Anterior-posterior patterning within the *Caenorhabditis elegans* endoderm. *Development* **125**, 4877-87.
- Shetty, P., Lo, M. C., Robertson, S. M. and Lin, R.** (2005). *C. elegans* TCF protein, POP-1, converts from repressor to activator as a result of Wnt-induced lowering of nuclear levels. *Dev Biol* **285**, 584-92.
- Shibuya, H., Iwata, H., Masuyama, N., Gotoh, Y., Yamaguchi, K., Irie, K., Matsumoto, K., Nishida, E. and Ueno, N.** (1998). Role of TAK1 and TAB1 in BMP signaling in early *Xenopus* development. *EMBO J* **17**, 1019-28.
- Shibuya, H., Yamaguchi, K., Shirakabe, K., Tonegawa, A., Gotoh, Y., Ueno, N., Irie, K., Nishida, E. and Matsumoto, K.** (1996). TAB1: an activator of the TAK1 MAPKKK in TGF-beta signal transduction. *Science* **272**, 1179-82.
- Shin, T. H., Yasuda, J., Rocheleau, C. E., Lin, R., Soto, M., Bei, Y., Davis, R. J. and Mello, C. C.** (1999). MOM-4, a MAP kinase kinase kinase-related protein, activates WRM-1/LIT-1 kinase to transduce anterior/posterior polarity signals in *C. elegans*. *Mol Cell* **4**, 275-80.
- Siegfried, K. R., Kidd, A. R., 3rd, Chesney, M. A. and Kimble, J.** (2004). The *sys-1* and *sys-3* genes cooperate with Wnt signaling to establish the proximal-distal axis of the *Caenorhabditis elegans* gonad. *Genetics* **166**, 171-86.
- Siegfried, K. R. and Kimble, J.** (2002). POP-1 controls axis formation during early gonadogenesis in *C. elegans*. *Development* **129**, 443-53.
- Slusarski, D. C. and Pelegri, F.** (2007). Calcium signaling in vertebrate embryonic patterning and morphogenesis. *Dev Biol* **307**, 1-13.
- Smit, L., Baas, A., Kuipers, J., Korswagen, H., van de Wetering, M. and Clevers, H.** (2004). Wnt activates the Tak1/Nemo-like kinase pathway. *J Biol Chem* **279**, 17232-40.
- Srivastava, M., Begovic, E., Chapman, J., Putnam, N. H., Hellsten, U., Kawashima, T., Kuo, A., Mitros, T., Salamov, A., Carpenter, M. L. et al.** (2008). The *Trichoplax* genome and the nature of placozoans. *Nature* **454**, 955-60.
- Sulston, J. E., Schierenberg, E., White, J. G. and Thomson, J. N.** (1983). The embryonic cell lineage of the nematode *Caenorhabditis elegans*. *Dev Biol* **100**, 64-119.

- Takeshita, H. and Sawa, H.** (2005). Asymmetric cortical and nuclear localizations of WRM-1/beta-catenin during asymmetric cell division in *C. elegans*. *Genes Dev* **19**, 1743-8.
- Thomas-Virnig, C. L., Sims, P. A., Simske, J. S. and Hardin, J.** (2004). The inositol 1,4,5-trisphosphate receptor regulates epidermal cell migration in *Caenorhabditis elegans*. *Curr Biol* **14**, 1882-7.
- Thorpe, C. J. and Moon, R. T.** (2004). nemo-like kinase is an essential co-activator of Wnt signaling during early zebrafish development. *Development* **131**, 2899-909.
- Thorpe, C. J., Schlesinger, A., Carter, J. C. and Bowerman, B.** (1997). Wnt signaling polarizes an early *C. elegans* blastomere to distinguish endoderm from mesoderm. *Cell* **90**, 695-705.
- Timmons, L. and Fire, A.** (1998). Specific interference by ingested dsRNA. *Nature* **395**, 854.
- van de Wetering, M., Cavallo, R., Dooijes, D., van Beest, M., van Es, J., Loureiro, J., Ypma, A., Hursh, D., Jones, T., Bejsovec, A. et al.** (1997). Armadillo coactivates transcription driven by the product of the *Drosophila* segment polarity gene dTCF. *Cell* **88**, 789-99.
- Vazquez-Manrique, R. P., Nagy, A. I., Legg, J. C., Bales, O. A., Ly, S. and Baylis, H. A.** (2008). Phospholipase C-epsilon regulates epidermal morphogenesis in *Caenorhabditis elegans*. *PLoS Genet* **4**, e1000043.
- Waterman, M. L.** (2004). Lymphoid enhancer factor/T cell factor expression in colorectal cancer. *Cancer Metastasis Rev* **23**, 41-52.
- Wu, M. and Herman, M. A.** (2006). A novel noncanonical Wnt pathway is involved in the regulation of the asymmetric B cell division in *C. elegans*. *Dev Biol* **293**, 316-29.
- Xiao, H., Pearson, A., Coulombe, B., Truant, R., Zhang, S., Regier, J. L., Triezenberg, S. J., Reinberg, D., Flores, O., Ingles, C. J. et al.** (1994). Binding of basal transcription factor TFIID to the acidic activation domains of VP16 and p53. *Mol Cell Biol* **14**, 7013-24.
- Yamada, M., Ohnishi, J., Ohkawara, B., Iemura, S., Satoh, K., Hyodo-Miura, J., Kawachi, K., Natsume, T. and Shibuya, H.** (2006). NARF, an nemo-like kinase (NLK)-associated ring finger protein regulates the ubiquitylation and degradation of T cell factor/lymphoid enhancer factor (TCF/LEF). *J Biol Chem* **281**, 20749-60.
- Yamaguchi, K., Shirakabe, K., Shibuya, H., Irie, K., Oishi, I., Ueno, N., Taniguchi, T., Nishida, E. and Matsumoto, K.** (1995). Identification of a member of the MAPKKK family as a potential mediator of TGF-beta signal transduction. *Science* **270**, 2008-11.
- Zarubin, T. and Han, J.** (2005). Activation and signaling of the p38 MAP kinase pathway. *Cell Res* **15**, 11-8.

- Zeng, Y. A. and Verheyen, E. M.** (2004). Nemo is an inducible antagonist of Wingless signaling during *Drosophila* wing development. *Development* **131**, 2911-20.
- Zhou, F., Xue, Y., Yao, X. and Xu, Y.** (2006). CSS-Palm: palmitoylation site prediction with a clustering and scoring strategy (CSS). *Bioinformatics* **22**, 894-6.
- Zhou, F. F., Xue, Y., Chen, G. L. and Yao, X.** (2004). GPS: a novel group-based phosphorylation predicting and scoring method. *Biochem Biophys Res Commun* **325**, 1443-8.
- Zhu, J., Fukushige, T., McGhee, J. D. and Rothman, J. H.** (1998). Reprogramming of early embryonic blastomeres into endodermal progenitors by a *Caenorhabditis elegans* GATA factor. *Genes Dev* **12**, 3809-14.
- Zhu, J., Hill, R. J., Heid, P. J., Fukuyama, M., Sugimoto, A., Priess, J. R. and Rothman, J. H.** (1997). end-1 encodes an apparent GATA factor that specifies the endoderm precursor in *Caenorhabditis elegans* embryos. *Genes Dev* **11**, 2883-96.